

## Final Report

# Axle Equivalent Transverse Loading on Segmental Bridge Decks

Contract Number BDK83-977-16  
FSU Project ID 030964

---

*Submitted to:*

Florida Department of Transportation  
Research Center  
605 Suwannee Street  
Tallahassee, Florida 32399-0450



Jean Ducher, P.E.  
Project Manager  
FDOT Office of Maintenance

---

*Submitted by:*



Michelle Roddenberry, Ph.D., P.E.  
Principal Investigator  
Sungmoon Jung, Ph.D.  
Co-Principal Investigator  
Atul Patil  
Graduate Research Assistant

FAMU-FSU College of Engineering  
Department of Civil and Environmental Engineering  
2525 Pottsdamer Street, Rm. A129  
Tallahassee, FL 32310-6046

---

April 2014

## **DISCLAIMER**

This report was prepared in cooperation with the State of Florida Department of Transportation. The opinions, findings, and conclusions expressed in this publication are those of the authors and not necessarily those of the State of Florida Department of Transportation. This report does not constitute a standard, specification, or regulation.

## SI\* (MODERN METRIC) CONVERSION FACTORS

### *APPROXIMATE CONVERSIONS TO SI UNITS*

SYMBOL	WHEN YOU KNOW	MULTIPLY BY	TO FIND	SYMBOL
<b>LENGTH</b>				
<b>in</b>	inches	25.4	millimeters	mm
<b>ft</b>	feet	0.305	meters	m
<b>yd</b>	yards	0.914	meters	m
<b>mi</b>	miles	1.61	kilometers	km
<b>AREA</b>				
<b>in<sup>2</sup></b>	square inches	645.2	square millimeters	mm <sup>2</sup>
<b>ft<sup>2</sup></b>	square feet	0.093	square meters	m <sup>2</sup>
<b>yd<sup>2</sup></b>	square yard	0.836	square meters	m <sup>2</sup>
<b>ac</b>	acres	0.405	hectares	ha
<b>mi<sup>2</sup></b>	square miles	2.59	square kilometers	km <sup>2</sup>
<b>VOLUME</b>				
<b>fl oz</b>	fluid ounces	29.57	milliliters	mL
<b>gal</b>	gallons	3.785	liters	L
<b>ft<sup>3</sup></b>	cubic feet	0.028	cubic meters	m <sup>3</sup>
<b>yd<sup>3</sup></b>	cubic yards	0.765	cubic meters	m <sup>3</sup>
NOTE: volumes greater than 1000 L shall be shown in m <sup>3</sup>				
<b>MASS</b>				
<b>oz</b>	ounces	28.35	grams	g
<b>lb</b>	pounds	0.454	kilograms	kg
<b>T</b>	short tons (2000 lb)	0.907	Megagrams (or "metric ton")	Mg (or "t")
<b>TEMPERATURE (exact degrees)</b>				
<b>°F</b>	Fahrenheit	5(F-32)/9 or (F-32)/1.8	Celsius	°C
<b>ILLUMINATION</b>				
<b>fc</b>	foot-candles	10.76	lux	lx
<b>fl</b>	foot-Lamberts	3.426	candela/m <sup>2</sup>	cd/m <sup>2</sup>
<b>FORCE and PRESSURE or STRESS</b>				
<b>lbf</b>	pound force	4.45	newtons	N
<b>k</b>	kip	4.45	kilonewtons	kN
<b>lbf/in<sup>2</sup> (or psi)</b>	pound force per square inch	6.89	kilopascals	kPa
<b>k/in<sup>2</sup> (or ksi)</b>	kips per square inch	6.89	megapascals	MPa

\*SI is the symbol for the International System of Units. Appropriate rounding should be made to comply with Section 4 of ASTM E380.

## SI\* (MODERN METRIC) CONVERSION FACTORS

### APPROXIMATE CONVERSIONS FROM SI UNITS

SYMBOL	WHEN YOU KNOW	MULTIPLY BY	TO FIND	SYMBOL
<b>LENGTH</b>				
mm	millimeters	0.039	inches	in
m	meters	3.28	feet	ft
m	meters	1.09	yards	yd
km	kilometers	0.621	miles	mi
<b>AREA</b>				
mm <sup>2</sup>	square millimeters	0.0016	square inches	in <sup>2</sup>
m <sup>2</sup>	square meters	10.764	square feet	ft <sup>2</sup>
m <sup>2</sup>	square meters	1.195	square yards	yd <sup>2</sup>
ha	hectares	2.47	acres	ac
km <sup>2</sup>	square kilometers	0.386	square miles	mi <sup>2</sup>
<b>VOLUME</b>				
mL	milliliters	0.034	fluid ounces	fl oz
L	liters	0.264	gallons	gal
m <sup>3</sup>	cubic meters	35.314	cubic feet	ft <sup>3</sup>
m <sup>3</sup>	cubic meters	1.307	cubic yards	yd <sup>3</sup>
<b>MASS</b>				
g	grams	0.035	ounces	oz
kg	kilograms	2.202	pounds	lb
Mg (or "t")	megagrams (or "metric ton")	1.103	short tons (2000 lb)	T
<b>TEMPERATURE (exact degrees)</b>				
°C	Celsius	1.8C+32	Fahrenheit	°F
<b>ILLUMINATION</b>				
lx	lux	0.0929	foot-candles	fc
cd/m <sup>2</sup>	candela/m <sup>2</sup>	0.2919	foot-Lamberts	fl
<b>FORCE and PRESSURE or STRESS</b>				
N	newtons	0.225	pound force	lbf
kN	kilonewtons	0.225	kip	k
kPa	kilopascals	0.145	pound force per square inch	lbf/in <sup>2</sup> (psi)
MPa	megapascals	0.145	kips per square inch	k/in <sup>2</sup> (ksi)

\*SI is the symbol for the International System of Units. Appropriate rounding should be made to comply with Section 4 of ASTM E380.

**Technical Report Documentation Page**

1. Report No.		2. Government Accession No.		3. Recipient's Catalog No.	
4. Title and Subtitle Axle Equivalent Transverse Loading on Segmental Bridge Decks				5. Report Date April 2014	
				6. Performing Organization Code	
7. Author(s) M. Roddenberry, S. Jung, and A. Patil				8. Performing Organization Report No. FSU Project ID 030964	
9. Performing Organization Name and Address FAMU-FSU College of Engineering Department of Civil and Environmental Engineering 2525 Pottsdamer St. Rm. A129 Tallahassee, FL 32310-6046				10. Work Unit No. (TRAIS)	
				11. Contract or Grant No. BDK83-977-16	
12. Sponsoring Agency Name and Address Florida Department of Transportation Research Center 605 Suwannee Street, MS 30 Tallahassee, FL 32399-0450				13. Type of Report and Period Covered Final Report November 2011 – April 2014	
				14. Sponsoring Agency Code	
15. Supplementary Notes					
16. Abstract <p>For a prestressed concrete segmental box girder bridge, both design and load rating are determined by longitudinal and transverse analyses. A transverse analysis is performed for the top slab, typically by using Homberg charts (an engineer's design tool), to account for transverse bending effects due to truck wheel loads. The FDOT Office of Maintenance issues thousands of permits annually for heavy trucks. These trucks may have different axle weights and spacings than the trucks that are analyzed in the engineer's design or load rating.</p> <p>In this research, a Homberg-based tool was developed in Excel for analyzing vehicles for their effect on transverse bending moments in a prestressed concrete segmental box girder bridge. The tool allows the user to analyze vehicle loads quickly and provides a simple way to compare effects of different vehicles. For example, the effects of vehicles that were analyzed in the designer's load rating could be compared to vehicles with axle weights and spacings that were not analyzed in the initial load rating.</p> <p>In addition, Finite Element Modeling (FEM) was performed to study the effect on transverse bending moment of elements such as barriers, barrier joints, diaphragms, supports, and expansion joints. The effect of axle load spacing was also studied to give insight into the Office of Maintenance's formerly-used "8-foot rule." Calculated bending moments from Homberg analysis and FEM were compared for a few "Blanket" Permit Vehicles. "Blanket" Permit Vehicles are those vehicles permitted to travel an unrestricted number of times on unrestricted routes within one calendar year.</p>					
17. Key Word transverse analysis, load rating, segmental box girder bridge, vehicle permit			18. Distribution Statement No restrictions.		
19. Security Classif. (of this report) Unclassified.		20. Security Classif. (of this page) Unclassified.		21. No. of Pages 78	22. Price

## **ACKNOWLEDGEMENTS**

The authors would like to thank the Florida Department of Transportation (FDOT) for providing funding for this research. In particular, thanks to Jean Ducher, P.E., for his guidance and management of the project, as well as his insight on the FDOT Office of Maintenance operations and permit process. Thanks also to Jeff Pouliotte, P.E., Will Potter, P.E., and Bryan Hubbard, P.E., for their participation and valuable discussions on the research.

## EXECUTIVE SUMMARY

For a prestressed concrete segmental box girder bridge, both design and load rating are determined by longitudinal and transverse analyses. A transverse analysis is performed for the top slab, typically by using Homberg charts (an engineer's design tool), to account for transverse bending effects due to truck wheel loads.

The FDOT Office of Maintenance issues thousands of permits annually for heavy trucks. These trucks may have different axle weights and spacings than the trucks that are analyzed in the engineer's design or load rating.

In this research, a Homberg-based tool was developed in Excel for analyzing vehicles for their effect on transverse bending moments in a prestressed concrete segmental box girder bridge. The tool allows the user to analyze vehicle loads quickly and provides a simple way to compare effects of different vehicles. For example, the effects of vehicles that were analyzed in the designer's load rating could be compared to vehicles with axle weights and spacings that were not analyzed in the initial load rating.

In addition, Finite Element Modeling (FEM) was performed to study the effect on transverse bending moment of elements such as barriers, barrier joints, diaphragms, supports, and expansion joints. The effect of axle load spacing was also studied to give insight into the Office of Maintenance's formerly-used "8-foot rule." Calculated bending moments from Homberg analysis and FEM were compared for a few "Blanket" Permit Vehicles. "Blanket" Permit Vehicles are those vehicles permitted to travel an unrestricted number of times on unrestricted routes within one calendar year.

# TABLE OF CONTENTS

<b>Disclaimer .....</b>	<b>ii</b>
<b>SI Conversion Factors .....</b>	<b>iii</b>
<b>Technical Report Documentation Page .....</b>	<b>v</b>
<b>Acknowledgements .....</b>	<b>vi</b>
<b>Executive Summary .....</b>	<b>vii</b>
<b>List of Figures.....</b>	<b>x</b>
<b>List of Tables .....</b>	<b>xii</b>
<b>1 Introduction.....</b>	<b>1</b>
1.1 Background.....	1
1.2 Objectives .....	1
<b>2 Finite Element Modeling.....</b>	<b>3</b>
2.1 Introduction.....	3
2.2 Element Choice.....	3
2.3 Simple Beam Analysis.....	4
2.4 Results: SHELL281 Element vs. SOLID186 Element.....	6
<b>3 Analyses of Channel Five Bridge.....</b>	<b>12</b>
3.1 Finite Element Modeling .....	12
3.2 Analysis for Various Loading Cases and Barrier Models .....	13
3.2.1 Effect of Span Support.....	14
3.2.2 Effect of Expansion Joint at End of Span .....	16
3.2.3 Effect of Expansion Joint as Load Moves Away from End of Span .....	18
3.2.4 Effect of Barrier .....	20
3.2.5 Effect of Barrier Joint .....	22
3.2.6 Effect of Diaphragm at the End Support.....	24
3.3 Verification of the 8-foot Rule.....	25
<b>4 FEM-Based Moment Approximation .....</b>	<b>30</b>
4.1 Introduction.....	30
4.2 Approach.....	31
4.2.1 Plate Model vs. Scaled Bridge .....	31
4.2.2 Replicating Homberg Influence Surfaces with FE Model Results .....	33
4.2.3 Explanation of Moment Calculations .....	38
4.2.4 Results.....	39
4.3 Moment Comparison Analyses on Blanket Permit Vehicles.....	44

<b>5</b>	<b>Tool Development .....</b>	<b>48</b>
5.1	Introduction.....	48
5.2	Overview of Tool.....	48
5.3	Explanation of Code and Visual Basic Functions.....	53
<b>6</b>	<b>How to Use the Tool (Tutorial).....</b>	<b>60</b>
	<b>References.....</b>	<b>66</b>

# LIST OF FIGURES

2.1	Sample I-shaped Beam for (a) SHELL281 Model and (b) SOLID186 Model.....	3
2.2	SHELL281 Element Geometry (ANSYS 2010).....	4
2.3	SOLID186 Element Geometry (ANSYS 2010).....	4
2.4	Beam Model with SHELL281 Elements: (a) Complete Beam (b) Enlarged Section.....	5
2.5	Beam Model with SOLID186 Elements: (a) Complete Beam (b) Enlarged Section .....	5
2.6	Deflected Shape of Beam under Pressure Load (Deflection Exaggerated) .....	6
2.7	Comparison of SHELL281, SOLID186 and Manual (Analytical) Solutions.....	7
2.8	Percentage Variation in Deflection vs. Degrees of Freedom for SHELL281, SOLID186 and Manual (Analytical) Solutions .....	7
2.9	Cross Section of I-shaped Beam Showing the Reading Locations.....	8
2.10	Normal Stress at Location 2 with Increasing Degrees of Freedom .....	8
2.11	Normal Stress at Location 3 with Increasing Degrees of Freedom .....	9
2.12	Shear Stress at Location 1 with Increasing Degrees of Freedom .....	9
2.13	Shear Stress at Location 2 with Increasing Degrees of Freedom .....	10
3.1	Channel Five Bridge Cross Section .....	12
3.2	FE Bridge Model: (a) Oblique View (b) Sectional View .....	13
3.3	FE Bridge Model (a) Reading Locations (b) Global Cartesian Axis.....	14
3.4	Loading Conditions for Cases A1 and A2 .....	15
3.5	Deflection for Cases A1 and A2 .....	15
3.6	Normal Stress X Direction for Cases A1 and A2 .....	16
3.7	Loading Conditions for Cases A1 and A3-A.....	16
3.8	Comparison of Deflections for Cases A1 and A3-A .....	17
3.9	Comparison of Normal Stress Z Direction for Cases A1 and A3-A.....	17
3.10	Comparison of Normal Stress X Direction for Cases A1 and A3-A .....	18
3.11	Exaggerated Deflected Shape for Case A3-A.....	18
3.12	Loading Condition for Cases A3-A and A3-B .....	19
3.13	Comparison of Deflection for Cases A3-A and A3-B.....	19
3.14	Comparison of Normal Stress in Z Direction for Cases A3-A and A3-B .....	19
3.15	Comparison of Normal Stress in X Direction for Cases A3-A and A3-B.....	20
3.16	Loading Condition for Cases A1 and B1 .....	20
3.17	Comparison of Deflection for Cases A1 and B1 .....	21
3.18	Comparison of Normal Stress in Z Direction for Cases A1 and B1 .....	21
3.19	Comparison of Normal Stress in X Direction for Cases A1 and B1 .....	22
3.20	Loading Condition for Cases B1 and B2 .....	22
3.21	Comparison of Deflection for Cases B1 and B2.....	23
3.22	Comparison of Normal Stress in Z Direction for Cases B1 and B2 .....	23
3.23	Comparison of Normal Stress in X Direction for Cases B1 and B2.....	24
3.24	Load Positions with No Diaphragm Modeled at Support.....	24
3.25	Load Positions with Diaphragm Modeled at Support.....	24
3.26	Variation of Top Stresses: (a) No Diaphragm at Support (b) Diaphragm at Support.....	25
3.27	Load Positions on Wing 30 Inches from Edge of Wing Slab .....	26
3.28	Load Positions at 2-foot Intervals up to 16 Feet from Mid Span (Not to Scale) .....	26

3.29	Reading Locations across the Width of Bridge, in Inches.....	27
3.30	Normal Stress X Direction at Top Surface .....	27
3.31	Normal Stress X Direction at Mid Depth .....	28
3.32	Normal Stress X Direction at Bottom Surface.....	28
3.33	Comparison of Normal Stress in X Direction for FEM Results and Homberg Chart (Stress from Top Surface).....	29
3.34	Comparison of Normal Stress in X Direction for FEM Results and Homberg Chart (Stress from Bottom Surface) .....	29
4.1	Influence Surface Moment Coefficients at Location 2 (m2x) .....	30
4.2	Moment Reading Locations for Various Boundary Conditions (from Homberg Charts) ..	31
4.3	ANSYS Cantilever Plate SOLID186 Element Model with Applied Unit Load .....	32
4.4	Comparison of Moment Function for SHELL281 vs. SOLID186 Element Models .....	33
4.5	Comparison of Moment Coefficients for the Cantilever Plate and the Scaled Bridge .....	34
4.6	Comparison of Influence Surfaces from (a) Homberg Chart m2x (b) FE Plate Model (c) Scaled Bridge FE Model.....	36
4.7	Comparison of Influence Surfaces from (a) Homberg Chart m3x (b) FE Plate Model (c) Scaled Bridge FE Model.....	37
4.8	Elements and Stress Reading Locations .....	38
4.9	Schematic Representation of Stress Envelope.....	39
4.10	Comparison of m2x Wing Case from (a) Homberg Chart (b) Scaled Bridge FE Model ..	40
4.11	Comparison of m3x Wing Case from (a) Homberg Chart (b) Scaled Bridge FE Model ..	41
4.12	Comparison of m3x Mid Span Fixed-edge Case from (a) Homberg Chart (b) Scaled Bridge FE Model.....	42
4.13	Comparison of m5x Mid Span Simply-supported from (a) Homberg Chart (b) Scaled Bridge FE Model.....	43
4.14	Bridge Section Showing m2x Wing with Applied HS20 Truck Load.....	44
5.1	Figure Showing (a) Tabs (b) WA, WB, and WC Entries .....	48
5.2	Schematic Representation of Required Data for Tool .....	49
5.3	Selecting Two Trucks and Two Types of Homberg Charts .....	49
5.4	Results for m2x Wing and m3x Mid Span.....	50
5.5	Button to Plot Wheel Locations for Maximum Moment.....	51
5.6	Sample Wheel Location for Maximum Moment.....	51
5.7	Custom Truck Details .....	52
5.8	Sample Custom Truck Plot.....	52
5.9	Flow Chart of the Tool.....	53
5.10	The Data Passed on to the Visual Basic ‘Main’ Function (Only Part of Data Shown) .....	54
5.11	Visual Basic ‘Main’ Function Code .....	55
5.12	HS20 Function Code.....	56
5.13	Sample Result for HS20, m2x Wing Span.....	56
5.14	Homberg Chart for m3x Wing Span with Additional Grid at 0.1 Interval .....	58
5.15	Moment Function for y = 0.4 Grid Line for m3x Wing Span .....	59

# LIST OF TABLES

4.1	Homberg Chart Tool and FEM Analysis Moments for m2x Wing Span .....	45
4.2	Moment Ratio HS20 / Blanket Permit Vehicle for m2x Wing Span .....	45
4.3	Homberg Chart Tool and FEM Analysis Moments for m3x Wing Span .....	45
4.4	Moment Ratio HS20 / Blanket Permit Vehicle for m3x Wing Span .....	46
4.5	Homberg Chart Tool and FEM Analysis Moments for m3x Mid Span Fixed Edge .....	46
4.6	Moment Ratio HS20 / Blanket Permit Vehicle for m3x Mid Span Fixed Edge .....	46
4.7	Homberg Chart Tool and FEM Analysis Moments for m5x Mid Span Simply Supported .....	46
4.8	Moment Ratio HS20 / Blanket Permit Vehicle for m5x Mid Span Simply Supported .....	47
5.1	Digitized Data for $y = 0.4$ Grid Line, m3x Wing Span Homberg Chart .....	58

# CHAPTER 1

## Introduction

### 1.1 Background

For a prestressed concrete segmental box girder bridge, both design and load rating are determined by longitudinal and transverse analyses. A transverse analysis is performed for the top slab, typically by using Homberg charts (an engineer's design tool), to account for transverse bending effects due to truck wheel loads. Homberg charts are influence surfaces that are based on plate behavior and idealized support conditions; they are for specific slab geometry and tapering (variable slab thickness). Previous Florida Department of Transportation (FDOT) research showed that Homberg charts can give conservative values for transverse bending moments (Roddenberry and Kuhn, 2008). Furthermore, the presence of a barrier or barrier joints on the bridge can significantly affect the transverse analysis. Similarly, expansion joints could affect the distribution of transverse load effects.

The FDOT Office of Maintenance issues thousands of permits annually for heavy trucks. These trucks may have different axle weights and spacings than the trucks that are analyzed in the engineer's design or load rating, but yet they must be analyzed for their effects on transverse bending moments in the slab. However, it is impractical for the permit office to do a Homberg analysis for every permit application that involves crossing a segmental box girder bridge. Thus, they currently use a simplified method that involves calculating the equivalent effect of a single axle or tandem axle (4 feet apart), while neglecting the effects of any axle more than 8 feet away from the axle under consideration.

### 1.2 Objectives

The goal of this research is for the FDOT Office of Maintenance to be able to safely route permit vehicles by using existing load rating information and known bridge data such as cross-sectional dimensions. The main objective was to develop a method for the FDOT Office of Maintenance to analyze permit vehicles for transverse bending effects on the top slab of a prestressed concrete segmental box girder bridge. The other objective was to gain insight into the transverse behavior of a segmental bridge, by studying the differences between (1) analyses using Homberg charts, which are based on idealized plates and support conditions, and (2) analyses using finite element modeling on an existing box girder cross section.

Channel Five Bridge, located in the Florida Keys, was used as a representative prestressed concrete segmental box girder bridge and was modeled and analyzed extensively. Finite Element Modeling (FEM) was performed to study the bending moments due to several vehicles such as the AASHTO HS20 truck and FDOT Blanket Permit Vehicles. Blanket Permit Vehicles are those vehicles permitted to travel an unrestricted number of times on unrestricted routes within one calendar year. The effect of elements such as barriers, barrier joints, diaphragms, supports, and expansion joints was studied using FEM. The effect of axle load spacing on transverse bending moments was also studied to give insight into the Office of Maintenance's formerly-used "8-foot rule." Calculated bending moments from Homberg analysis and FEM were compared for a few Blanket Permit Vehicles.

Lastly, an Excel-based tool was developed for analyzing vehicles for their effect on transverse bending moments in a prestressed concrete segmental box girder bridge. This tool allows the user to analyze vehicle loads quickly and provides a simple way to compare effects of different vehicles. For example, the effects of vehicles that were analyzed in the designer's load rating could be compared to vehicles with axle weights and spacings that were not analyzed in the initial load rating.

# CHAPTER 2

## Finite Element Modeling

### 2.1 Introduction

Commercial software ANSYS was used to create the finite element models for this study. In order to identify the performance of candidate element types, preliminary analyses were conducted. The preliminary study was carried out by modeling an I-shaped beam, using shell or solid elements. Figure 2.1(a) shows the SHELL281 model, and Figure 2.1(b) shows the SOLID186 model.

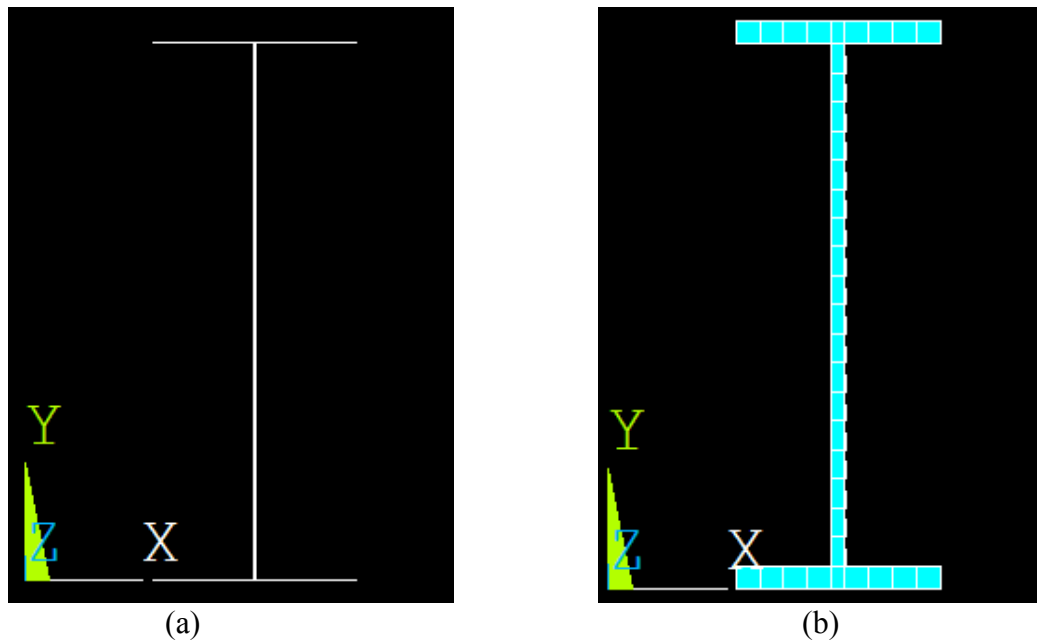


Figure 2.1: Sample I-shaped Beam for (a) SHELL281 Model and (b) SOLID186 Model

### 2.2 Element Choice

The beam model was first constructed by using SHELL281 elements, which are suitable for analyzing thin to moderately thick shell structures with linear, large rotations (ANSYS 2010). The SHELL281 element has eight (8) nodes with six (6) degrees of freedom (dof) at each node: three (3) translational degrees of freedom along x, y, and z axes and three (3) rotational degrees of freedom about x, y, and z axes. The load applied to the structure passes from one element to another through the eight (8) peripheral nodes. The thickness of the structural element is modeled mathematically. Because the number of nodes along the thickness direction is only one, the thickness is entered into the program as a parameter rather than being computed from the geometry. A sample SHELL281 element is shown in Figure 2.2.

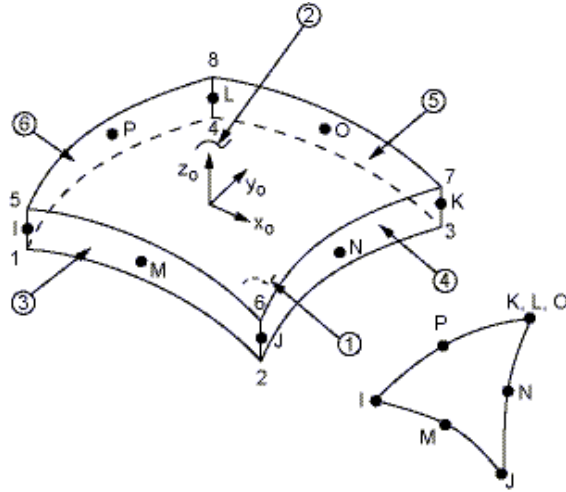


Figure 2.2: SHELL281 Element Geometry (ANSYS 2010)

The beam was next modeled in ANSYS by using SOLID186 elements, which are higher order elements, used for three-dimensional (3-D) modeling. The SOLID186 element has 20 nodes, and each node has three (3) translational degrees of freedom (along x, y, and z axes). The load applied to the structure passes through the nodes of the adjacent elements. The element is suitable for cases where plasticity, stress stiffening, creep, and large deflections are anticipated under the action of load (ANSYS 2010), but it also can be used to solve less complex 3-D problems. A sample SOLID186 element is shown in Figure 2.3.

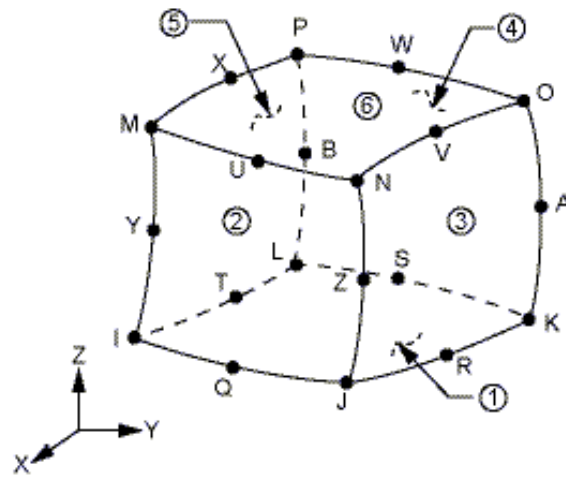


Figure 2.3: SOLID186 Element Geometry (ANSYS 2010)

### 2.3 Simple Beam Analysis

The simple beam analysis was carried out as a preliminary analysis for two reasons: 1) to study the mesh size and its sensitivity towards the final results and 2) to study the difference in the

performance between SHELL281 and SOLID186 elements for modeling the bridge structure. The beam models with SHELL281 and with SOLID186 elements are shown in Figures 2.4 and 2.5, respectively.

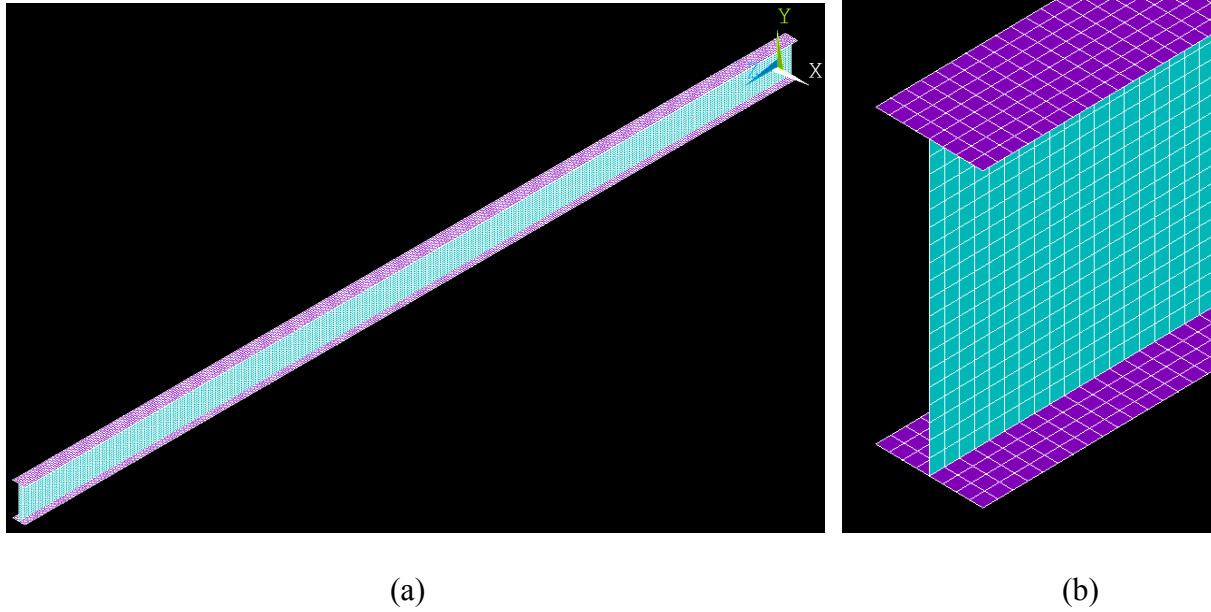


Figure 2.4: Beam Model with SHELL281 Elements: (a) Complete Beam (b) Enlarged Section

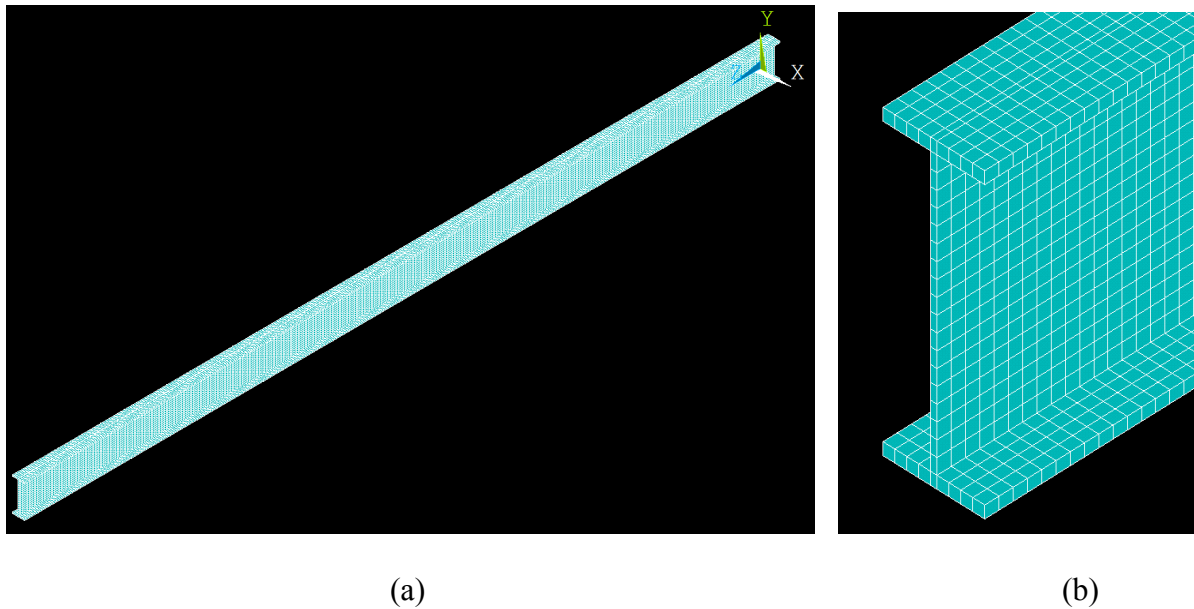


Figure 2.5: Beam Model with SOLID186 Elements: (a) Complete Beam (b) Enlarged Section

The modeled beam had 16-inch-wide top and bottom flanges, had a 44-inch-tall web, and was 1000 inches long. The material was modeled as linear and isotropic with a modulus of elasticity of 29,000,000 psi and a Poisson's ratio of 0.3. The beam was supported with a hinge at one end and a roller at the other end. A pressure load of 1.25 psi was applied on the top flange. The exaggerated deflected shape of the beam modeled with SOLID186 elements is shown in Figure 2.6.

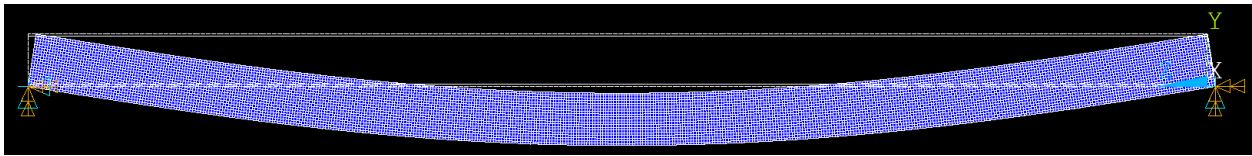


Figure 2.6: Deflected Shape of Beam under Pressure Load (Deflection Exaggerated)

#### 2.4 Results: SHELL281 Element vs. SOLID186 Element

After the modeling, an analysis was carried out in order to study the mesh size sensitivity and the difference between the SHELL281 element and the SOLID186 element. The comparative assessment was done based on three parameters: deflection, normal stress, and shear stress.

The mesh size sensitivity was carried out with decreasing mesh size: 8, 4.25, 3, and 2.25 inches. The number of degrees of freedom (DOFs) was calculated by multiplying the number of nodes by the DOFs per node corresponding to the element type, i.e., for SOLID186 element type, the number of elements was multiplied by 3, and for SHELL281 element type, by 6. The result was compared with a manual (analytical) solution. A sample result for deflection from SHELL281, SOLID186 and manual solutions is shown in Figure 2.7. The percentage variation of deflection for SHELL281 and SOLID186 solutions with respect to the manual solution is shown in Figure 2.8, which illustrates that decreasing the mesh size affected the results up to a certain point, and decreasing the mesh size below that certain limit had no effect on the final outcome. The study was carried out for normal stress and shear stress by taking readings at locations shown in Figure 2.9. The percentage variation in normal stress at locations 2 and 3 is shown in Figures 2.10 and 2.11, respectively. The variation in shear stress for locations 1 and 2 is shown in Figures 2.12 and 2.13, respectively.

The manual (analytical) solution in this section used the Euler-Bernoulli beam theory because shear deformation is negligible for a long beam. For a simple beam with a symmetric cross section such as the beam analyzed here, theoretical equations provide exact answers and are often used as the reference to check the performance of the FE analysis (Reddy, 1997). After deciding the type of element and mesh density, the FE analysis then can be used for a similar problem, but one that does not have theoretical solutions. The reason that the FE solution has error is because it is an approximate solution of theoretical equations. The theoretical equations have infinite DOFs, whereas the FE approach has finite DOFs (hence the name begins with “finite”). The FE solution is influenced by, for example, the number of DOFs, formulation of the element, and the integration rule.

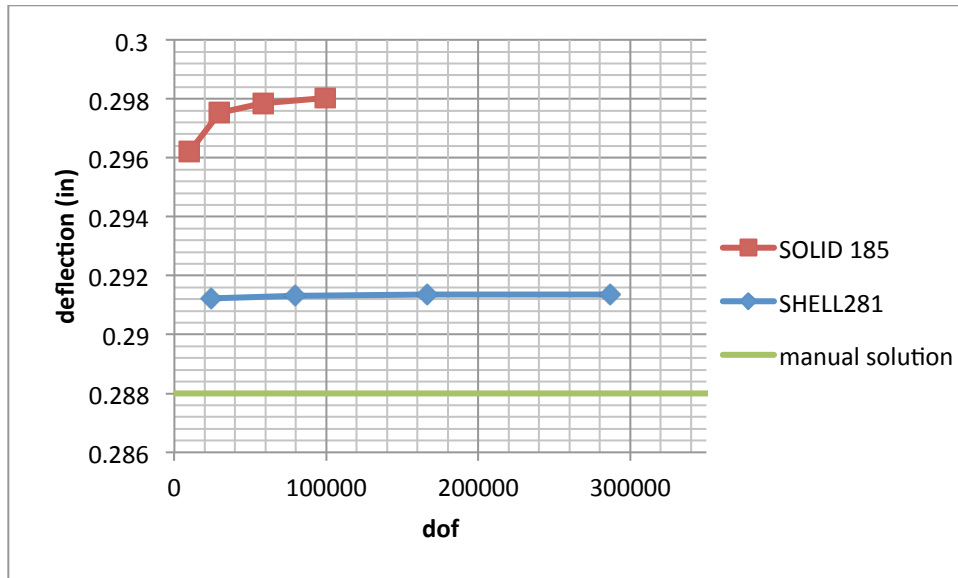


Figure 2.7: Comparison of SHELL281, SOLID186 and Manual (Analytical) Solutions

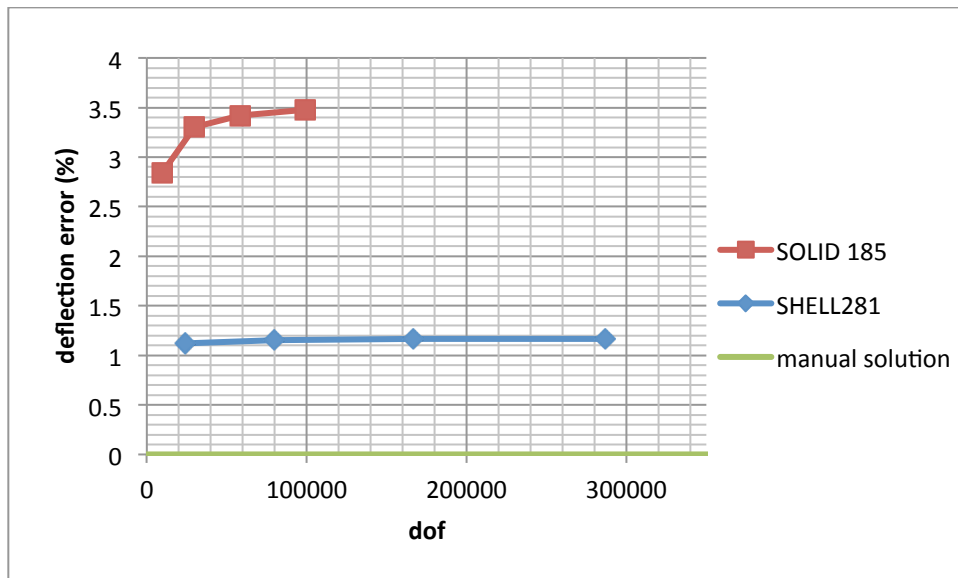


Figure 2.8: Percentage Variation in Deflection vs. Degrees of Freedom for SHELL281, SOLID186 and Manual (Analytical) Solutions

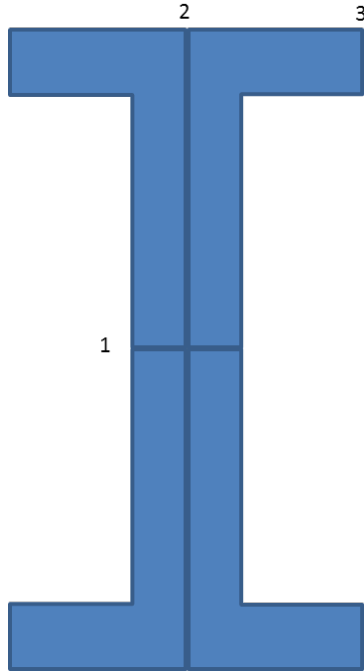


Figure 2.9: Cross Section of I-shaped Beam Showing the Reading Locations

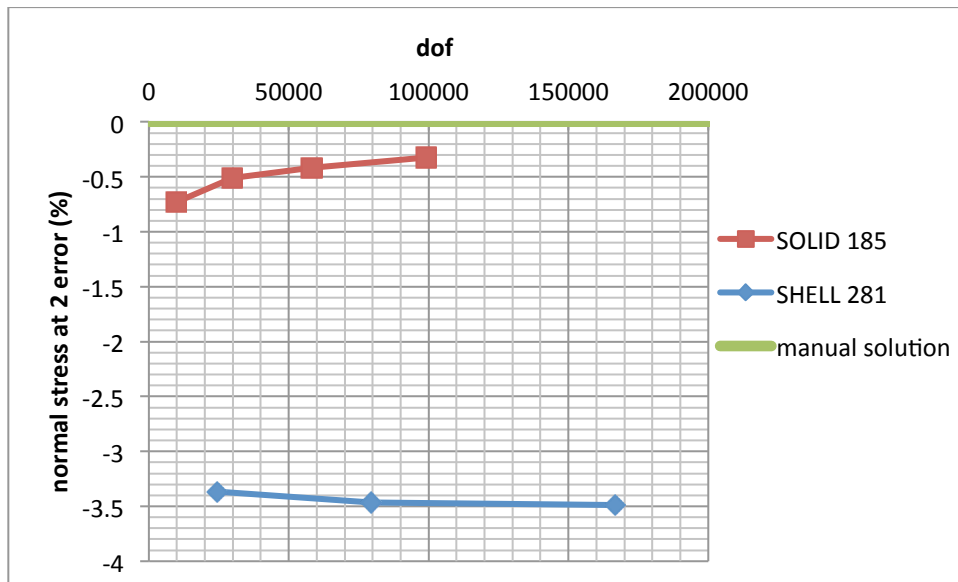


Figure 2.10: Normal Stress at Location 2 with Increasing Degrees of Freedom

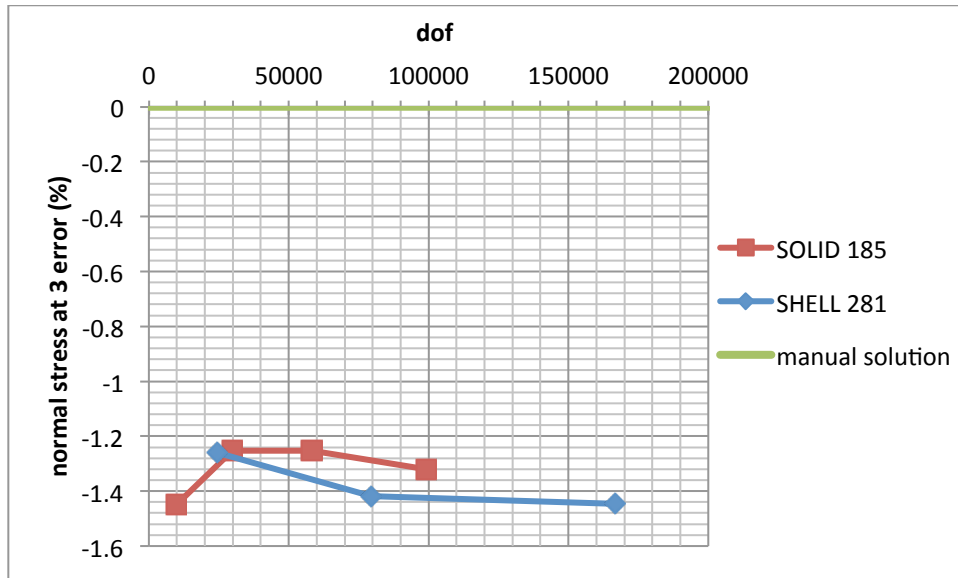


Figure 2.11: Normal Stress at Location 3 with Increasing Degrees of Freedom

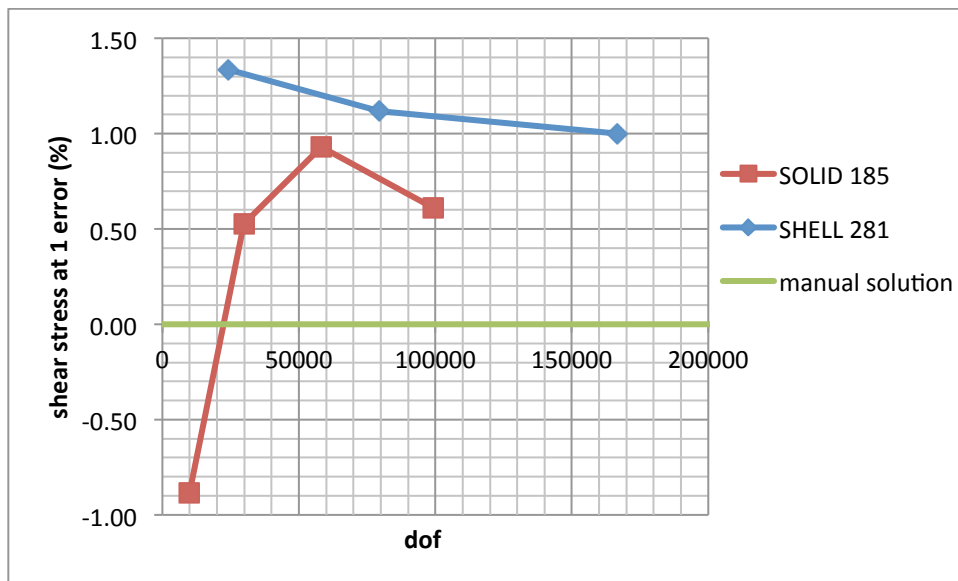


Figure 2.12: Shear Stress at Location 1 with Increasing Degrees of Freedom

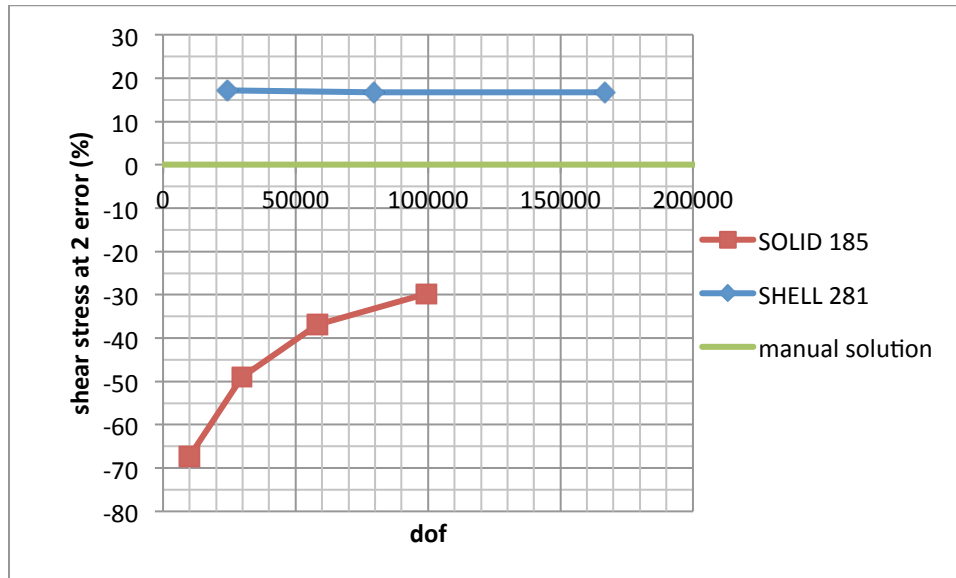


Figure 2.13: Shear Stress at Location 2 with Increasing Degrees of Freedom

The results from the preliminary analysis are as follows (for the smallest mesh size):

- Compared to the analytical solution, the error in deflection was 3.5% for the solid element and 1.2% for the shell element.
- The error in normal stress was up to 1.3% for the solid element and up to 3.5% for the shell element.
- The error in shear stress, where the maximum shear stress occurs, was 0.6% for the solid element and 1.0% for the shell element.
- At the junction of the web and the flange, the error in shear stress was very high for both elements. The solid element had 30% error and the shell element had 17% error compared to the analytical solution. However, the “error” may not be the true error as the accuracy of the analytical solution at this location is not very good.

Based on the results of this preliminary analysis, solid elements were then used to model the bridge. This decision was based on two reasons. First, they provide better accuracy for the normal stress, which would later be used to calculate the moment in the transverse direction, which was the main focus of this research. Second, they enable a more accurate representation of the geometry of a bridge with a box girder cross section, in which the variation in thickness is continuous and some parts (e.g., web-to-flange transition) cannot be accurately described using shell elements. The solid element type will be a better choice as long as the bridge is primarily under bending and is not a deep beam, which were the conditions of the analysis in this section.

Since the I-beam shape and the box girder shape resist bending similarly, the solid element type is a better choice for the box girder shape also.

Although the shear stress in the web-to-flange transition zone was quite different from the analytical solution, further analysis was not conducted. The shear stress would not be needed in this research, so further investigations on shear stress were not necessary. (Although, FDOT sometimes uses shear stresses from load ratings to evaluate torsional effects of permit vehicles.) As noted earlier, the large difference may simply be due to the inaccuracy of the analytical solution as noted earlier.

One disadvantage of using the solid element is its inconvenience in obtaining the moment. Unlike the shell element that directly provides the moment, the solid element due to its formulation does not do so. However, this is not a limitation, but rather an inconvenience, because the moment can be easily calculated. The calculation of the moment will be explained in a later section.

Finally, the preliminary analysis provided the number of elements to use (per the dimension of the flange and the web) in order to achieve convergence in accuracy. The information was used in subsequent modeling.

# CHAPTER 3

## Analyses of Channel Five Bridge

### 3.1 Finite Element Modeling

The Channel Five Bridge – a precast, prestressed concrete segmental box girder bridge in Florida – was studied using finite element models (FEM). The bridge was modeled with commercial software ANSYS and based on the available drawings and details.

The Channel Five Bridge has 17 spans at 135 feet in length and one (1) span at 99 feet 5.5 inches. Each segment is 38 feet 4.5 inches wide and 84 inches tall. The barriers are 2 feet 9.5 inches high. The cross section of the bridge girder is shown in Figure 3.1. SOLID186 elements, as discussed in the previous chapter, were used to model the bridge.

The FEM results presented herein are also applicable to Niles Channel Bridge and Long Key Bridge, which have the same cross section as Channel Five Bridge and therefore exhibit the same transverse behavior. These three bridges are located on US Highway 1 in the Florida Keys and carry two (2) lanes of traffic. Because they are prestressed both transversely in the top slab and longitudinally, it is assumed that the concrete material behaves as linear elastic and that the cross section is uncracked. Also in the Florida Keys, Seven Mile Bridge has the same cross section; however, its top slab is reinforced with mild steel and is not prestressed, so the assumption that the section is uncracked should not be made, and therefore the FEM results do not apply.

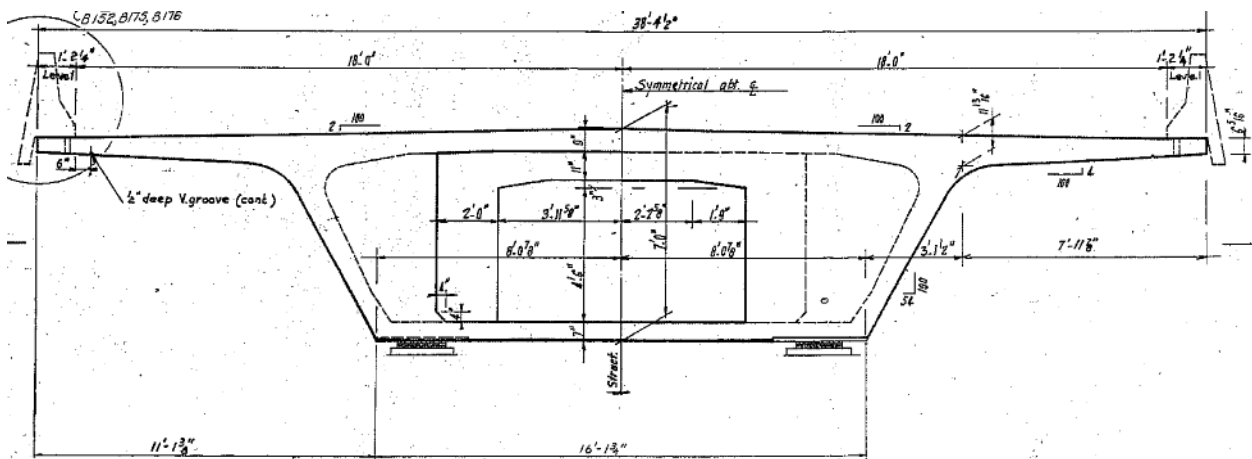


Figure 3.1: Channel Five Bridge Cross Section

The bridge section shown in Figure 3.1 was simplified for the finite element (FE) analyses. As for simplification, the smooth curves at the junctions of different parts of the bridge were replaced by straight lines joining at one point. The span was modeled as simply supported at one end and roller supported at the other end, with the supports placed under the bottom slab where the bearings are located (Figure 3.1). The internal diaphragms and other components such as

small ducts were not modeled. The simplified FE model of the bridge is shown in Figure 3.2. Because the focus was to be on the top slab moment and stresses, the top slab of the bridge was modeled with a fine mesh size. The webs and the bottom slab were modeled with a comparatively large mesh size. This decision was made to achieve computational efficiency and accelerated computational speed.

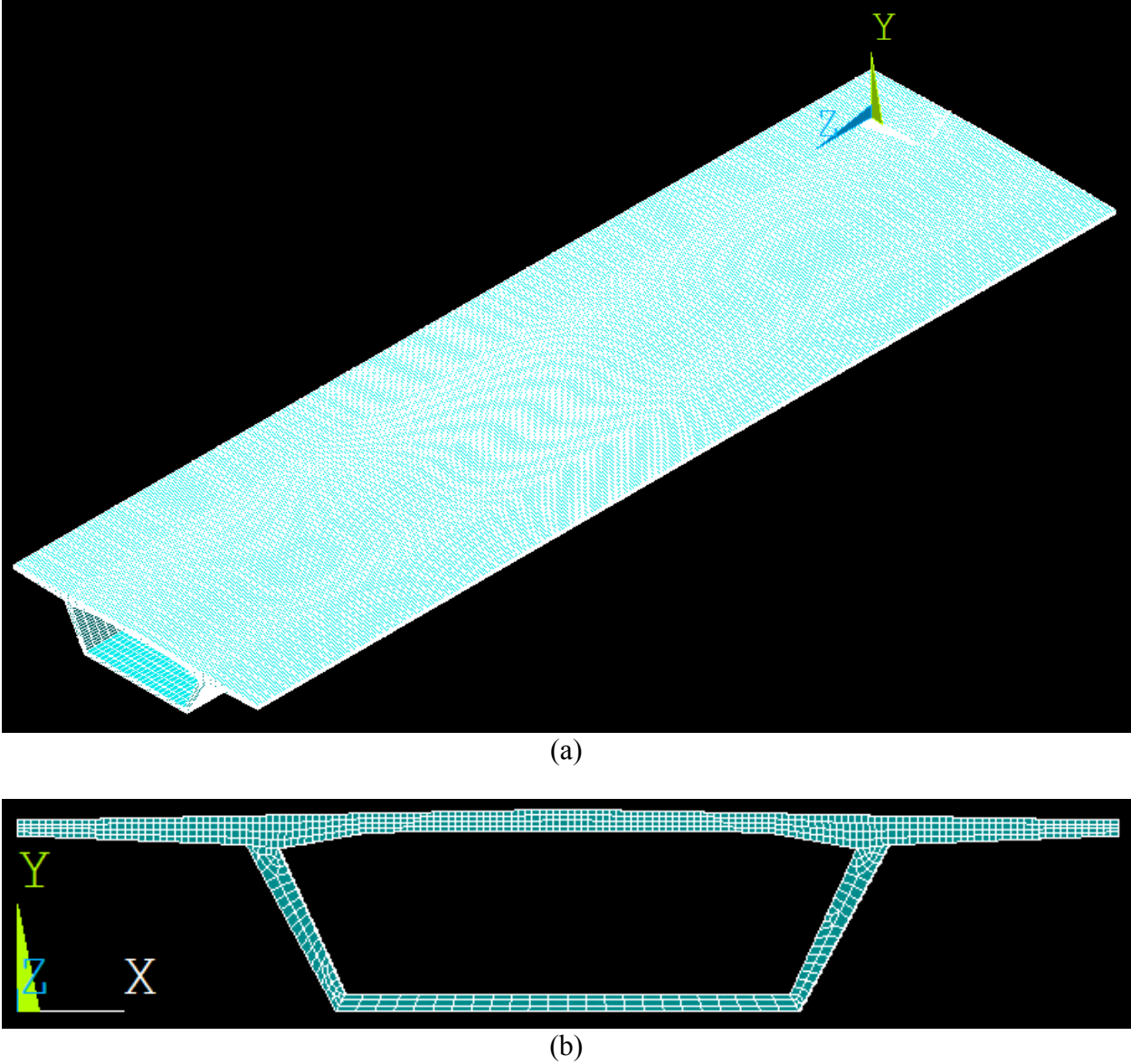


Figure 3.2: FE Bridge Model: (a) Oblique View (b) Sectional View

### 3.2 Analysis for Various Loading Cases and Barrier Models

The FE bridge model was analyzed for various load locations and barrier conditions. The analyses were compared for deflection and normal stress at different locations as shown in Figure 3.3. Although all stress components were checked to validate the analyses, the primary

focus will be given to the results relevant to the transverse direction, while also showing longitudinal results whenever necessary. The 1-kip concentrated load was always placed 30 inches away from the edge of the wing slab (tip of cantilever). The readings were taken at four (4) locations shown in Figure 3.3(a) and were taken at top, middle, and bottom surfaces at each location.

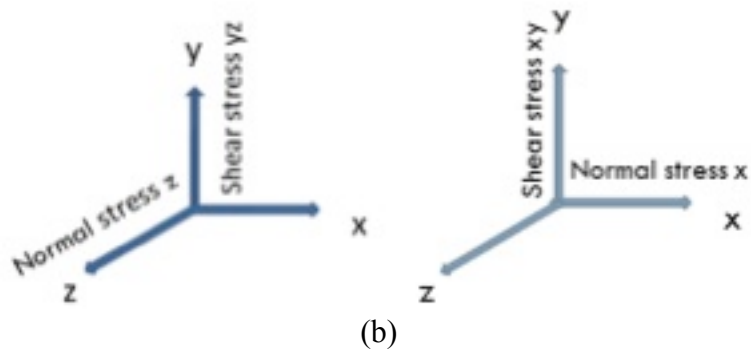
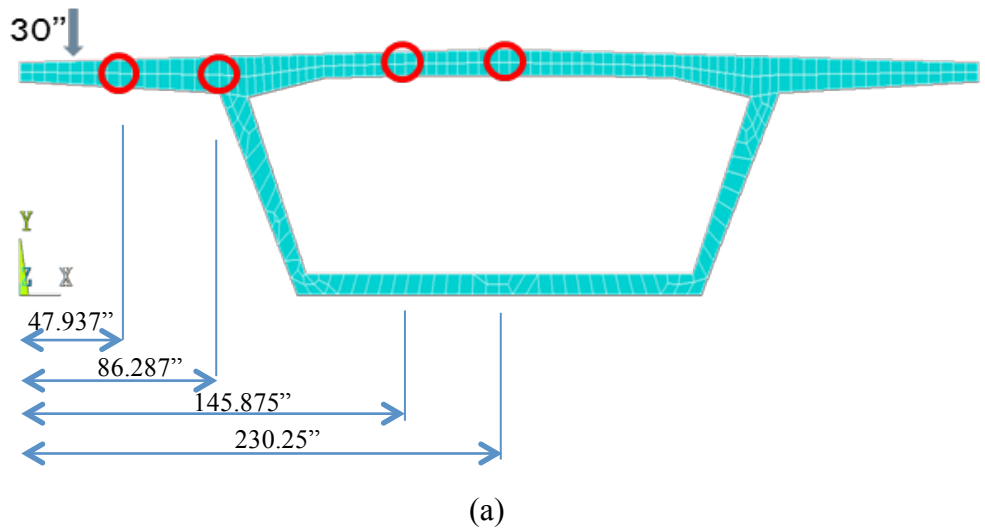


Figure 3.3: FE Bridge Model (a) Reading Locations (b) Global Cartesian Axis

### 3.2.1 Effect of Span Support

In case A1, the load was placed on the bridge with the simply-supported boundary condition. In case A2, an additional support was placed at the mid length of the span. Both loading conditions are schematically shown in Figure 3.4.

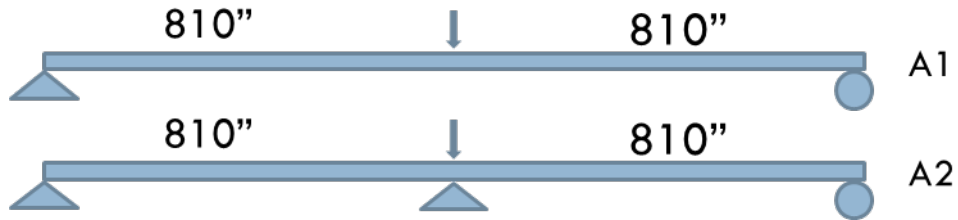


Figure 3.4: Loading Conditions for Cases A1 and A2

The deflections at four (4) locations in Figure 3.3 are shown in Figure 3.5. The locations near the load position had a higher deflection. Case A2, where the additional support was provided, exhibited less deflection than case A1.

The normal stress in the x direction (Figure 3.3(b)) at four (4) locations (Figure 3.3(a)) for case A1 and case A2 is shown in Figure 3.6. The results show that placing the load near a support (case A2) causes a larger normal stress in the x direction in the deck between the webs than when the load is placed at mid span (case A1).

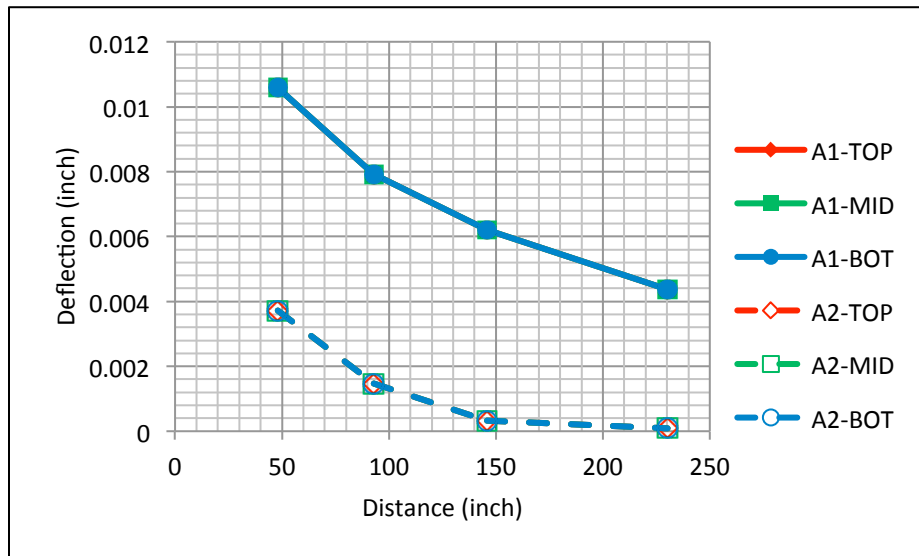


Figure 3.5: Deflection for Cases A1 and A2

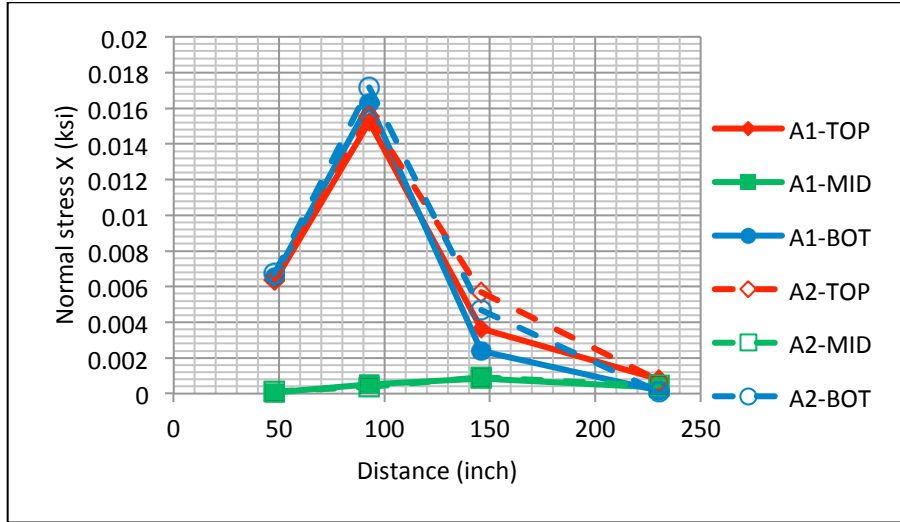


Figure 3.6: Normal Stress X Direction for Cases A1 and A2

### 3.2.2 Effect of Expansion Joint at End of Span

The next analyses were carried out by placing the load at 12 inches away from the support. This condition depicts the situation when the vehicle enters the span of the bridge (case A3-A). Transversely, the load was again at 30 inches from the edge of the wing. A schematic representation of the compared loading conditions is shown in Figure 3.7. The deflections at the four (4) locations for the two (2) loading conditions are shown in Figure 3.8. The respective normal stresses in the z and x directions are shown in Figures 3.9 and 3.10, respectively.

The exaggerated deflected shape of the bridge deck for case A3-A where the load was placed at 12 inches away from the support is shown in Figure 3.11.

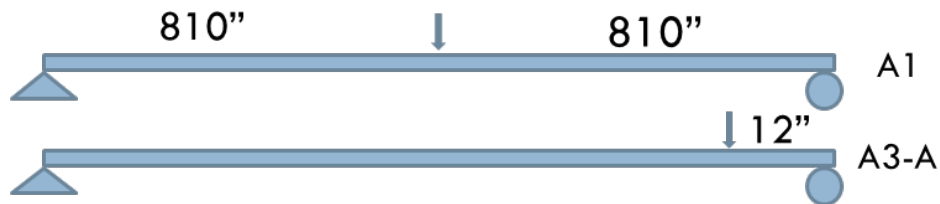


Figure 3.7: Loading Conditions for Cases A1 and A3-A

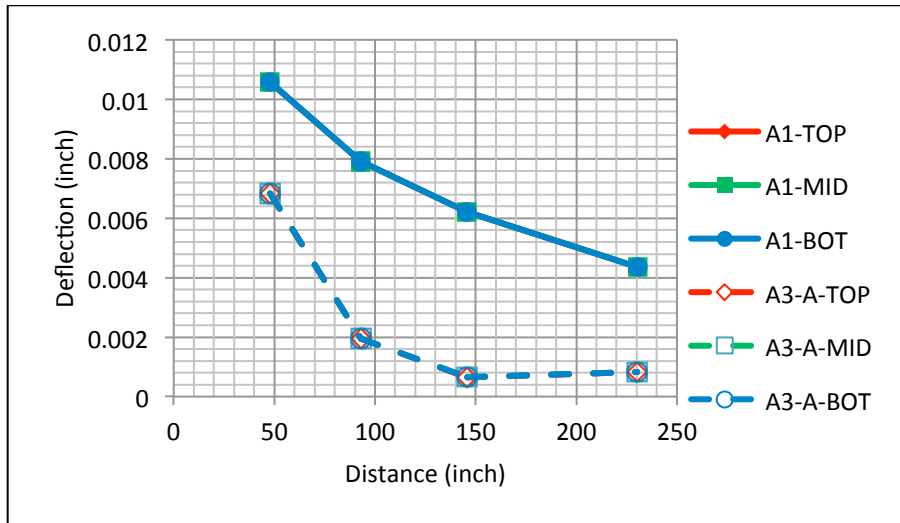


Figure 3.8: Comparison of Deflections for Cases A1 and A3-A

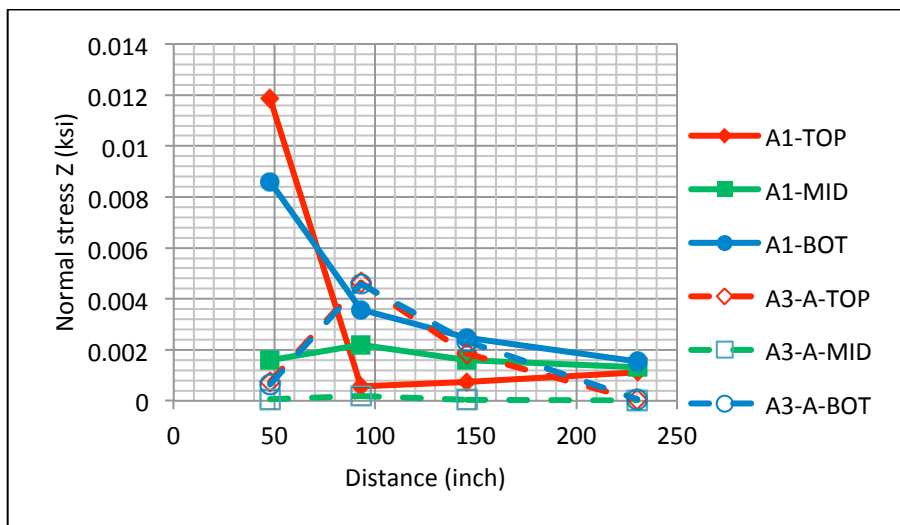


Figure 3.9: Comparison of Normal Stress Z Direction for Cases A1 and A3-A

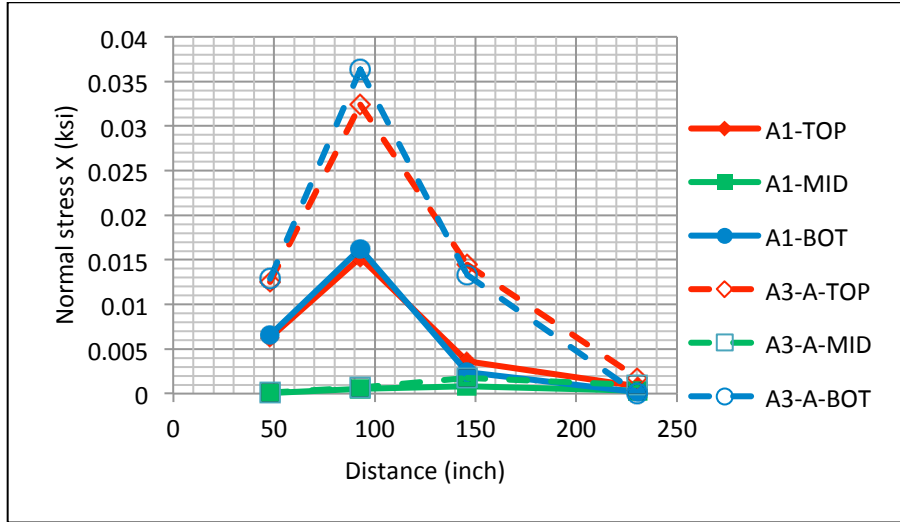


Figure 3.10: Comparison of Normal Stress X Direction for Cases A1 and A3-A

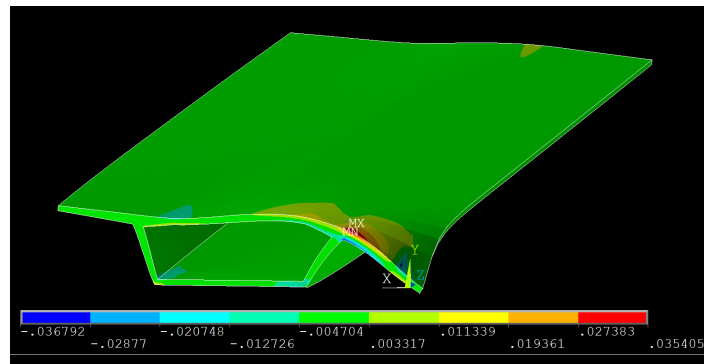


Figure 3.11: Exaggerated Deflected Shape for Case A3-A

### 3.2.3 Effect of Expansion Joint as Load Moves Away from End of Span

The next study was performed to compare the effect of loading as it moves away from the support. Load case A3-A, explained earlier, was compared to case A3-B, in which the load was applied at 48 inches away from the support. The 48-inch distance was chosen because it is the minimum spacing of truck axles and because it lies in the region where an expansion joint segment diaphragm would typically be located. The schematic representation of the loading is shown in Figure 3.12. The displacements at four (4) locations are plotted in Figure 3.13, the corresponding normal stress in the z direction is shown in Figure 3.14, and the normal stress in the x direction is shown in Figure 3.15.



Figure 3.12: Loading Condition for Cases A3-A and A3-B

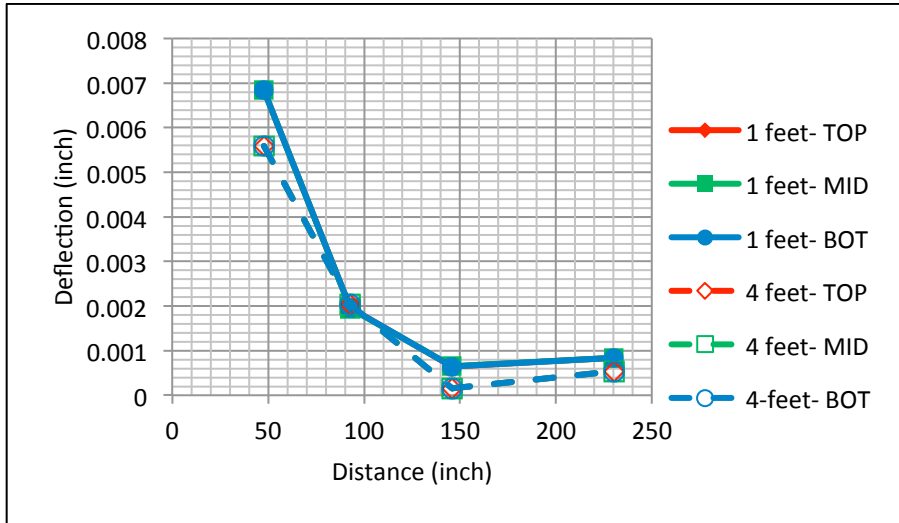


Figure 3.13: Comparison of Deflection for Cases A3-A and A3-B

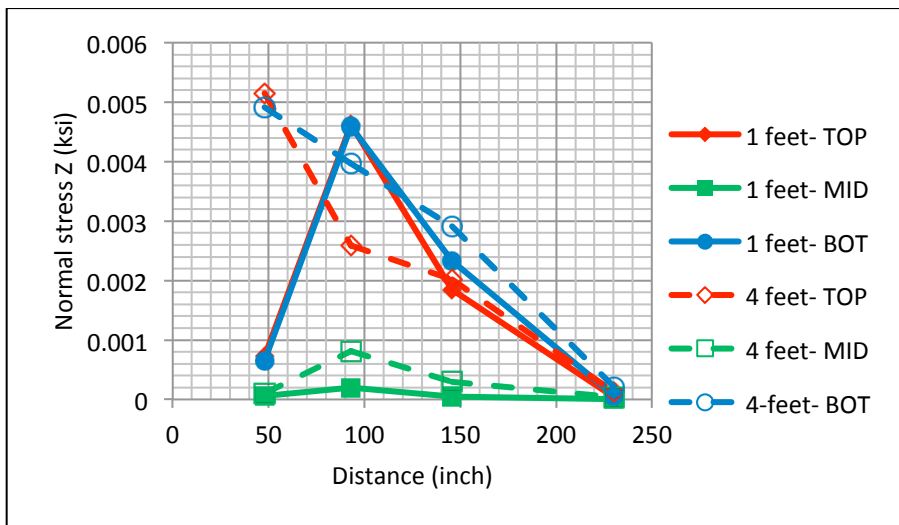


Figure 3.14: Comparison of Normal Stress in Z Direction for Cases A3-A and A3-B

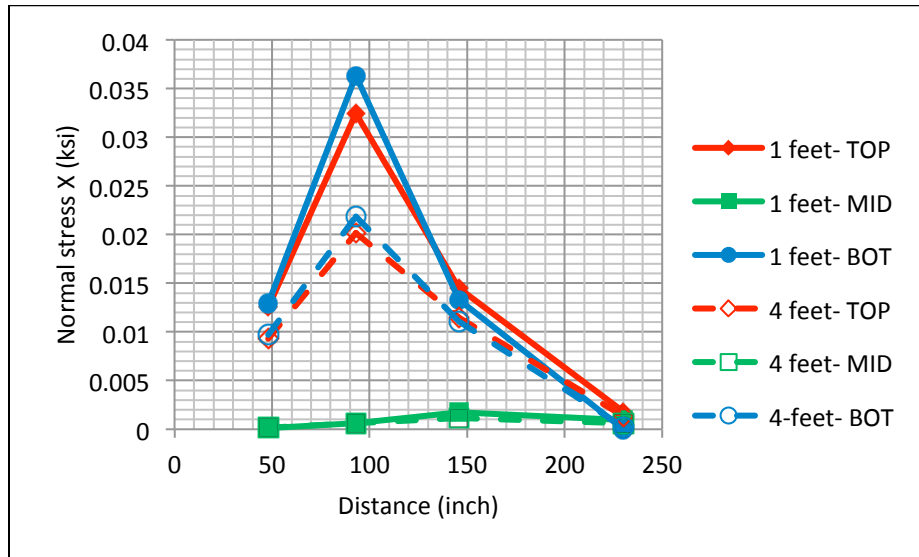


Figure 3.15: Comparison of Normal Stress in X Direction for Cases A3-A and A3-B

### 3.2.4 Effect of Barrier

The effect of the barriers was studied next. The load placed was at 30 inches from the tip of the wing in all the related models.

The first study was performed on a model with a continuous barrier on the entire length of the bridge (case B1). The results were compared with case A1, which was without a barrier. A schematic representation of the loading is shown in Figure 3.16. The deflection is shown in Figure 3.17. The variation of normal stress in the z direction is compared and shown in Figure 3.18, and the variation of normal stress in the x direction is compared and shown in Figure 3.19.

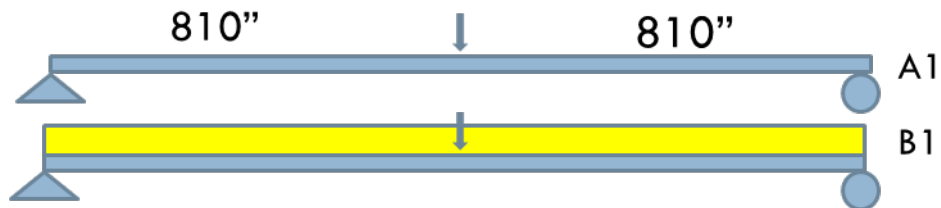


Figure 3.16: Loading Condition for Cases A1 and B1

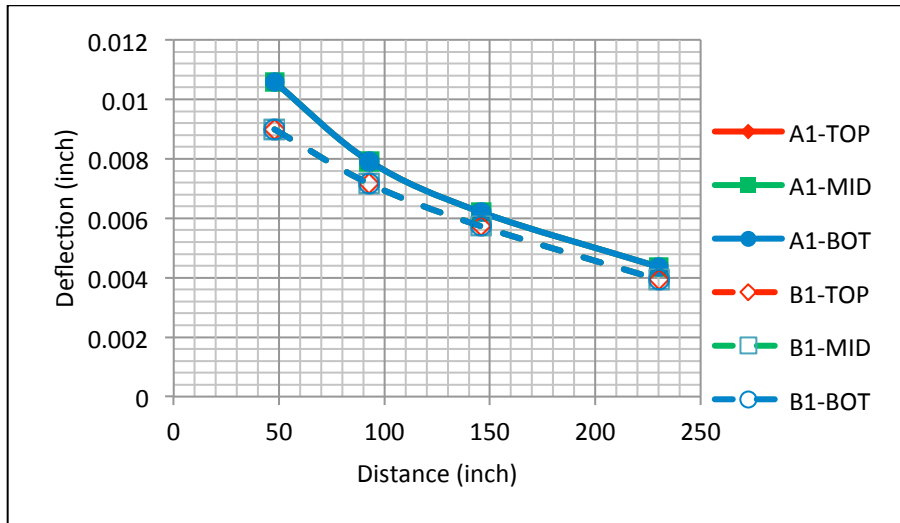


Figure 3.17: Comparison of Deflection for Cases A1 and B1

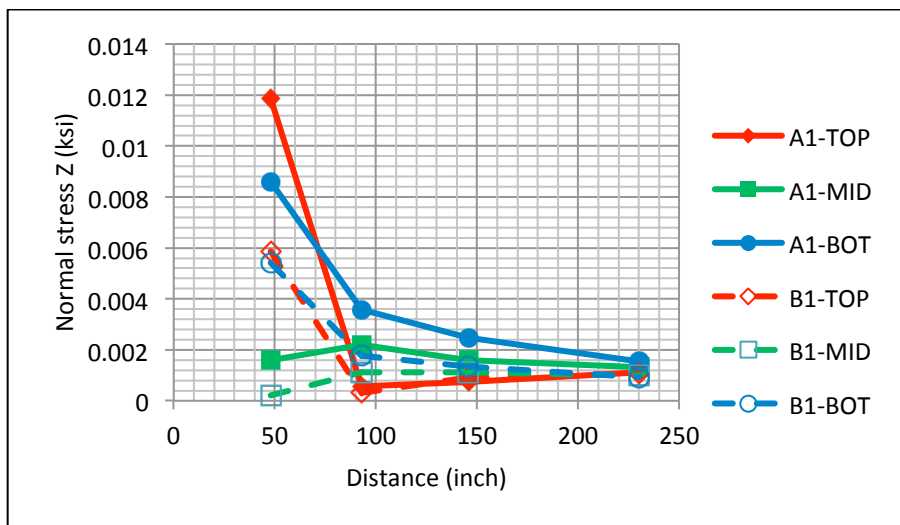


Figure 3.18: Comparison of Normal Stress in Z Direction for Cases A1 and B1

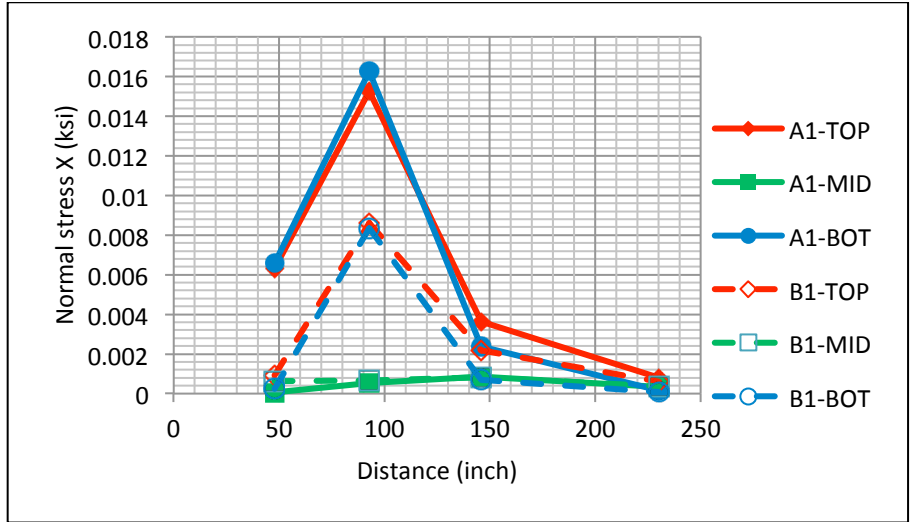


Figure 3.19: Comparison of Normal Stress in X Direction for Cases A1 and B1

### 3.2.5 Effect of Barrier Joint

Barriers are often constructed with an open joint in them, sometimes placed at mid span. This discontinuity affects the longitudinal and transverse stresses. In the next FEM study, the stresses and deflections for the continuous barrier condition (case B1) were compared to the discontinuous barrier condition (case B2). The load was applied at 30 inches away from the edge of the wing slab and at mid length of the span. A schematic representation of the loading condition and barrier cases is shown in Figure 3.20.

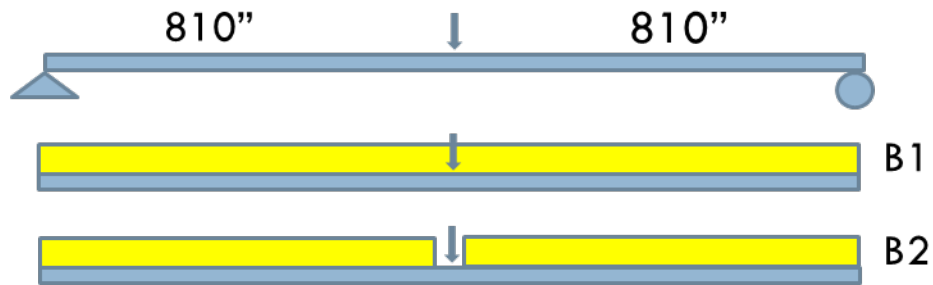


Figure 3.20: Loading Condition for Cases B1 and B2

The deflections for cases B1 and B2 are compared in Figure 3.21. The normal stress in the z direction is shown in Figure 3.22, and the normal stress in the x direction is shown in Figure 3.23.

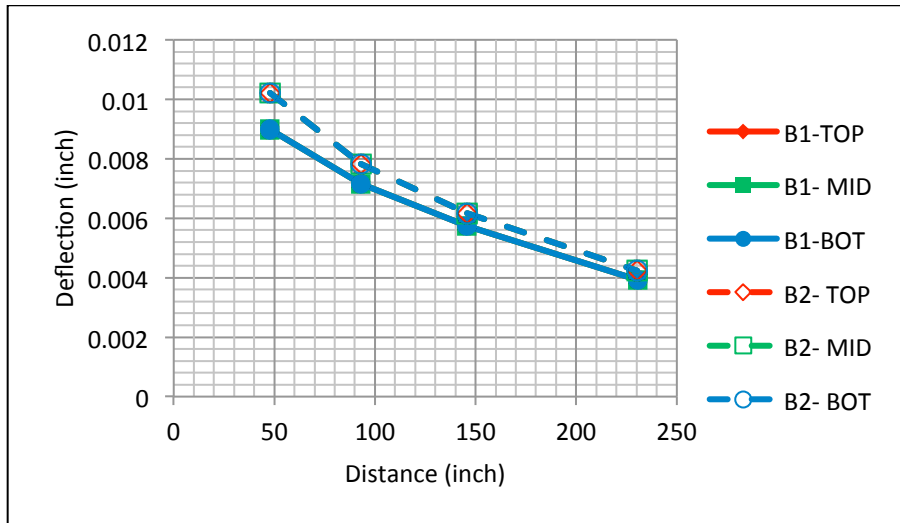


Figure 3.21: Comparison of Deflection for Cases B1 and B2

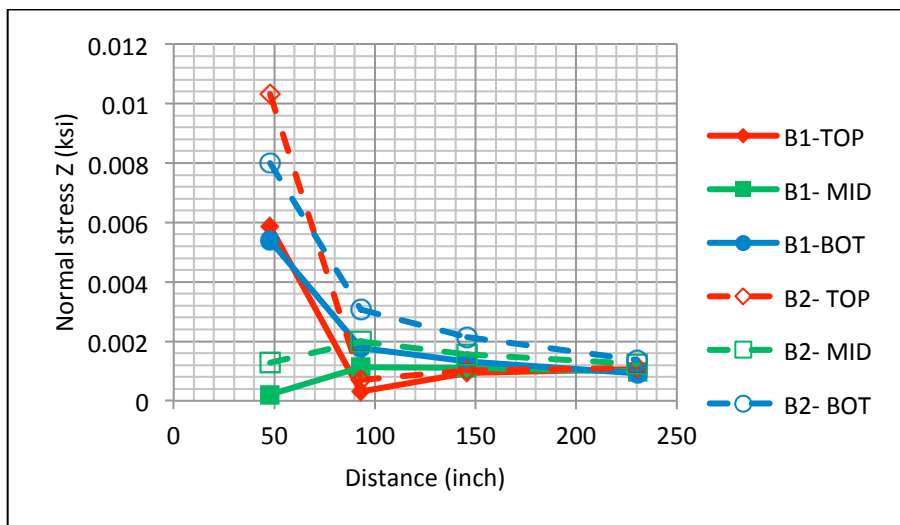


Figure 3.22: Comparison of Normal Stress in Z Direction for Cases B1 and B2

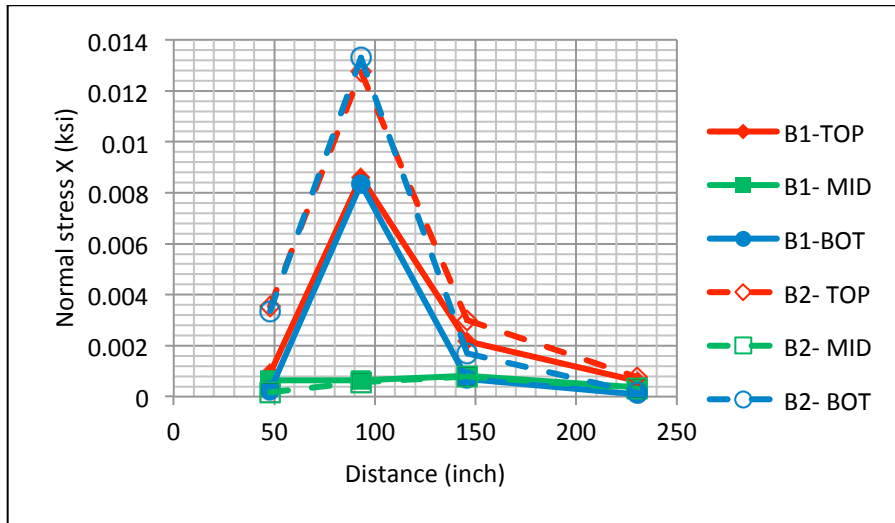


Figure 3.23: Comparison of Normal Stress in X Direction for Cases B1 and B2

### 3.2.6 Effect of Diaphragm at the End Support

Precast, prestressed concrete, segmental box girder bridges have internal diaphragms at the supports in which to anchor prestressing tendons. The effect on transverse moments due to having a diaphragm at the support was studied next. The FE model was modified so that the internal void of the cross section was filled with concrete, using SOLID186 elements, for a length of 3.5 feet over the region at the span's end support (case CB). The load was applied at 30 inches from the edge of the wing slab and placed along the length at various locations as shown in Figures 3.24 and 3.25. The top stress variation in the x direction is shown in Figure 3.26.

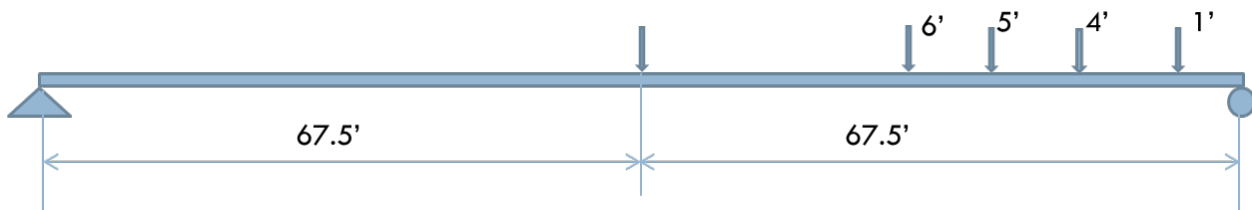


Figure 3.24: Load Positions with No Diaphragm Modeled at Support

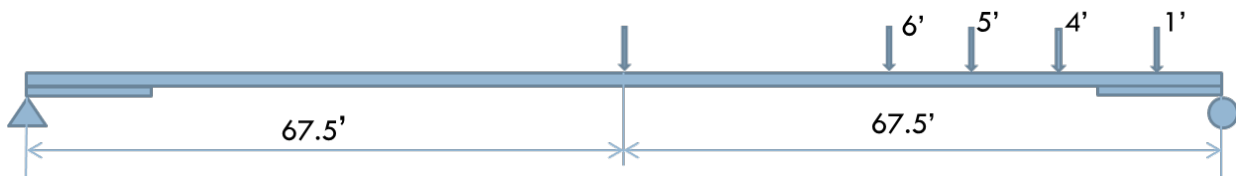
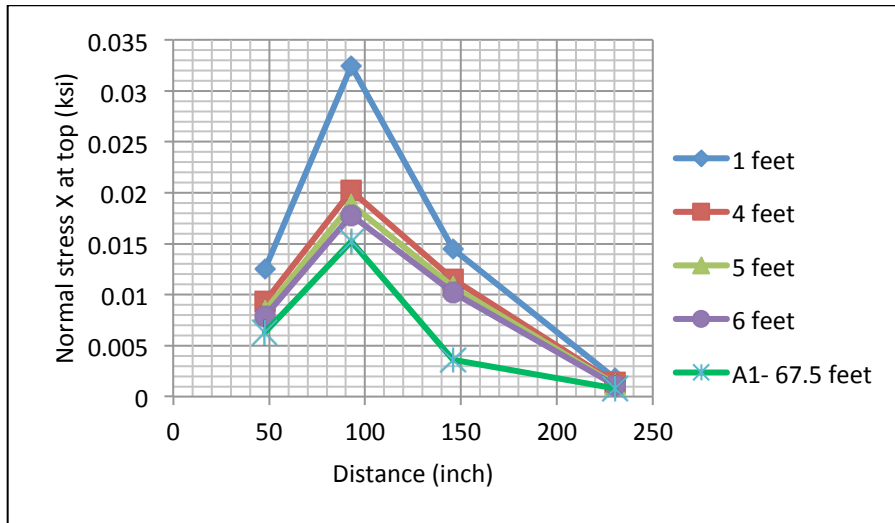
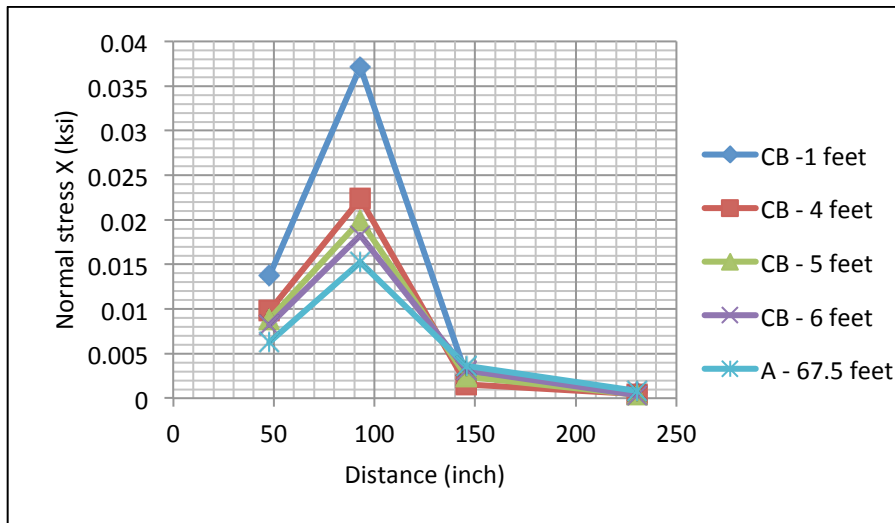


Figure 3.25: Load Positions with Diaphragm Modeled at Support



(a)



(b)

Figure 3.26: Variation of Top Stresses: (a) No Diaphragm at Support (b) Diaphragm at Support

### 3.3 Verification of the 8-foot Rule

To evaluate a segmental box girder bridge for transverse effects due to a permit vehicle, FDOT formerly used an in-house “8-foot rule”, in which all axles within an 8-foot range (longitudinally) are considered when calculating transverse moments using Homberg charts. The effect of load from axles beyond the 8 feet is considered to be negligible. This “rule” was studied using FE models, and this section summarizes these analysis results. The ANSYS model of the Channel Five Bridge created earlier was used. The 1-kip load was applied to the bridge at 30 inches from the edge of the wing slab (Figure 3.27). Longitudinally along the top slab, the load was applied at 2-foot intervals in the z direction, from the mid span to 16 feet away (Figure 3.28).

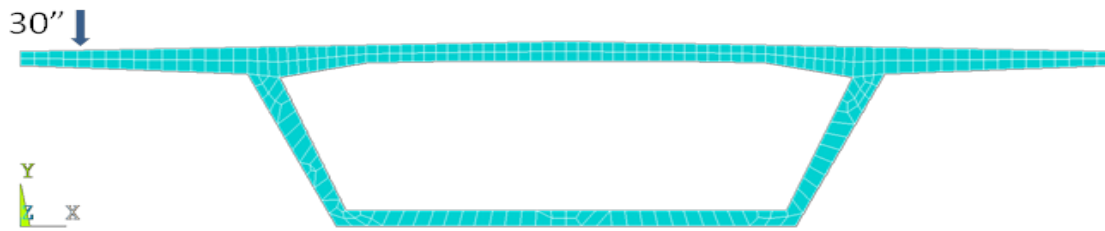


Figure 3.27: Load Positions on Wing 30 Inches from Edge of Wing Slab

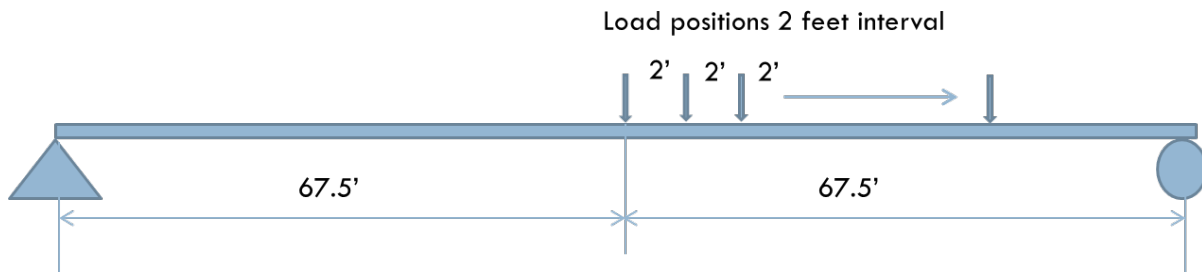


Figure 3.28: Load Positions at 2-foot Intervals up to 16 Feet from Mid Span (Not to Scale)

The normal stress in the x direction was read at ten (10) different locations across the width of the bridge deck (Figure 3.29) and at the top, middle, and bottom at each location. These stresses are plotted in Figures 3.30, 3.31, and 3.32. The results labeled “810 inches” correspond to the cases where load was applied at the mid span. Likewise, the result labeled “786 inches” corresponds to the loading applied at  $810 - 786 = 24$  inches away from the mid span in the z direction. Note that the results from the mid span loading case contain a singular point at  $x = 29.96$  inches (i.e., the data point is off the chart and causes a spike in the plot). This is due to the stress being read immediately under the loading point, and so it is understandably large.

The variation of normal stress in the x direction was also compared to the stresses calculated from moments obtained from a Homberg chart. Homberg charts will be discussed in more detail in the next chapter. The normal stresses at the top and bottom surfaces are shown in Figure 3.33 and 3.34, respectively.

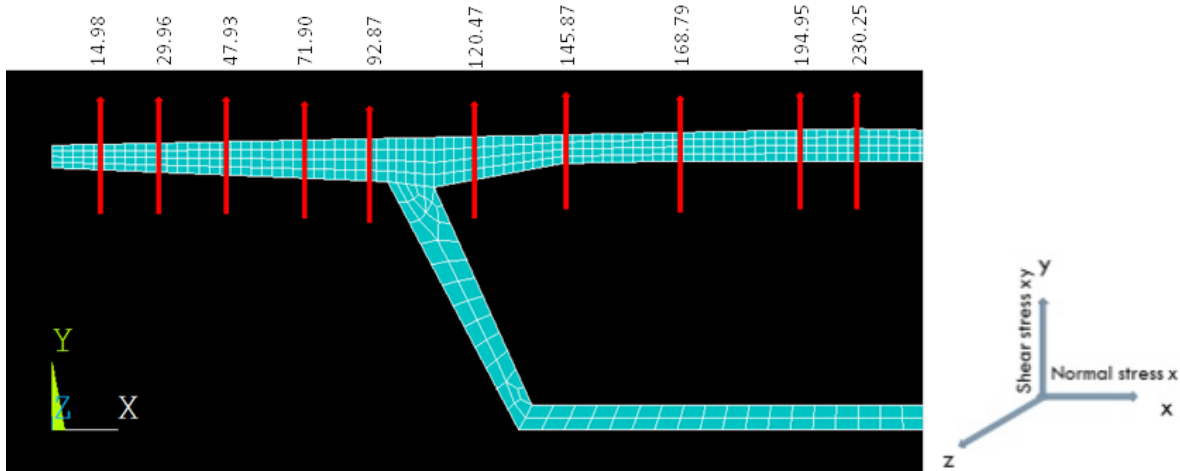


Figure 3.29: Reading Locations across the Width of Bridge, in Inches

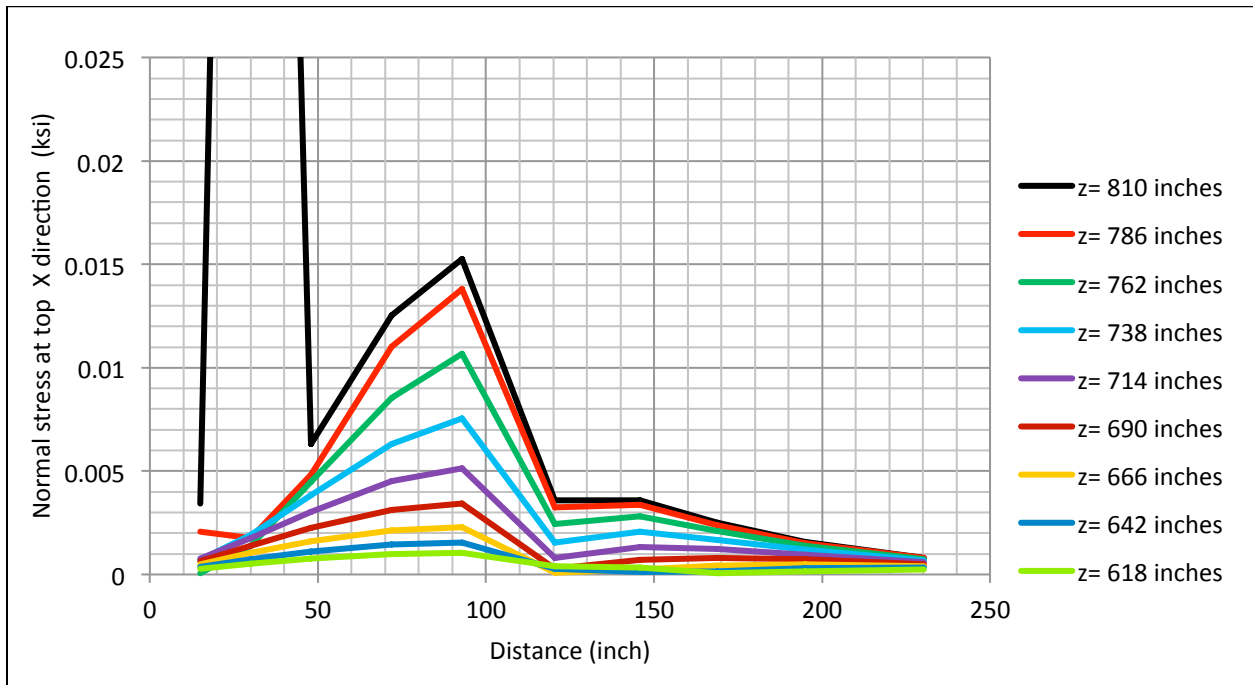


Figure 3.30: Normal Stress X Direction at Top Surface

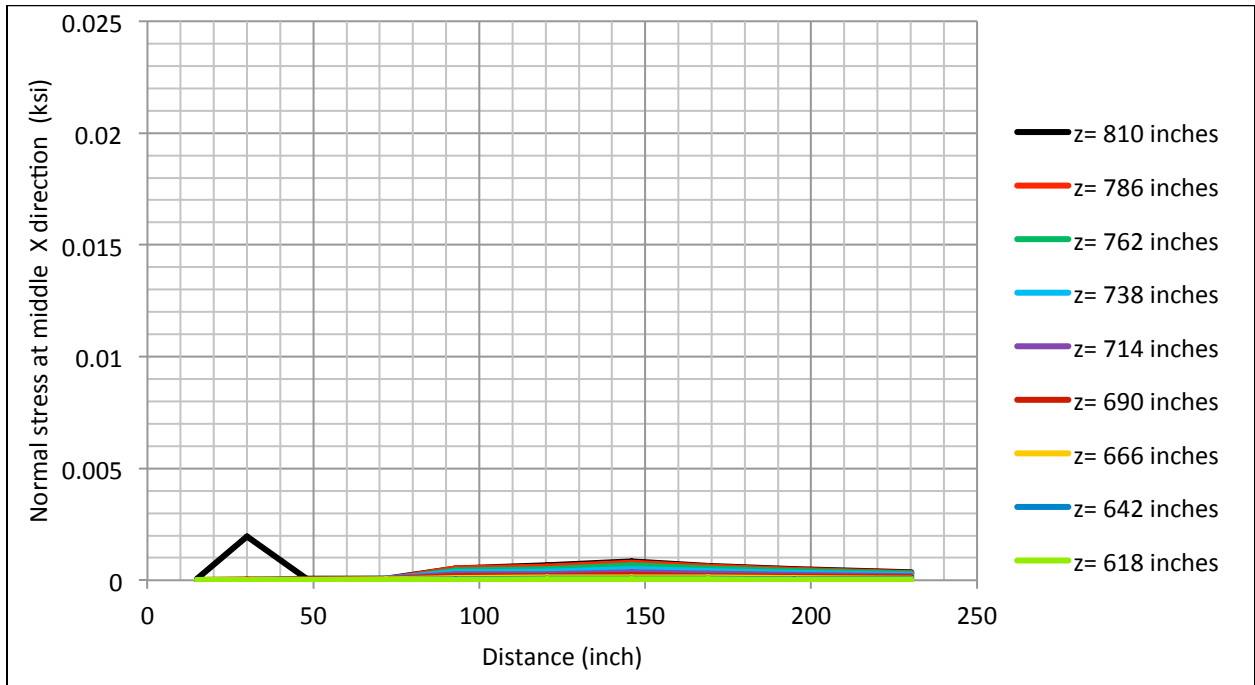


Figure 3.31: Normal Stress X Direction at Mid Depth

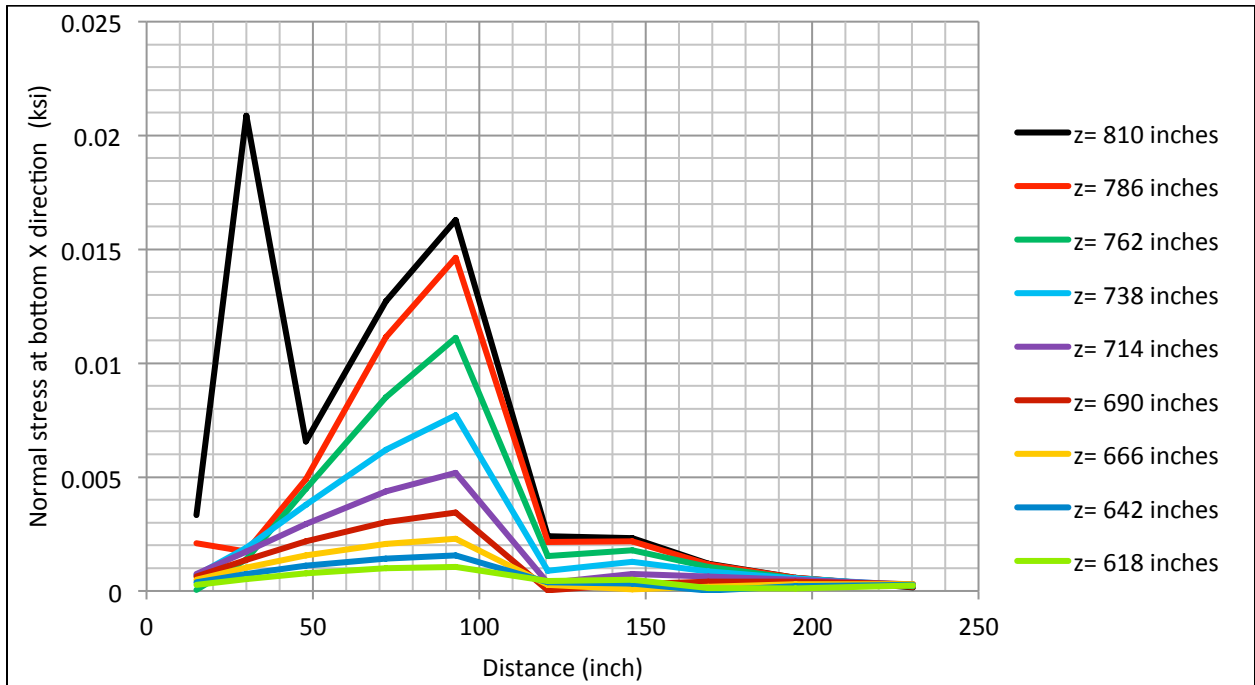


Figure 3.32: Normal Stress X Direction at Bottom Surface

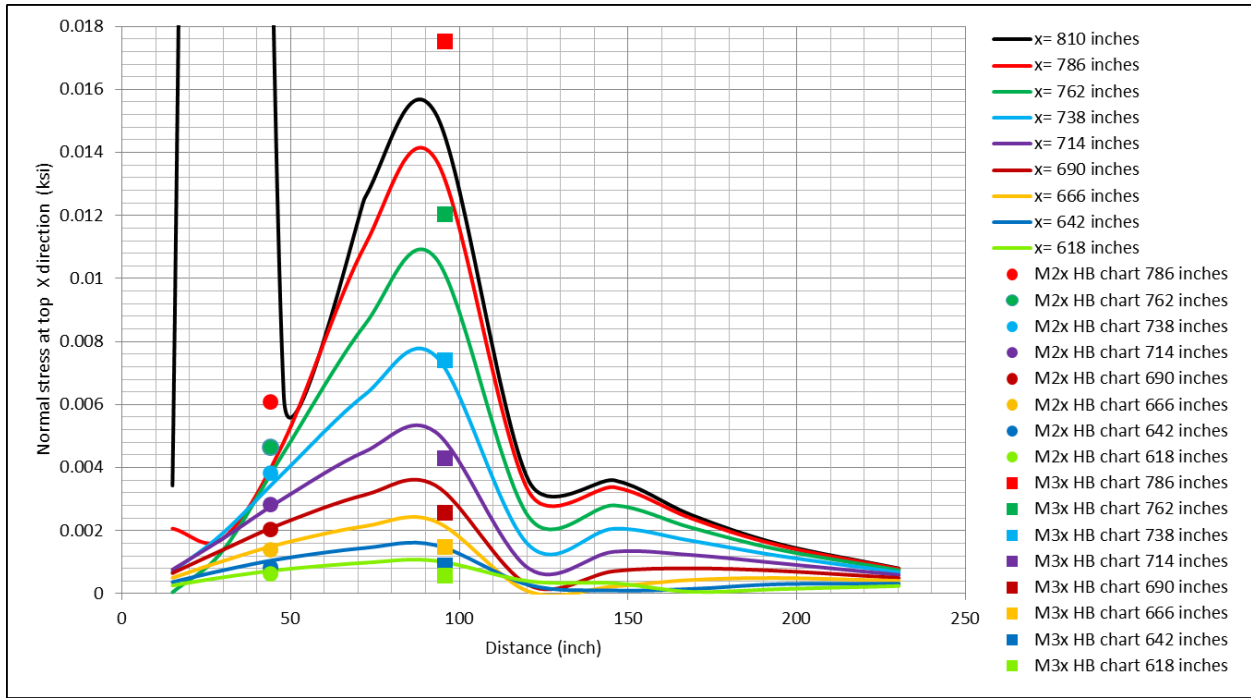


Figure 3.33: Comparison of Normal Stress in X Direction for FEM Results and Homberg Chart (Stress from Top Surface)

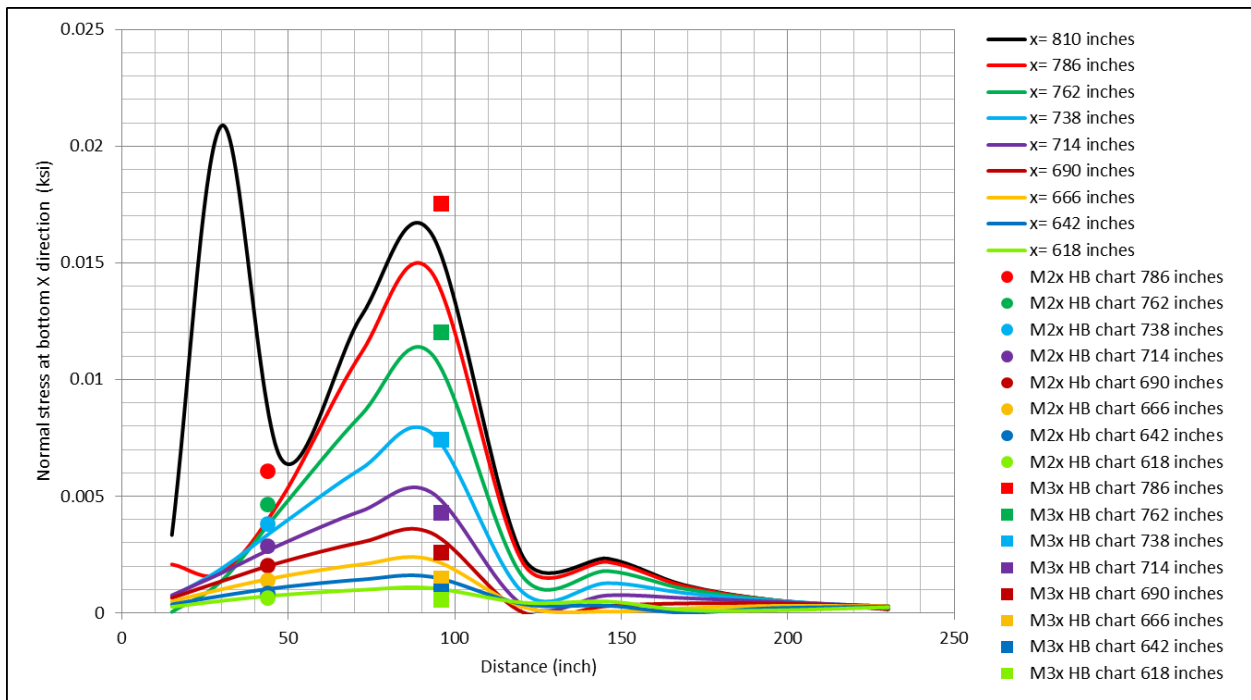


Figure 3.34: Comparison of Normal Stress in X Direction for FEM Results and Homberg Chart (Stress from Bottom Surface)

# CHAPTER 4

## FEM-Based Moment Approximation

### 4.1 Introduction

Homberg charts are influence surfaces for bending moments in a plate. They are often used to calculate transverse moments in the top slab of a precast, prestressed concrete segmental box girder bridge due to moving loads. A sample Homberg chart is shown in Figure 4.1. This particular chart would be used to analyze the bending moment at mid span of the cantilever portion of the top slab. The top edge of the chart (the y axis) represents the fixed edge that is shown as point “3” in the figure of the cantilever below the chart.

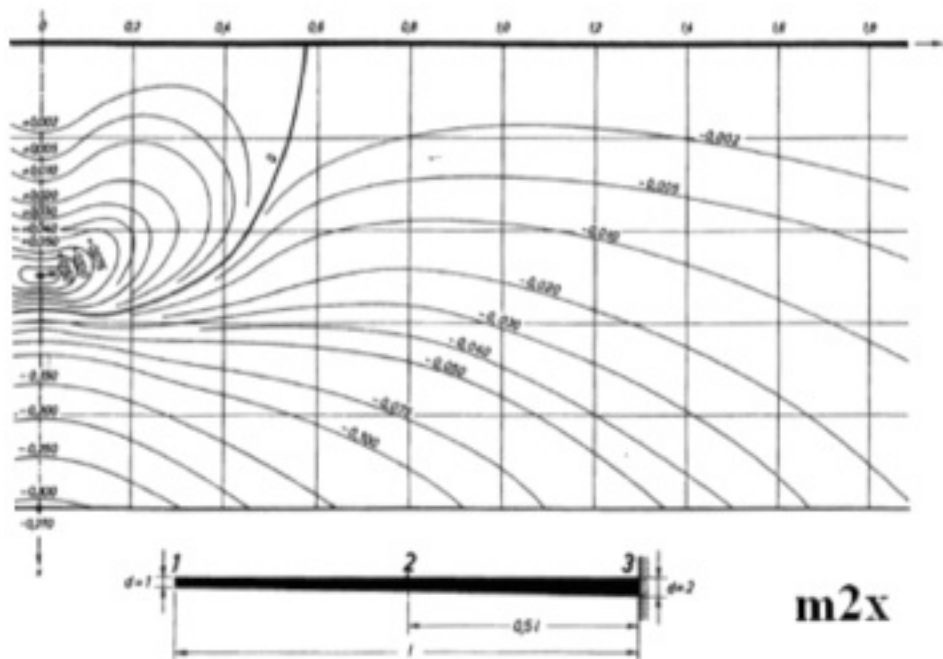


Figure 4.1: Influence Surface Moment Coefficients at Location 2 ( $m_{2x}$ )

Homberg charts are published and available for different support conditions, span configurations, and moment locations. In this study, the charts for  $m_{2x}$  wing span,  $m_{3x}$  wing span,  $m_{3x}$  mid span with edges fixed, and  $m_{5x}$  mid span with simple supports were used (Figure 4.2). To use the chart, the load is multiplied by the moment coefficient found on the chart at the location of the load; this results in the moment value at, using Figure 4.1 as an example, location 2. For load positions between the contour lines, the values for moment coefficients can be interpolated. Moment calculations in the design process are simplified with the help of Homberg charts, compared to, for example, doing a plate analysis for applied concentrated loads. In this study,

results showed that the moments found using Homberg charts were conservative compared to FE models of the Channel Five Bridge.

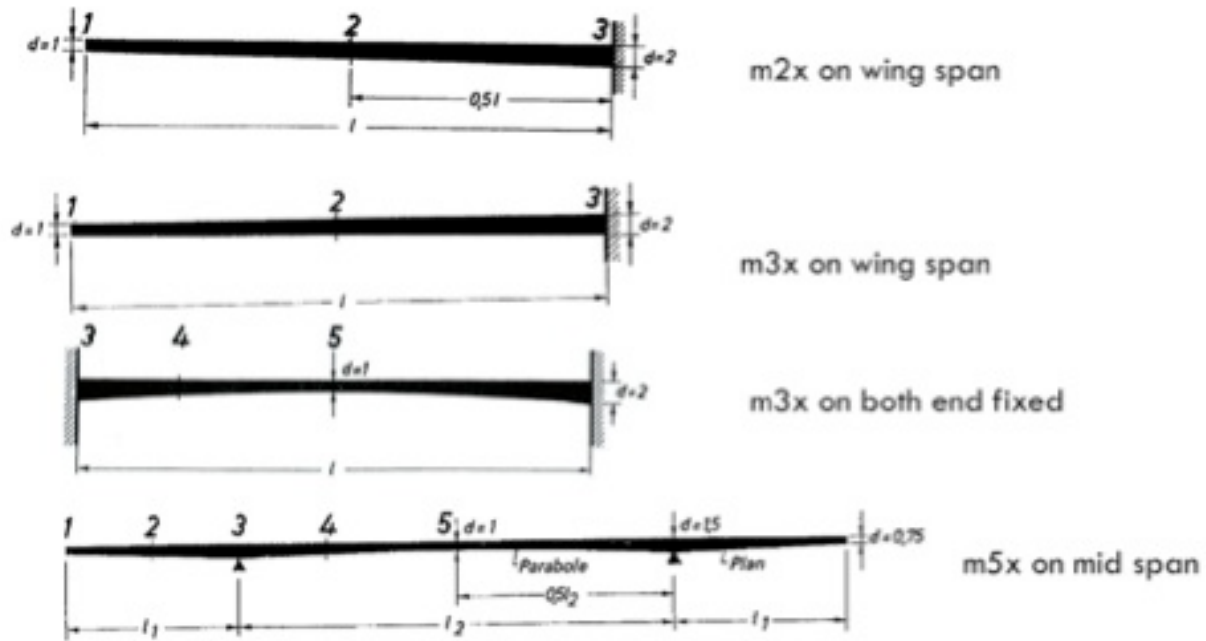


Figure 4.2: Moment Reading Locations for Various Boundary Conditions (from Homberg Charts)

## 4.2 Approach

The study started with comparing results of an FE model using SHELL281 elements, an FE model using SOLID186 elements, and an FE model of a scaled bridge (Section 4.2.1). The purpose was to validate the FE modeling approach and to decide whether to use shell or solid elements for the remaining analyses. Next, the Homberg chart for m2x wing span (at mid span of the cantilevered slab) and m3x wing span (at the fixed end of the cantilevered slab) were replicated by using results of FE analyses.

The scaled bridge FE model is identical to the full bridge model, except for geometric differences. The dimension of the bridge is scaled down proportionally so as to match the wing of the bridge deck with that of the plate model used to reproduce the Homberg chart. As explained and demonstrated in following section, the shell model and solid model results are identical. The scaled bridge is modeled with SOLID186 elements.

### 4.2.1 Plate Model vs. Scaled Bridge

ANSYS was used to model a cantilevered plate with a length of 600 inches, width of 12 inches, maximum thickness of 1 inch, and minimum thickness of 0.5 inches. Figure 4.3 shows a cross section of the ANSYS plate model with SOLID186 elements and SHELL281 elements.

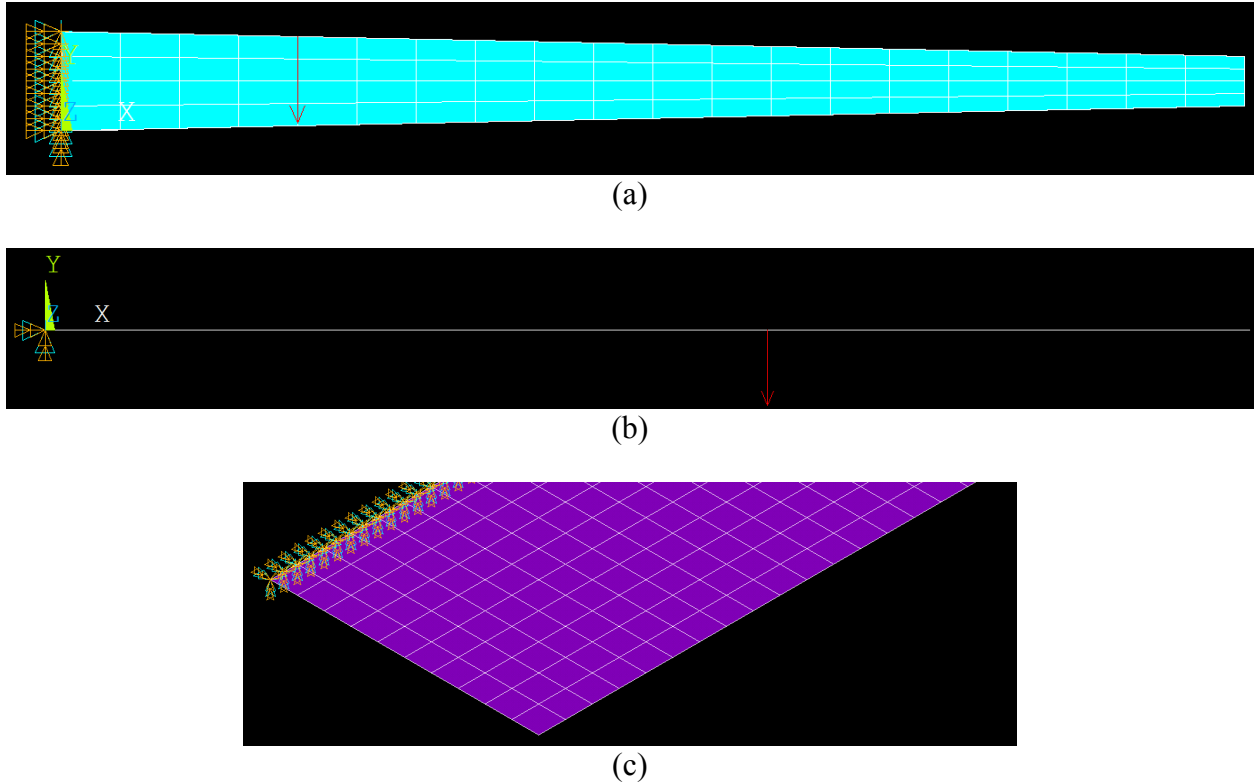


Figure 4.3: ANSYS Cantilever Plate (a) SOLID186 Element Model Cross-sectional View (b) SHELL281 Model Cross-sectional View (c) Oblique View of Plate Model

Both the SHELL281 and SOLID186 element models were simulated in ANSYS, and moment functions were created for the m2x location on the Homberg chart. The load was modeled to act at the 0.2 grid intersection of the Homberg chart as shown in Figure 4.1. A comparison of moment functions developed for solid and shell element models is shown in Figure 4.4, which shows that the shell model results match the solid model results. Thus, further analyses with shell models were deemed not necessary.

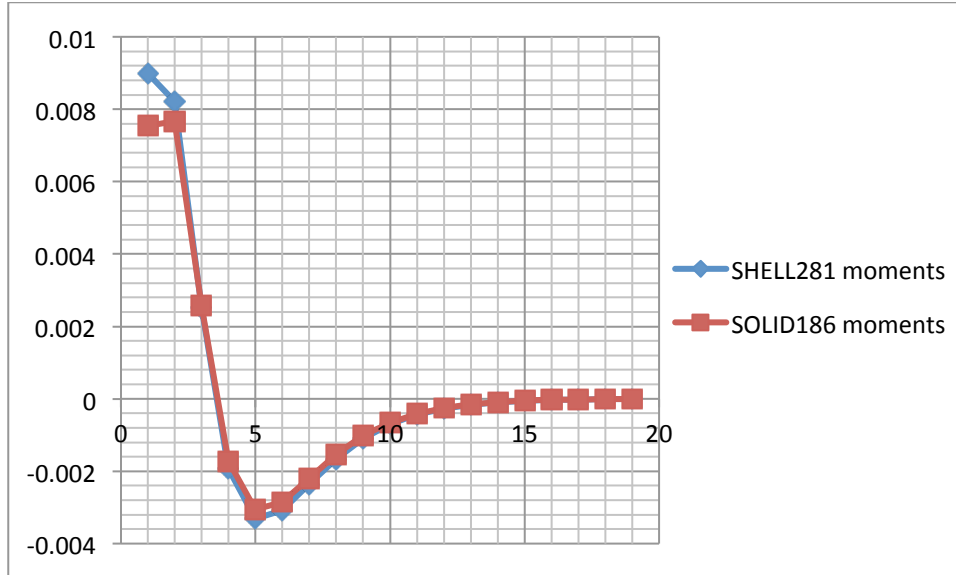


Figure 4.4: Comparison of Moment Function for SHELL281 vs. SOLID186 Element Models

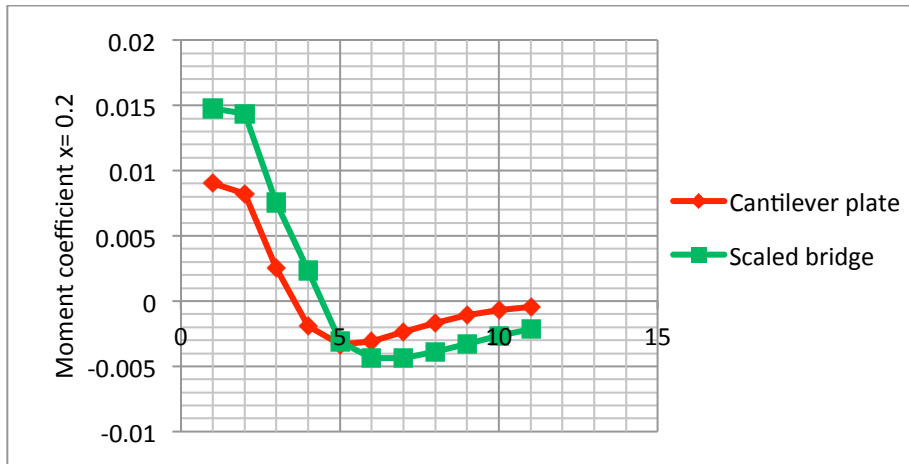
In order to further confirm the results, the plate analysis results were compared to results from a scaled FE model of the Channel Five Bridge. The details of the bridge are discussed in Chapter 3. The FE model was scaled for convenience. A comparison of the moment coefficients for the simple plate and scaled models is shown in Figure 4.5 (a) to (e), and it follows that the results are comparable. As expected, the negative moments of the scaled bridge are less conservative, because the wing of the scaled bridge is supported by the web, whereas the cantilever plate has a fixed support.

#### 4.2.2 Replicating Homberg Influence Surfaces with FE Model Results

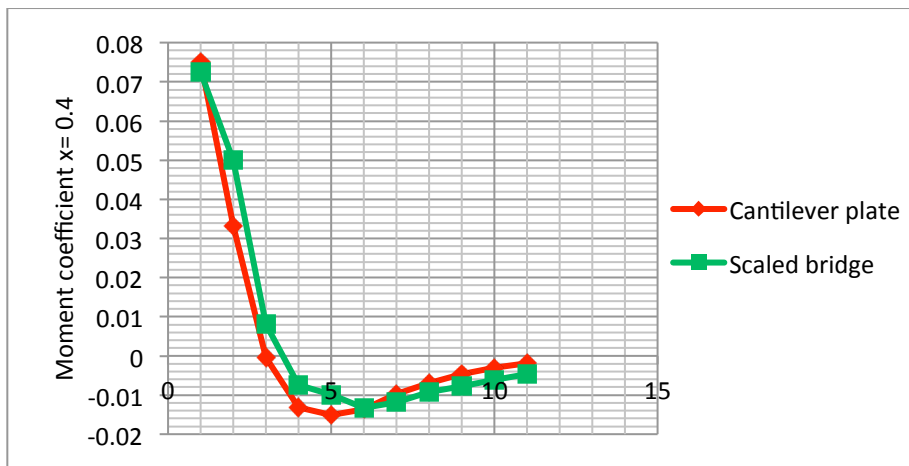
The influence surfaces drawn from results of the simple plate and scaled bridge models were compared to the Homberg chart for m2x from Figure 4.1. A comparison of these moment influence surfaces is shown in Figure 4.6. A similar comparison was made for the Homberg chart for m3x (Figure 4.7).

In order to explain how the Homberg charts were replicated by the FE models, the m2x wing chart in Figure 4.1 will be used as an example. A load of magnitude 1 kip was applied to the FE models at the grid intersection points along the length of the scaled bridge. The load was first applied at location (0, 0), i.e., the origin of the Homberg chart, and the stresses were read at the location that corresponded to location 2 on the m2x Homberg chart. The moments were calculated based on the slab thickness at that location and on the stress values. In the next iteration, the load was moved and applied at the location that corresponded with (0, 0.2) of the Homberg chart, and moments were calculated based on stress values and the slab thickness. This process was repeated four (4) more times, by moving the load to (0, 0.4), (0, 0.6), (0, 0.8), and (0, 1.0) positions. The next set of six (6) iterations were carried out by applying load at (0.2, 0) to (0.2, 1) and each grid intersection in between (see Homberg chart grids in Figure 4.6(a)). The

process was repeated several more times, for all the grid points, and stress values were used to calculate the moments each time.

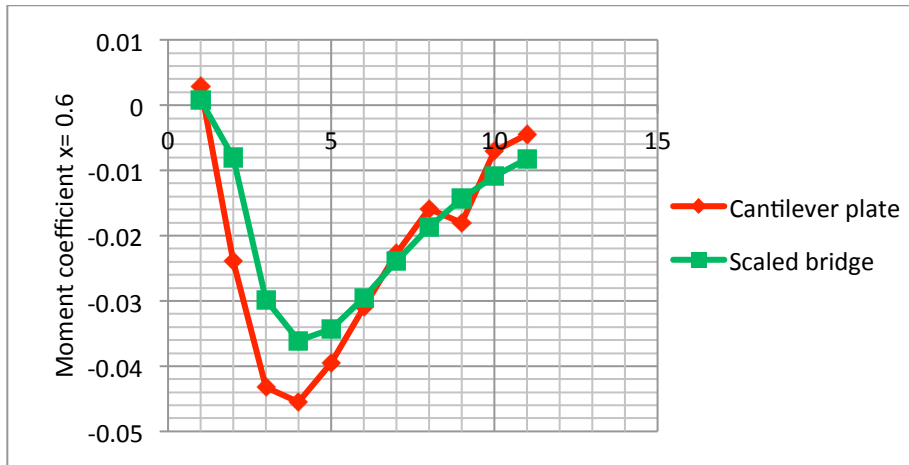


(a)

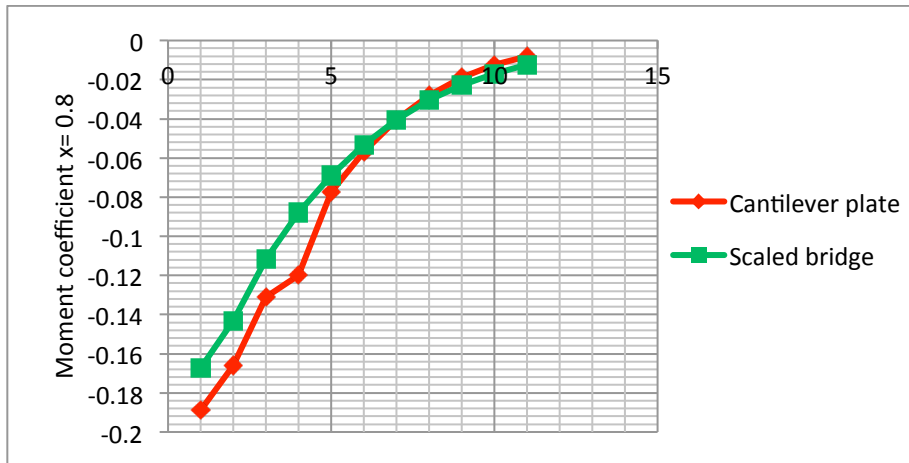


(b)

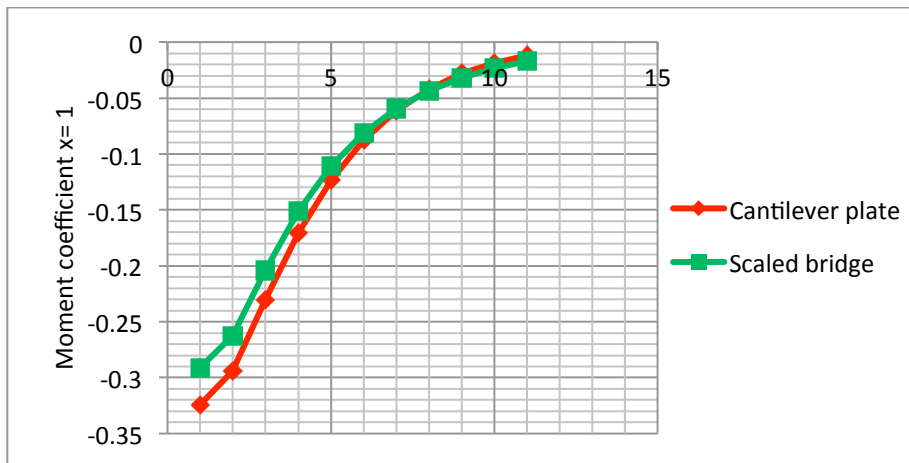
Figure 4.5: Comparison of Moment Coefficients for the Cantilever Plate and the Scaled Bridge



(c)

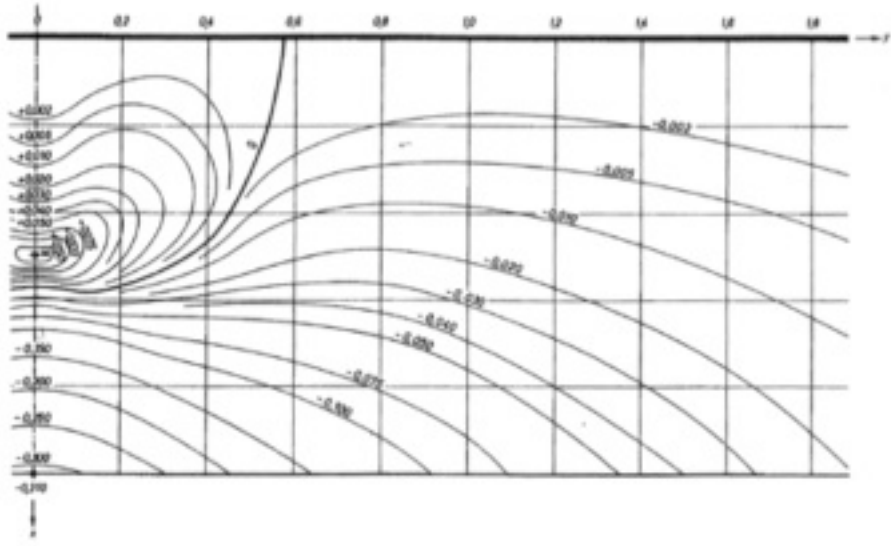


(d)

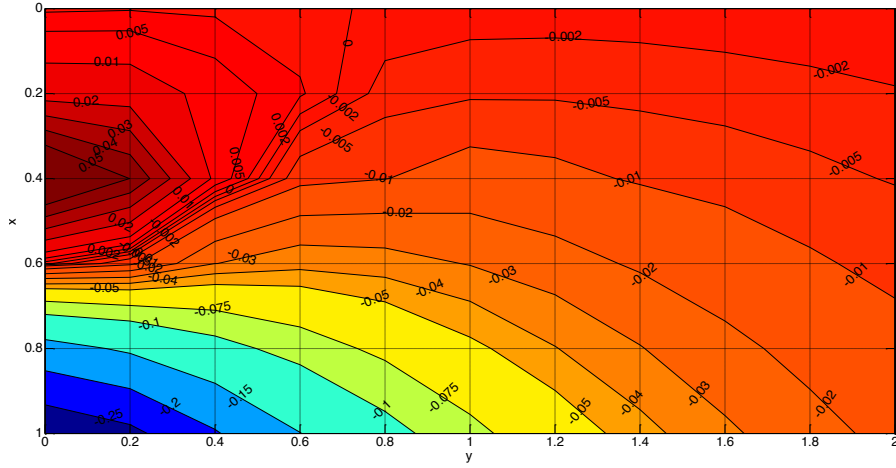


(e)

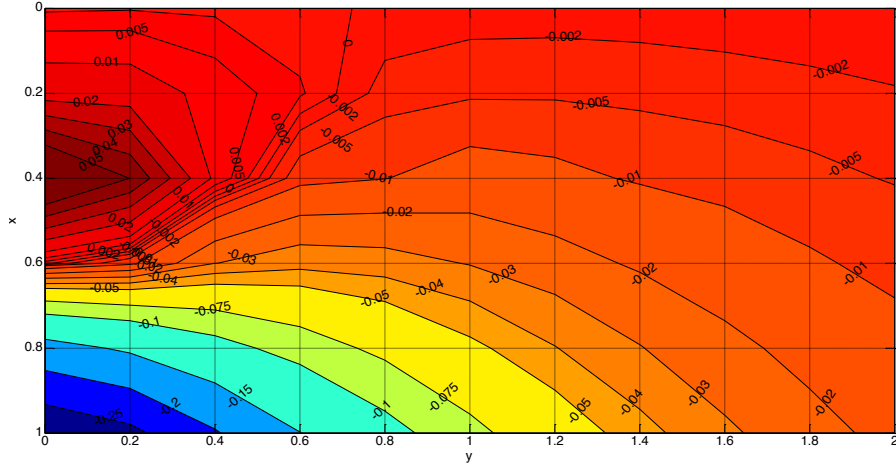
Figure 4.5 (cont'd.): Comparison of Moment Coefficients for the Cantilever Plate and the Scaled Bridge



(a)

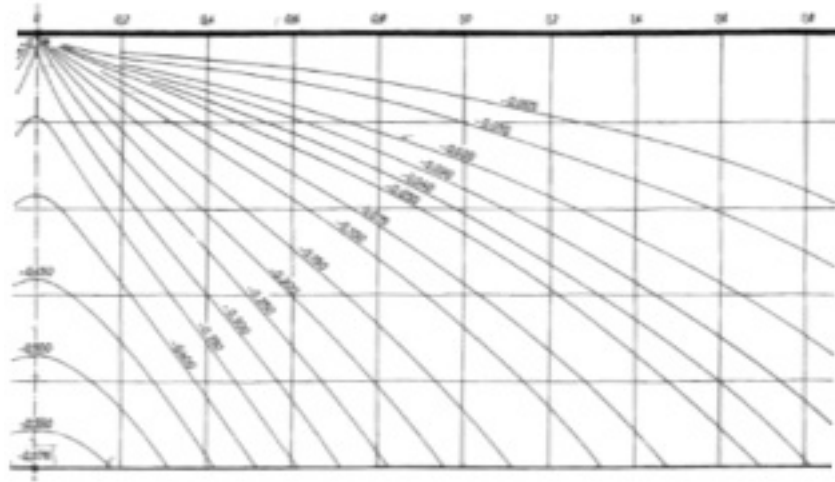


(b)

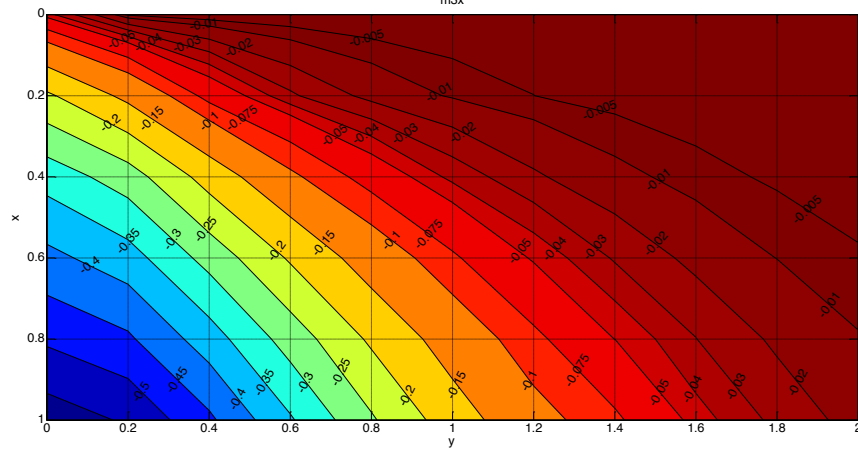


(c)

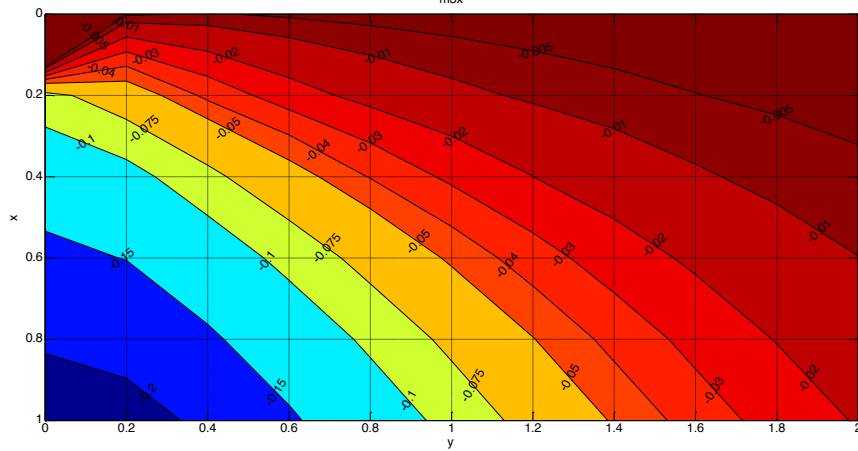
Figure 4.6: Comparison of Influence Surfaces from (a) Homberg Chart m2x (b) FE Plate Model (c) Scaled Bridge FE Model



(a)



(b)



(c)

Figure 4.7: Comparison of Influence Surfaces from (a) Homberg Chart m3x (b) FE Plate Model (c) Scaled Bridge FE Model

Now practically, it would be time consuming and inefficient to apply the load at each intersection point of grid line. So, instead of applying the load at each grid point, the unit load was applied at a point along the x axis (vertical), and multiple readings were taken along the y axis (horizontal) while moving away from the loading point. This approach required running only six (6) FE simulations to get all data points, instead of  $6 \times 10$  FE simulations.

### 4.2.3 Explanation of Moment Calculations

In the FE model of the top slab, the slab thickness was modeled with four (4) elements layered as shown in Figure 4.8. The stress readings were taken as explained above. For wing cases, the readings were taken at five (5) locations vertically (Figure 4.8).

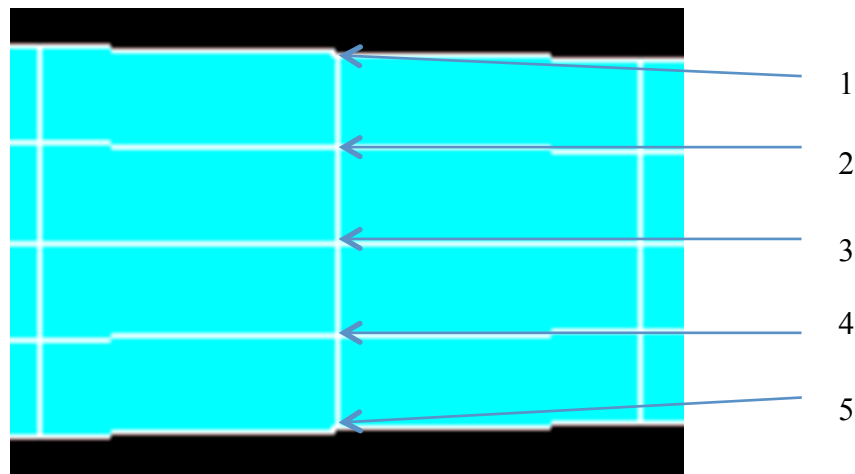


Figure 4.8: Elements and Stress Reading Locations

To calculate the moments, the area of the stress envelope was multiplied by the moment arm. The mid node stress was assumed to be zero. For example, from Figure 4.8, the normal stress in the x direction at point 1 was multiplied by the lever arm which is the distance from mid depth of the slab. Figure 4.9 shows a schematic representation of the stress envelope. For the top and bottom elements, the moments were calculated by considering the trapezoidal area of the stress envelope, and for the middle two elements, the moments were calculated by considering the triangular stress envelopes. As for m2x wing and m3x wing span, the stress envelope was used as shown in Figure 4.9. For m3x fixed-edge case and m5x simply-supported case, triangular stress envelopes were used in order to simplify the post-processing.

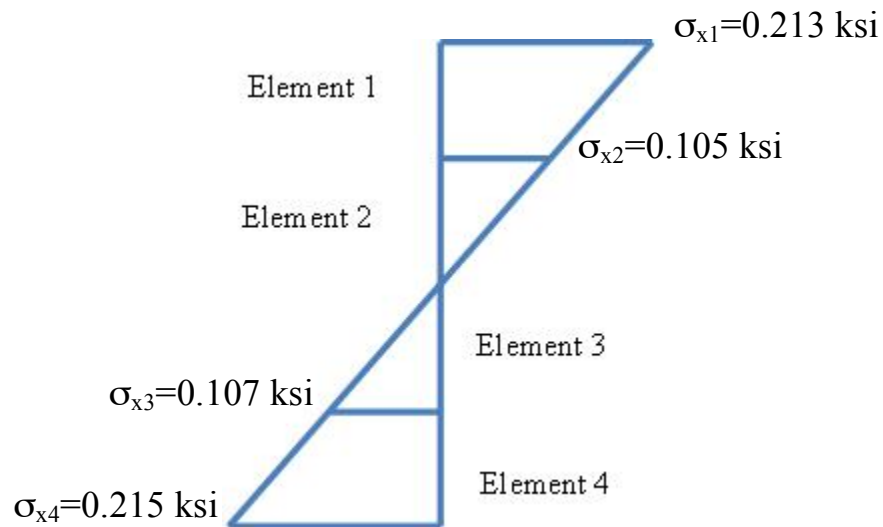
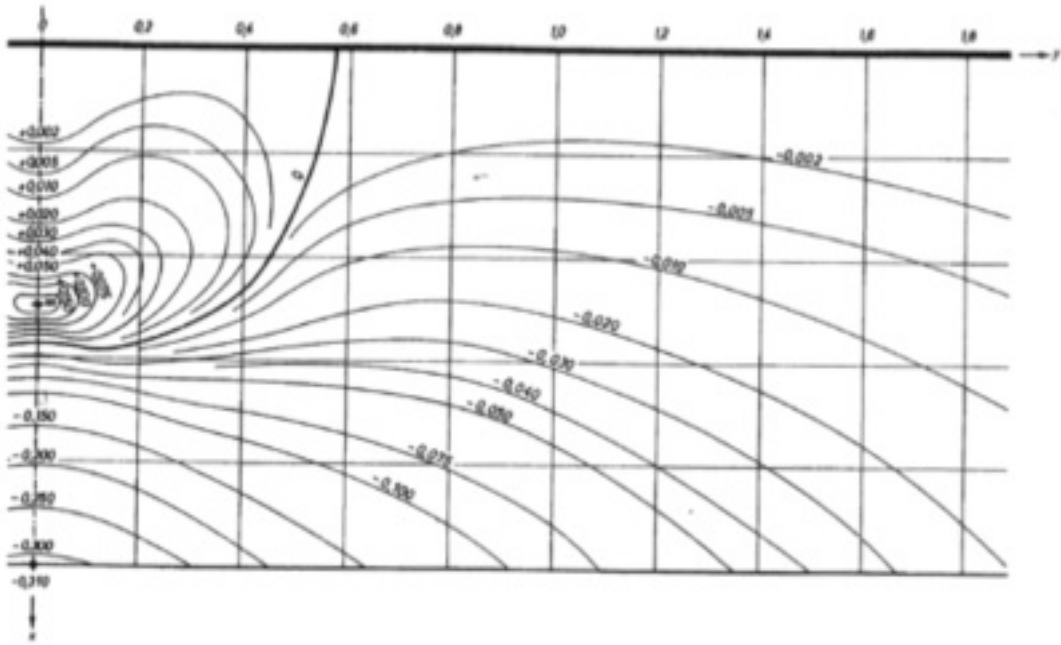


Figure 4.9: Schematic Representation of Stress Envelope (Sample Stresses in X Direction for TTT#3 Truck)

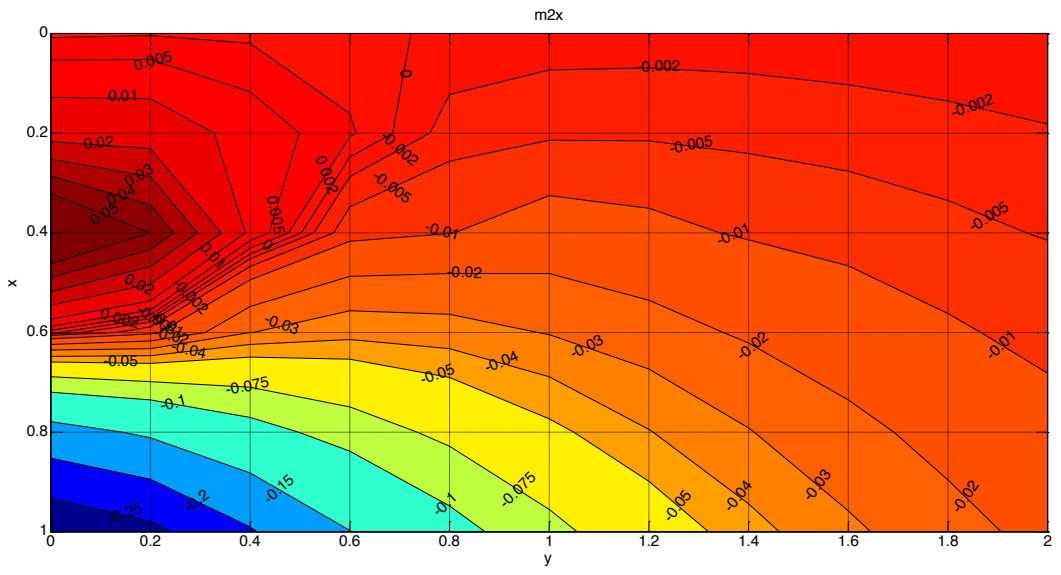
#### 4.2.4 Results

After establishing that the FE plate model and the scaled bridge FE model had comparable results for m2x wing span and m3x wing span, the study was further extended to other cases: Homberg charts m3x with both edges fixed and m5x with simple supports. Schematic representations of m2x wing, m3x wing, m3x fixed condition, and m5x simply-supported conditions are shown in Figure 4.2.

For each of these four support conditions, comparisons were made between the Homberg chart and the influence surface created from the scaled bridge FE model. Part of the results for m2x wing span and m3x wing span presented earlier are shown again for completeness. Figures 4.10 – 4.13 show comparisons for m2x wing case, m3x wing case, m3x mid span fixed-edge case, and m5x mid span simply-supported case, respectively.

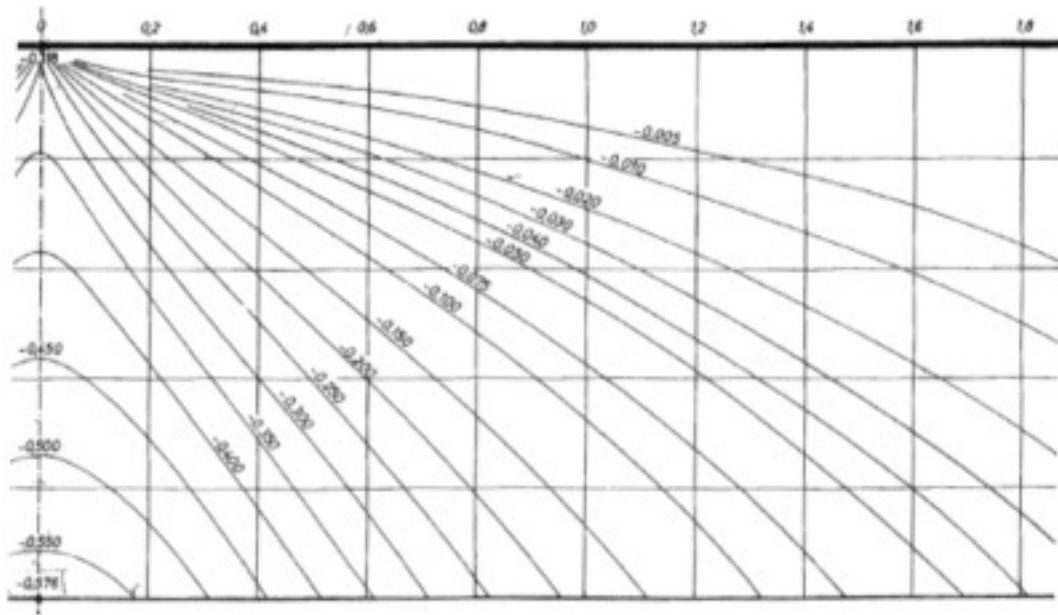


(a)

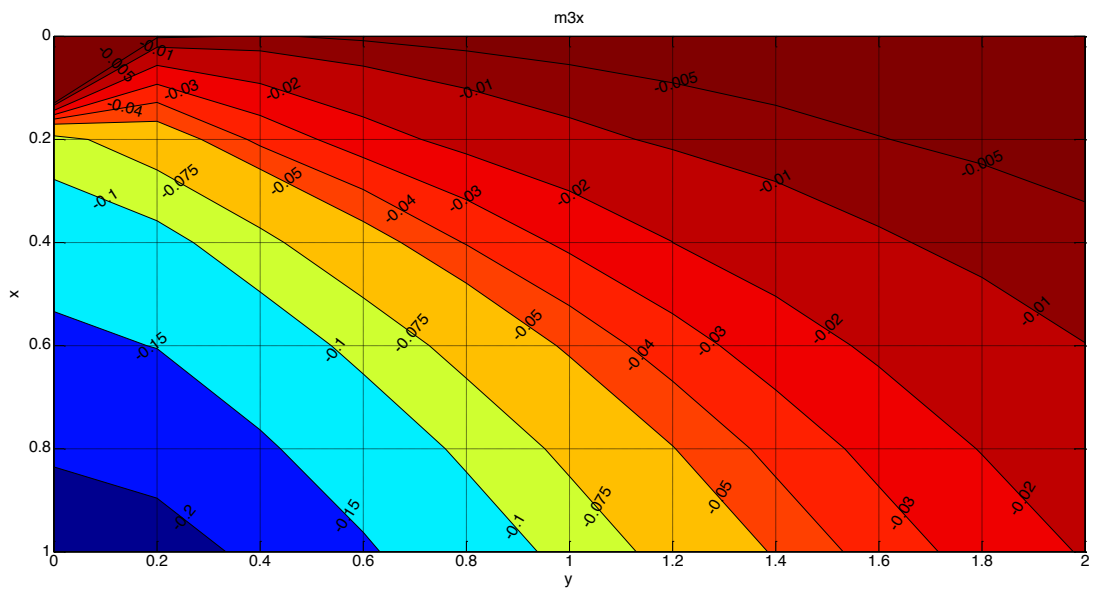


(b)

Figure 4.10: Comparison of m2x Wing Case from (a) Homberg Chart (b) Scaled Bridge FE Model

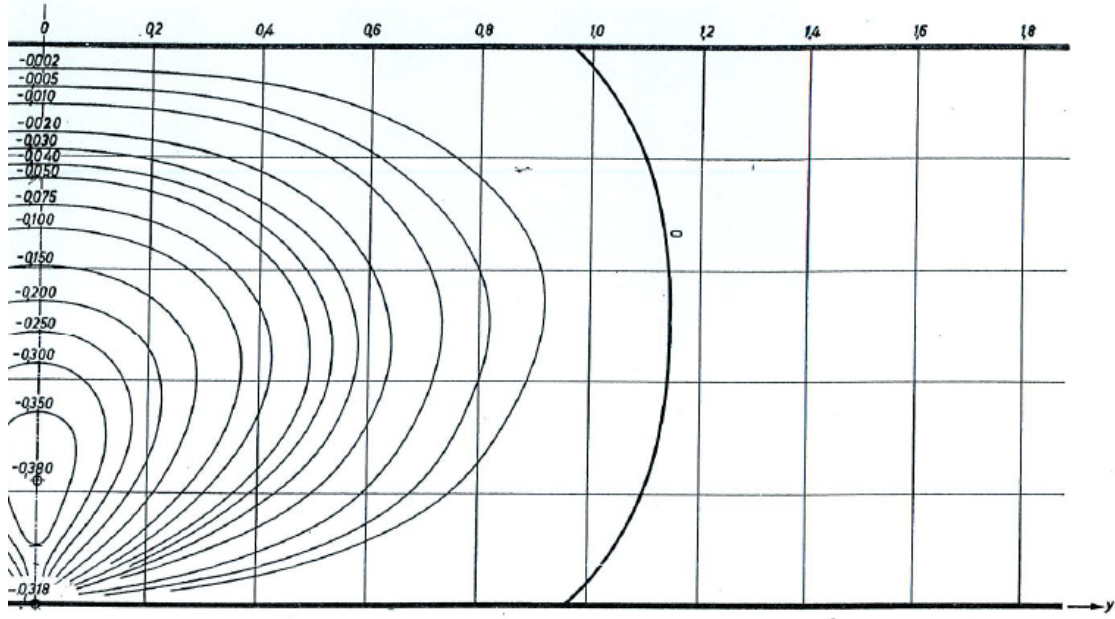


(a)



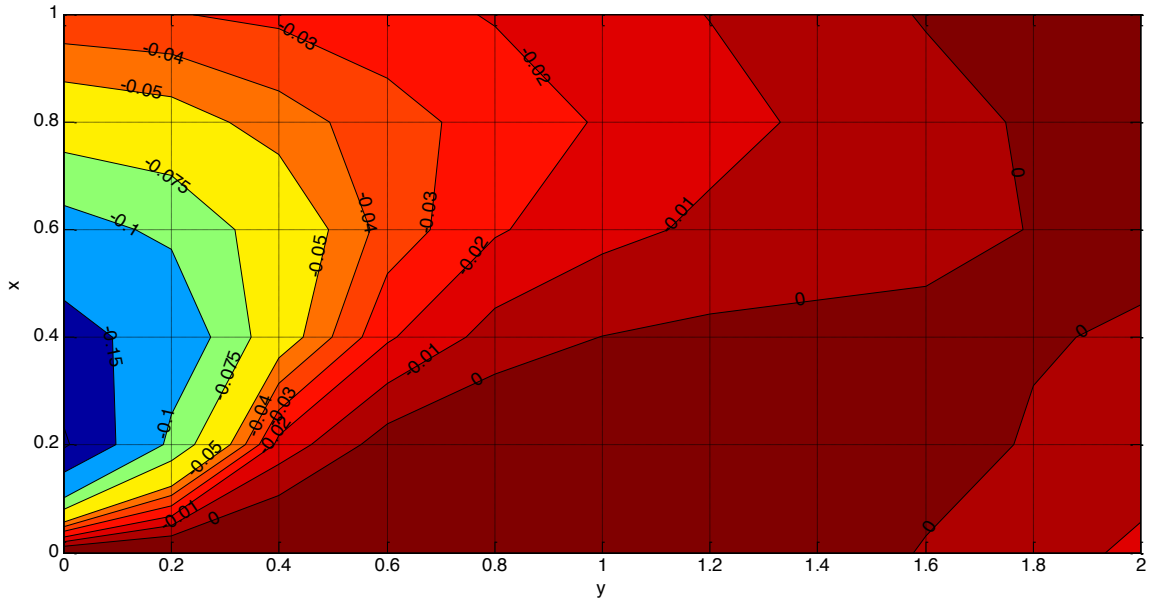
(b)

Figure 4.11: Comparison of m3x Wing Case from (a) Homberg Chart (b) Scaled Bridge FE Model



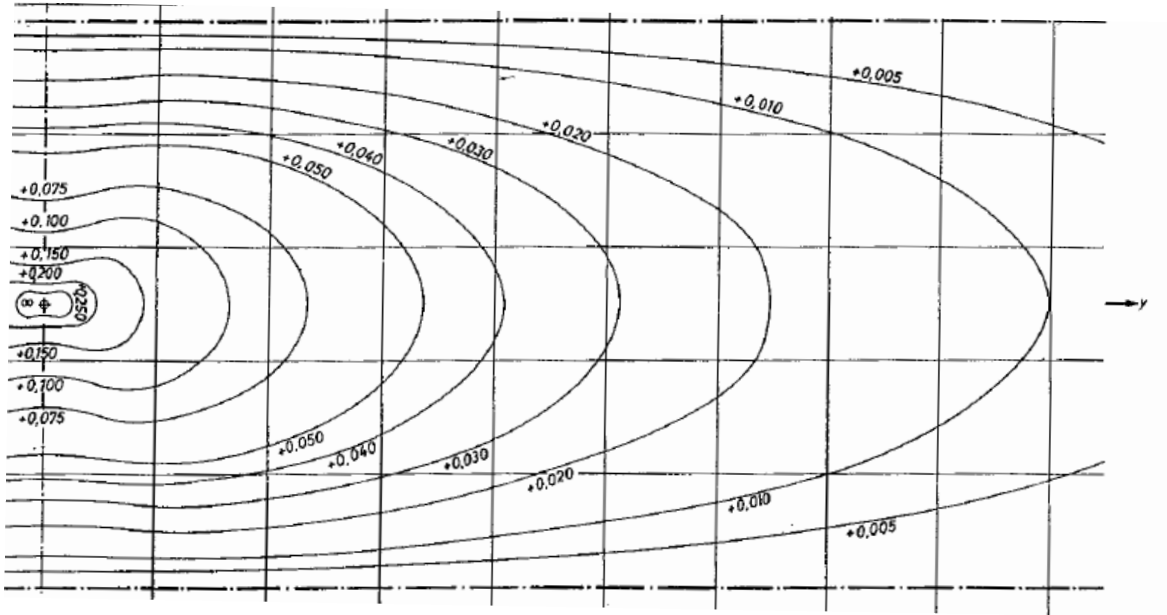
(a)

m3xmid



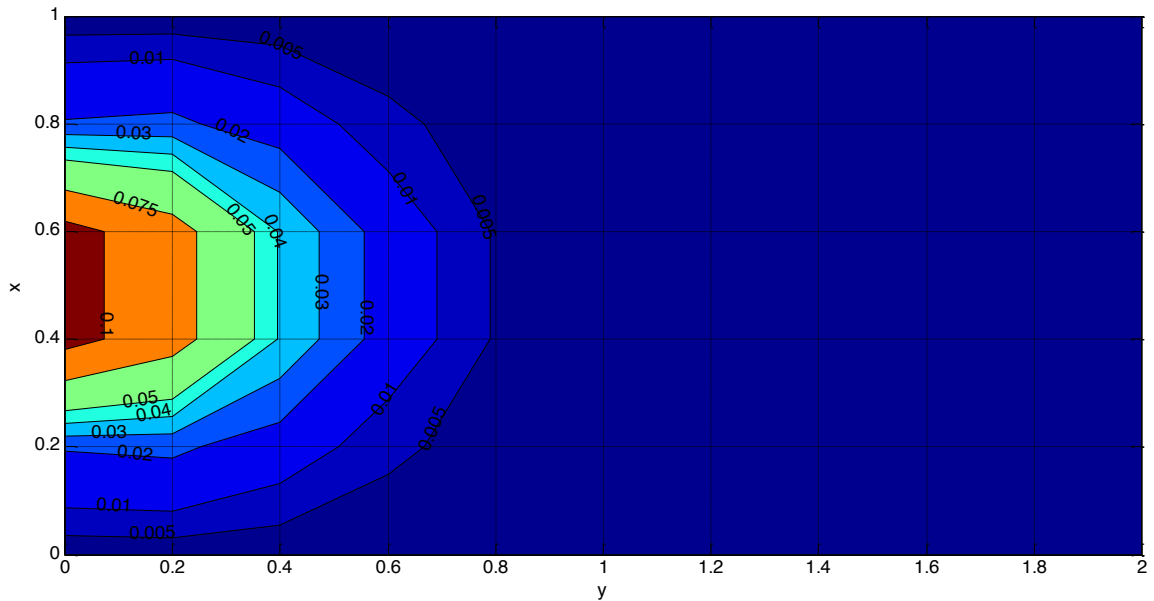
(b)

Figure 4.12: Comparison of m3x Mid Span Fixed-edge Case from (a) Homberg Chart (b) Scaled Bridge FE Model



(a)

m5xmid



(b)

Figure 4.13: Comparison of m5x Mid Span Simply-supported from (a) Homberg Chart (b) Scaled Bridge FE Model

Differences between the Homberg chart and FE-based chart were expected. They are due to the differing boundary conditions. Homberg charts were created based on infinitely-long plates with idealized support conditions (fixed or pinned). However, in the scaled bridge FE model, the top slab is supported by the two webs, which are connected by the bottom slab. For example, for the Homberg chart m2x and m3x wing cases, in the scaled bridge FE model, the wing slab is a

continuation of the middle section of the slab and is supported by the web. The fixed boundary condition of the Homberg chart would be representative of the web “support.” These differences mean that the boundary condition of the FE model (of the bridge) is not as stiff as the cantilever plates. The same explanations apply to the m3x mid span and m5x mid span cases: Homberg assumes idealized boundary conditions, but the FE model accounts for the flexibility of the web supports.

An additional cause of the difference is how the stresses were obtained in the FE analysis. For m3x wing and m3x mid span cases, the results were read one element away from the support location. This was done to overcome the potential stress concentration and rapid stress transition around the support. Also, the grid used in the FE analyses was not fine, which resulted in non-smooth curves in the FE-based charts.

### 4.3 Moment Comparison Analyses on Blanket Permit Vehicles

A final study was performed to analyze the effects of FDOT blanket permit vehicles on both the Homberg model and the scaled bridge FE model. Four trucks were used: AASHTO HS20 and three (3) FDOT blanket permit vehicles (TTT#1, TTT#3, and CR#1). Truck loads were applied to a full-scale FE model of the Channel Five Bridge as described in Section 3.1, and they were applied so as to cause maximum bending moment effect at the location under consideration (e.g., m2x wing span). Figure 4.14 shows an example truck load application. In order to calculate the maximum bending moment and the corresponding truck location on the bridge for the Homberg model, a computer program was written using Visual Basic in Excel. This software tool allows the user to select the type of truck to be analyzed and the Homberg chart to be used. The tool development and user instructions will be discussed in next chapter.

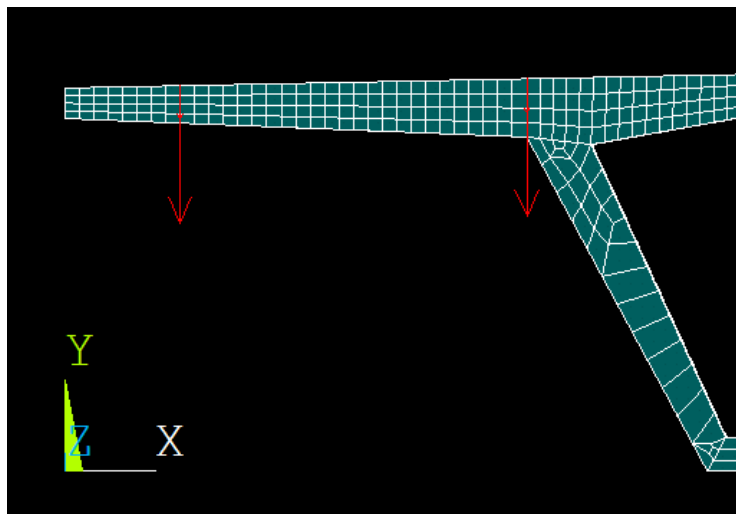


Figure 4.14: Bridge Section Showing m2x Wing with Applied HS20 Truck Load

The analysis results are provided in Tables 4.1 – 4.8. To explain the analysis method, take, for example, Tables 4.1 and 4.2, which show results for analyses at m2x wing span. First, the truck load was applied using the Homberg-based Excel tool. The maximum moment from the Homberg chart for m2x wing span is 2.468 kip-ft/ft, with the first axle of the truck being placed at 173.4 inches from the center of the bridge deck with one tire of the axle on the joint of wing and web. Secondly, the truck load was applied to the same location from the Homberg analysis so as to cause the maximum bending moment on the ANSYS bridge model. The normal stresses were read at location 2 in m2x wing span as shown in Figure 4.2, and the moments were calculated from the FEM normal stress envelope as discussed previously. For example, the FE moment for the HS20 truck was 2.513 kip-ft/ft.

The process was repeated for the remaining trucks, and the results are presented in Tables 4.1 - 4.8. Tables 4.1 and 4.2 show the results for m2x wing span case; Homberg gives very similar results as the FE bridge model.

Table 4.1: Homberg Chart Tool and FEM Analysis Moments for m2x Wing Span (Kip-Inch Units)

Location	HS20		TTT#1		TTT#3		CR#1	
	Homberg	FEM	Homberg	FEM	Homberg	FEM	Homberg	FEM
m2x wing	2.469	2.513	2.848	2.893	2.570	3.008	2.929	2.802

Table 4.2: Moment Ratio HS20 / Blanket Permit Vehicle for m2x Wing Span

Location	HS20/TTT#1		HS20/TTT#3		HS20/CR#1	
	Homberg	FEM	Homberg	FEM	Homberg	FEM
m2x wing	0.8669	0.8684	0.9605	0.8352	0.8426	0.8967

Tables 4.3 and 4.4, the results for the m3x wing span case, show that Homberg moments are considerably larger than FE model results. This is a reasonable result, since location 3 is fixed for Homberg condition but has the web as a flexible support in the FE model.

Table 4.3: Homberg Chart Tool and FEM Analysis Moments for m3x Wing Span (Kip-Inch Units)

Location	HS20		TTT#1		TTT#3		CR#1	
	Homberg	FEM	Homberg	FEM	Homberg	FEM	Homberg	FEM
m3x wing	8.292	6.375	11.089	9.091	9.997	8.541	10.469	7.362

Table 4.4: Moment Ratio HS20 / Blanket Permit Vehicle for m3x Wing Span

Location	HS20/TTT#1		HS20/TTT#3		HS20/CR#1	
	Homberg	FEM	Homberg	FEM	Homberg	FEM
m3x wing	0.7478	0.7012	0.8294	0.7464	0.7920	0.8659

Tables 4.5 and 4.6 show the results for the m3x mid span fixed-edge case. Homberg moments are considerably larger than the FE model results. Differences were expected, however: for the m3x mid span case, both edges are completely fixed and therefore attract negative moment, but in the FE model, the webs provide flexible support to the slab.

Table 4.5: Homberg Chart Tool and FEM Analysis Moments for m3x Mid Span Fixed Edge (Kip-Inch Units)

Location	HS20		TTT#1		TTT#3		CR#1	
	Homberg	FEM	Homberg	FEM	Homberg	FEM	Homberg	FEM
m3x mid span	10.530	3.346	13.990	5.597	12.570	4.931	12.920	5.246

Table 4.6: Moment Ratio HS20 / Blanket Permit Vehicle for m3x Mid Span Fixed Edge

Location	HS20/TTT#1		HS20/TTT#3		HS20/CR#1	
	Homberg	FEM	Homberg	FEM	Homberg	FEM
m3x mid span	0.7526	0.5978	0.8377	0.6785	0.8150	0.6378

The Homberg moments are also considerably larger for the m5x mid span simply-supported case (Tables 4.7 and 4.8). Differences were expected: in the m5x mid span case, the slab is simply supported, but in the FE model, the webs provide some rotational stiffness – reducing the positive moment at mid span.

Table 4.7: Homberg Chart Tool and FEM Analysis Moments for m5x Mid Span Simply Supported (Kip-Inch Units)

Location	HS20		TTT#1		TTT#3		CR#1	
	Homberg	FEM	Homberg	FEM	Homberg	FEM	Homberg	FEM
m5x mid span (whole width)	5.957	2.640	7.381	3.959	8.008	3.603	7.764	3.851

Table 4.8: Moment Ratio HS20 / Blanket Permit Vehicle for m5x Mid Span Simply Supported

Location	HS20/TTT#1		HS20/TTT#3		HS20/CR#1	
	Homberg	FEM	Homberg	FEM	Homberg	FEM
m5x mid span (whole width)	0.8069	0.6668	0.7438	0.7328	0.7672	0.6855

# CHAPTER 5

## Tool Development

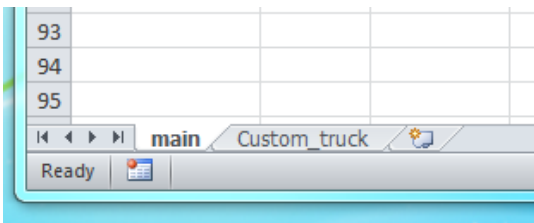
### 5.1 Introduction

The Homberg chart requires the user to look up the moment manually. FEM analysis, too, needs the manual lookup for the stresses in order to calculate the moments. An Excel-based tool was developed in this research with the aim to automate the process. The Homberg chart contours for m2x wing span, m3x wing span, m3x mid span with fixed edges, and m5x mid span with simple supports cases were digitized to extract the data points. The moment functions created from digitized data are used in tool. The FDOT Blanket Permit Trucks and others (HS20, FL120, TTT#1, TTT#2, TTT#3, CR#1) are modeled in the tool. In addition, a separate tab in the Excel file is provided to enter details for a Custom truck. The details of the various modules of the tool and use are explained in following sections.

### 5.2 Overview of Tool

The tool is an Excel sheet with Visual Basic code running behind it. There are two tabs in the Excel sheet, titled 'main' and 'Custom\_truck' as shown in Figure 5.1(a).

In the 'main' tab, the user is required to enter three (3) values for WA, WB, and WC. Refer to Figure 5.1(b). As shown in Figure 5.2, WA is the wing width, WB is the distance from the edge of the wing up to which the truck wheel can be placed, and WC is the deck mid width.



(a)

WA	102 inches
WB	30 inches
WC	268.75 inches

(b)

Figure 5.1: Figure Showing (a) Tabs (b) WA, WB, and WC Entries

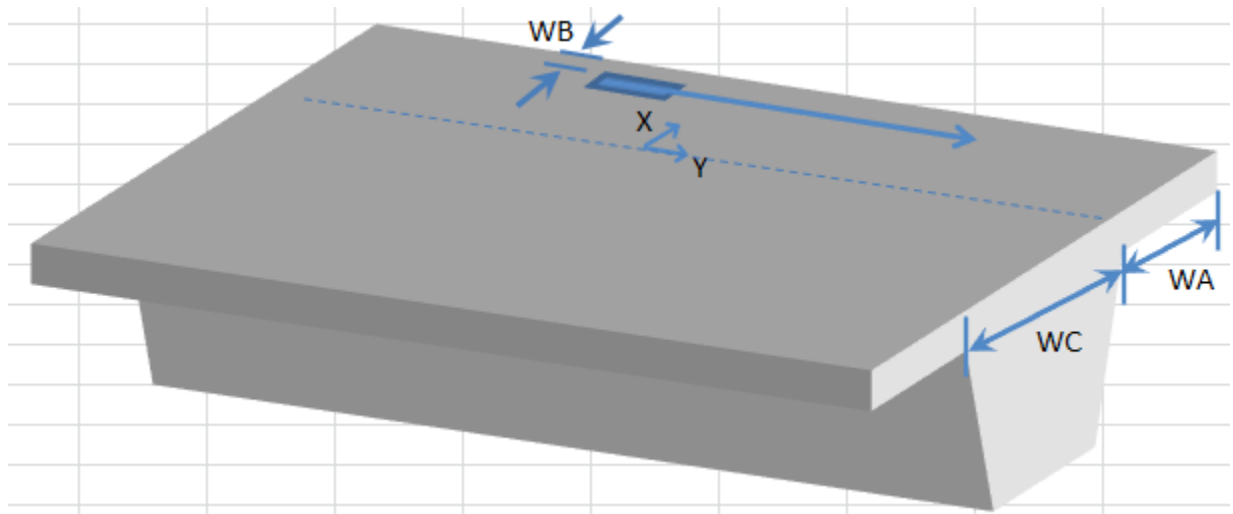


Figure 5.2: Schematic Representation of Required Data for Tool

In the next step, the user selects the type of truck and Homberg chart. The user can select two trucks at the same time from two different lists of trucks. Likewise, the user can select two types of Homberg charts at the same time. Figure 5.3 shows example windows in which to choose the truck and Homberg chart.

SELECT TRUCK A	SELECT TRUCK B
<input checked="" type="radio"/> HS20 <input type="radio"/> FL120 <input type="radio"/> TTT1	<input checked="" type="radio"/> HS20 <input type="radio"/> FL120 <input type="radio"/> TTT1
<input checked="" type="radio"/> m2x wing <input type="radio"/> m3x wing	<input checked="" type="radio"/> m3x mid span <input type="radio"/> m5x mid span

Figure 5.3: Selecting Two Trucks and Two Types of Homberg Charts

The calculation is done quickly, as the user selects from the choices, and the maximum moment and right tire location are displayed in the respective truck output data. The minimum moment and corresponding location of the right wheel are also displayed. Refer to Figures 5.4 and 5.5. The user can plot the wheel location of Trucks A and B on the wing span and mid span by clicking the respective buttons shown in Figure 5.5. The position of the truck wheels is with respect to the mid length of the bridge deck span. A sample truck wheel location is shown in Figure 5.6.

TRUCK A	HS20			
m2x wing		Normalized	Original	
Max moment		0	0	k-in/in
Location	x	0.1	10.2	inch
	y	-1.8	-183.6	inch
Min moment		-2.47	-2.47	k-in/in
Location	x	0	0	inch
	y	1.7	173.4	inch

TRUCK A	HS20			
m3x mid span		Normalized	Original	
Max moment		0	0	k-in/in
Location	x	0	0	inch
	y	-1.8	-483.75	inch
Min moment		0.00	0.00	k-in/in
Location	x	0	0	inch
	y	-1.8	-483.75	inch

(a) Truck A

TRUCK B	HS20			
m2x wing		Normalized	Original	
Max moment		0	0	k-in/in
Location	x	0.1	10.2	inch
	y	-1.8	-183.6	inch
Min moment		-2.44	-2.44	k-in/in
Location	x	0	0	inch
	y	1.7	173.4	inch

TRUCK B	HS20			
m3x mid span		Normalized	Original	
Max moment		0	0	k-in/in
Location	x	0	0	inch
	y	-1.8	-483.75	inch
Min moment		0.00	0.00	k-in/in
Location	x	0	0	inch
	y	-1.8	-483.75	inch

(b) Truck B

Figure 5.4: Results for m2x Wing and m3x Mid Span



Figure 5.5: Button to Plot Wheel Locations for Maximum Moment

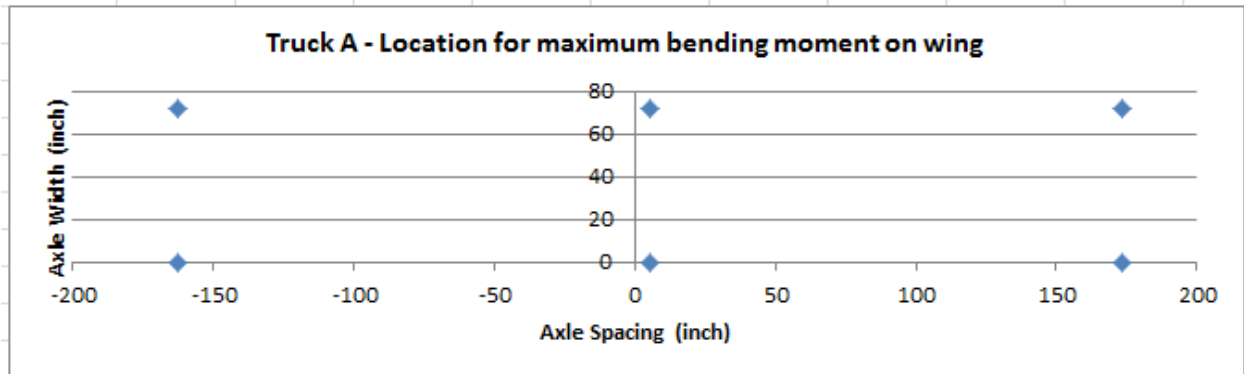


Figure 5.6: Sample Wheel Location for Maximum Moment

In the 'Custom\_truck' tab, the user is asked to enter the number of wheels. Each axle is considered to have two (2) wheels. Depending on the number of axles, a number of rows will be heighted – prompting the user to enter the x and y coordinates of the wheels and corresponding loads on each wheel. Each wheel is half the axle load. In order to cross check x and y coordinates, the user can click the 'Plot Tire Location'. If the plot does not exist or was accidentally deleted, then the user would be prompted to create the plot. Figures 5.7 and 5.8 show the details for sample custom truck.

	A	B	C
1	Enter no of tires	6	
2	X inch	Y inch	F kips
3	0	0	4
4	72	0	4
5	0	-168	16
6	72	-168	16
7	0	-336	16
8	72	-336	16

Figure 5.7: Custom Truck Details

**Define custom truck**

Enter number of tires in Cell B1. Maximum 100 tires could be entered

Enter coordinates of tire in the following sequence

top right, top left, middle right, middle left, bottom right, bottom left and so on

X = x coordinats, Y = y coordinate, F = force/ load on tire

The tire plot do not follow above sequence. The purpose of plot is just to view.

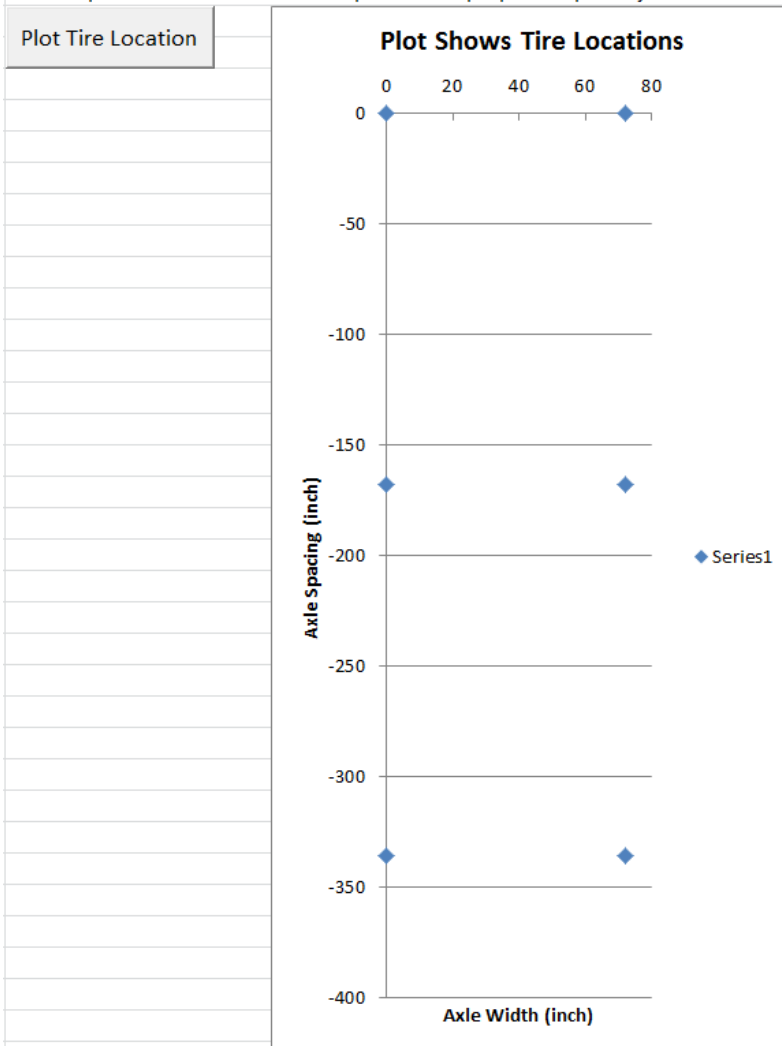


Figure 5.8: Sample Custom Truck Plot

### 5.3 Explanation of Code and Visual Basic Functions

In this section, the design steps in code development are discussed. The code broadly works with five building blocks and could be termed as data input, truck selection, Homberg chart selection, data processing and plotting. The flowchart for the code is shown in Figure 5.9.

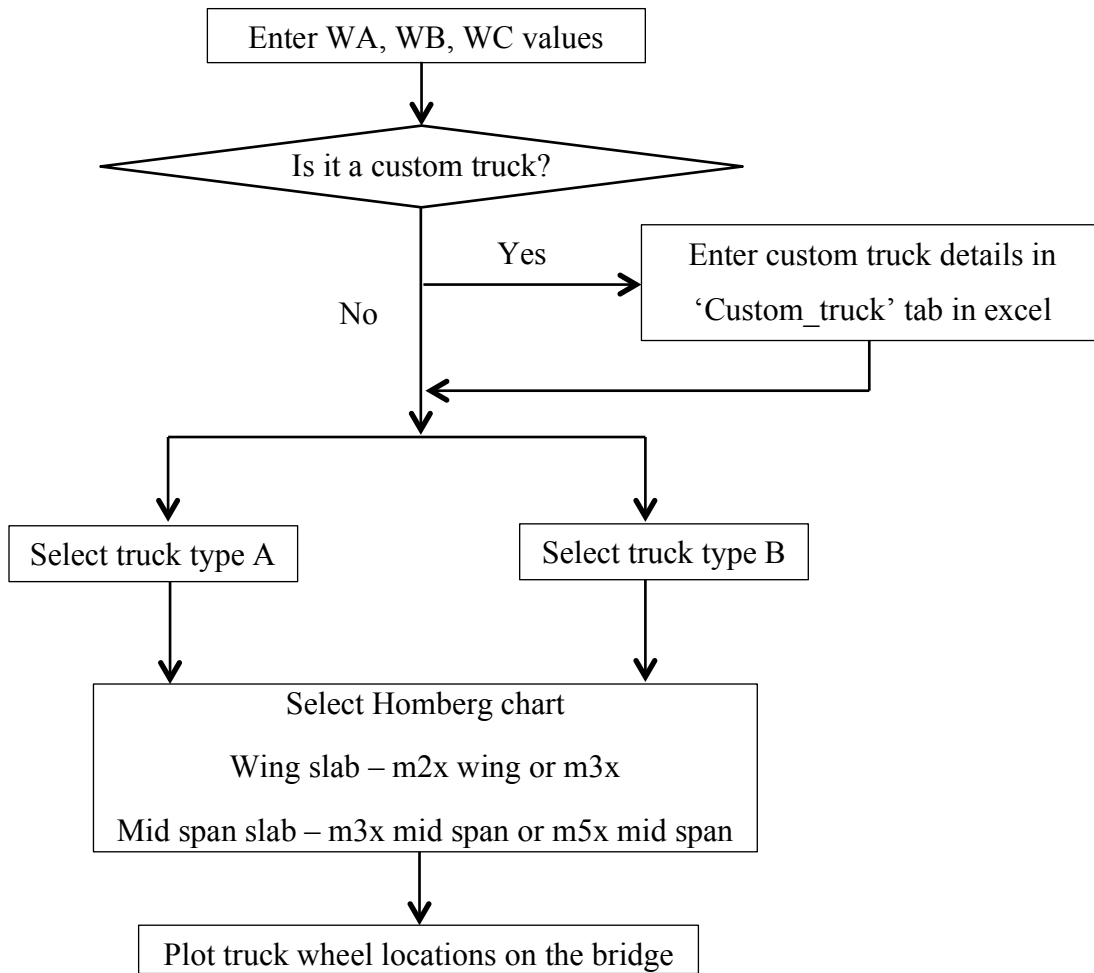


Figure 5.9: Flow Chart of the Tool

The 'main' tab in the Excel sheet is the "center" which controls and comprises all of the code building blocks. The data values WA, WB, and WC are three basic dimensions of the bridge slab. The Homberg chart is based on the unit width. It requires that while using the tool, the wing width must be normalized. The user then selects the type of truck A and B. In both truck lists A and B, the same types of trucks are available for selection. This is done so that the user can study the difference in moments for trucks and do a comparative assessment. Once the user selects the required data, the code executes Visual Basic code embedded in Excel.

All of the selected data is passed to Visual Basic code modules. The code execution is explained with HS20, truck A, m2xwing case. In the ‘main’ tab, cell numbers B37 to AX37 describe the length of the bridge deck. The bridge deck length ranges from –1.8 to 3 in normalized length. This resembles the plate lengths shown in the Homberg chart. The unit width of the plate in the Homberg chart is entered from cell number A30 to A48. Cell numbers B38 to AX48 define the right top tire location. Refer to Figure 5.2. From cell number B38 to AX48, each cell calls Visual Basic’s ‘main’ function with input data as truck type, Homberg chart name, WA, WB, x coordinate (which is the distance along the width of plate on the Homberg chart), and y coordinate (the distance along the length of plate on the Homberg chart). Figure 5.10 shows the part of the Excel sheet that reports the data.

36	HS20	Truck A					
37	m2x wing	-1.8	-1.7	-1.6	-1.5	-1.4	
38	0	-0.0475	-0.05646875	-0.07056	-0.08011	-0.09609	
39	0.1	0	0	0	0	0	
40	0.2	0	0	0	0	0	
41	0.3	0	0	0	0	0	
42	0.4	0	0	0	0	0	
43	0.5	0	0	0	0	0	
44	0.6	0	0	0	0	0	
45	0.7	0	0	0	0	0	
46	0.8	0	0	0	0	0	
47	0.9	0	0	0	0	0	
48	1	0	0	0	0	0	

Figure 5.10: The Data Passed on to the Visual Basic ‘Main’ Function (Only Part of Data Shown)

Visual Basic’s ‘main’ function accepts the data from Excel ‘main’ function as described earlier for further processing. The ‘main’ function is shown in Figure 5.11. The ‘main’ function in turn calls the function based on the truck type. In this explanation, we will use the HS20 function. Refer to Figure 5.12. In this function, truck HS20 is described, and the coordinates are normalized to a unit plate width. The truck wheel coordinates are normalized with the wing width. HS20 function then calls the corresponding Homberg chart moment functions in order to calculate the moment for each wheel location and the load on that wheel. The moments so computed are added and the values are passed onto the corresponding cell number in the Excel ‘main’ tab. The process repeats for the cells from B38 to AX38.

```

Function main_msB(vehicle As String, moment_location As String,
' vehicle: vehicle type
' WA, WB: wing length, barrier clearance
' (x,y) is the normalized coordinate of the top/right of th

If vehicle = "HS20" Then
    main_msB = HS20fn(moment_location, x, y, WA, WB, WC)
ElseIf vehicle = "FL120" Then
    main_msB = FL120(moment_location, x, y, WA, WB, WC)
ElseIf vehicle = "TTT1" Then
    main_msB = TTT1fn(moment_location, x, y, WA, WB, WC)
ElseIf vehicle = "TTT2" Then
    main_msB = TTT2fn(moment_location, x, y, WA, WB, WC)
ElseIf vehicle = "TTT3" Then
    main_msB = TTT3fn(moment_location, x, y, WA, WB, WC)
ElseIf vehicle = "CR1" Then
    main_msB = CR1fn(moment_location, x, y, WA, WB, WC)
ElseIf vehicle = "Custom" Then
    main_msB = Customfn(moment_location, x, y, WA, WB, WC)
End If

```

Figure 5.11: Visual Basic 'Main' Function Code

The minimum and maximum moments and the corresponding location are selected by using the Excel function, and results are displayed from cell number A15 to E23. The normalized x and y coordinates are converted to real x and y coordinates by multiplying by the corresponding normalization factor. The moment reported is the total moment. The wheel coordinates are, for the top right wheel when the truck moves in the direction as shown in Figure 5.2. The sample result for HS20 truck, m2x wing span Homberg chart, is shown in Figure 5.13.

The wheel locations for the selected type of truck for the corresponding maximum moment are plotted by clicking respective button created in the Excel 'main' tab. This was explained in detail earlier.

The same code is repeated for truck type B and different Homberg chart influence surfaces. In Visual Basic code, four modules were written. Module1 is for m2x and m3x wing Homberg chart for truck type A. Module2 is for m2x and m3x wing Homberg chart for truck type B. Module3 is for m3x mid span fixed edge and m5x mid span simply supported case of Homberg chart for truck type A. Module4 is for m3x mid span fixed edge and m5x mid span simply supported case of Homberg chart for truck type B. The formulation of moment functions for Homberg charts is described in following section separately.

```

Function HS20fn(moment_location As String, x As Double, y

    ' Define the truck: tire coordinates and forces. Top/
    Dim TireX, TireY, TireF ' x coordinate (inch), y coord
    TireX = Array(0, 72, 0, 72, 0, 72) ' order: top/right
    TireY = Array(0, 0, -168, -168, -336, -336)
    TireF = Array(4, 4, 16, 16, 16, 16)

    ' Normalize coordinates of the tire, and then consider
    Dim TireXN(6) As Double
    Dim TireYN(6) As Double
    Dim intI As Integer
    For intI = 0 To 5
        TireXN(intI) = TireX(intI) / WA + x
        TireYN(intI) = TireY(intI) / WA + y
    Next

    ' If the tire falls into the barrier clearance zone,
    ' (One side of the truck overlaps with the barrier).
    ' Assume that the second array entry is the left tire
    If TireXN(1) > (1 - WB / WA) Then
        HS20fn = 0
        Exit Function
    End If

    ' Loop over all tires and compute the total moment
    Dim MomentSum As Double
    MomentSum = 0
    For intI = 0 To 5
        If moment_location = "m2x wing" Then
            MomentSum = MomentSum + m2xWing(TireXN(intI),
        ElseIf moment_location = "m3x wing" Then
            MomentSum = MomentSum + m3xWing(TireXN(intI),
        End If
    Next

    HS20fn = MomentSum

End Function

```

Figure 5.12: HS20 Function Code

TRUCK A	HS20			
m2x wing		Normalized	Original	
Max moment		0	0	k-in/in
Location	x	0.1	10.2	inch
	y	-1.8	-183.6	inch
Min moment		-2.47	-2.47	k-in/in
Location	x	0	0	inch
	y	1.7	173.4	inch

Figure 5.13: Sample Result for HS20, m2x Wing Span

The Homberg chart moment functions were formulated by digitizing the Homberg chart. The process is discussed with m3x wing span Homberg chart. The Homberg chart shows the grid at every 0.2 interval. Refer to Figure 5.14. An additional grid at 0.1 intervals was created as shown by rectangles. Each rectangle is of 0.1 unit width. One long edge of the each rectangle is aligned with vertical grid lines of the Homberg chart. The other long edge gives the reading at 0.1 unit interval. The intersection points of these grid lines with contour lines were picked by Digitizer Engauge software. The software allows copying the graph and selecting the data points along graph and contour lines. The data points first selected along the x axis of the Homberg chart which is a vertical line passing through (0, 0) on the left side of the chart. The data points so collected were exported to the Excel file, and curve fitting was done in Excel to extract the equation, which is the moment equation for 0.0 grid line. Likewise, data points were selected for the remaining grid line parallel to the x axis, and corresponding moment functions were formulated.

The digitized points exported to the Excel file are the x coordinates of the data points. The contour data points are then typed against each x coordinate value. This is explained with Table 5.1(a) and (b). Table 5.1(a) shows the digitized data. The x coordinate goes from 0 to 1, and the y coordinate is 0.4 for each reading. The small fractional error is because of the manual picking of data points. In Table 5.1(b), the x coordinates are copied as is. The magnitude indicated on the contour lines is written against the x coordinates. The values in Table 5.1(b) are plotted as shown in Figure 5.15. The best-fit polynomial trend line gives the moment function, which is used in Visual Basic tool for moment calculation. The process was repeated for the rest of the Homberg charts considered in the analysis.

When the load moves to  $y = 0.4$  grid on normalized bridge coordinate which is P37 cell in Excel tool 'main' tab, its x coordinate and other data is passed onto the respective Visual Basic code functions as explained in earlier. Based on x and the location of the load, the corresponding moment function executes, and the calculated moment value is passed back to the respective Excel 'main' tab cell.

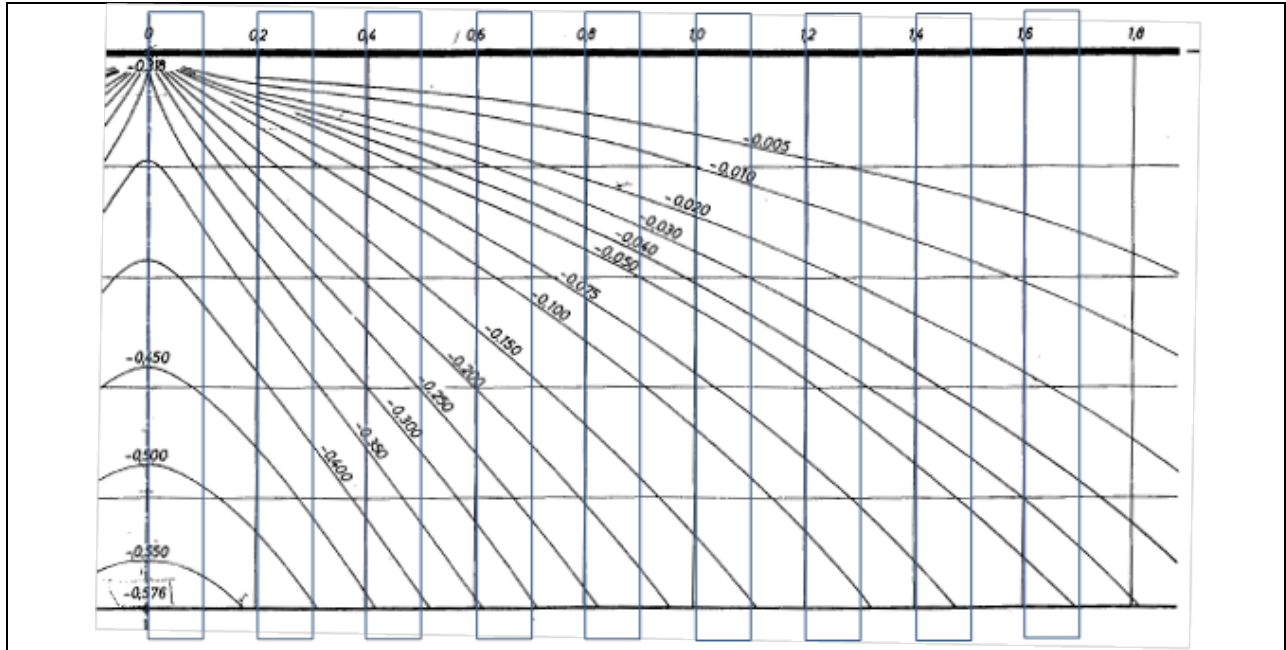


Figure 5.14: Homberg Chart for m3x Wing Span with Additional Grid at 0.1 Interval

Table 5.1: Digitized Data for  $y = 0.4$  Grid Line, m3x Wing Span Homberg Chart

x	Curve1
0	0.39658
0.061715	0.396977
0.08203	0.400566
0.11595	0.397351
0.136312	0.394044
0.156603	0.40108
0.173551	0.401197
0.21764	0.398053
0.261706	0.398357
0.336279	0.398871
0.414241	0.399409
0.499006	0.396545
0.604086	0.39727
0.719335	0.398064
0.837974	0.398883
0.973561	0.399818
1	0.396557

(a)

x	y0.4
0	0
0.061715	-0.005
0.08203	-0.01
0.11595	-0.02
0.136312	-0.03
0.156603	-0.04
0.173551	-0.05
0.21764	-0.075
0.261706	-0.1
0.336279	-0.15
0.414241	-0.2
0.499006	-0.25
0.604086	-0.3
0.719335	-0.35
0.837974	-0.4
0.973561	-0.45
1	-0.4555

(b)

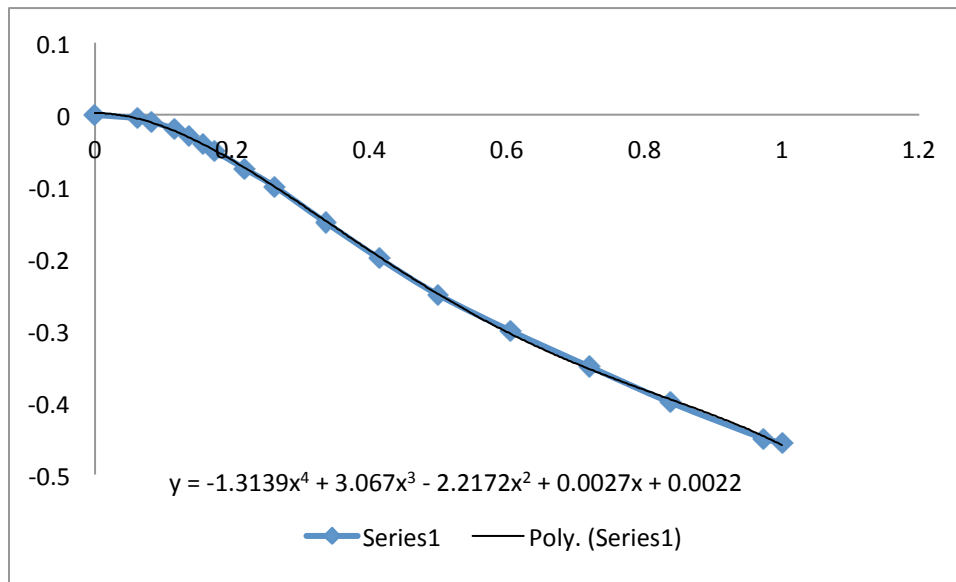


Figure 5.15: Moment Function for y = 0.4 Grid Line for m3x Wing Span

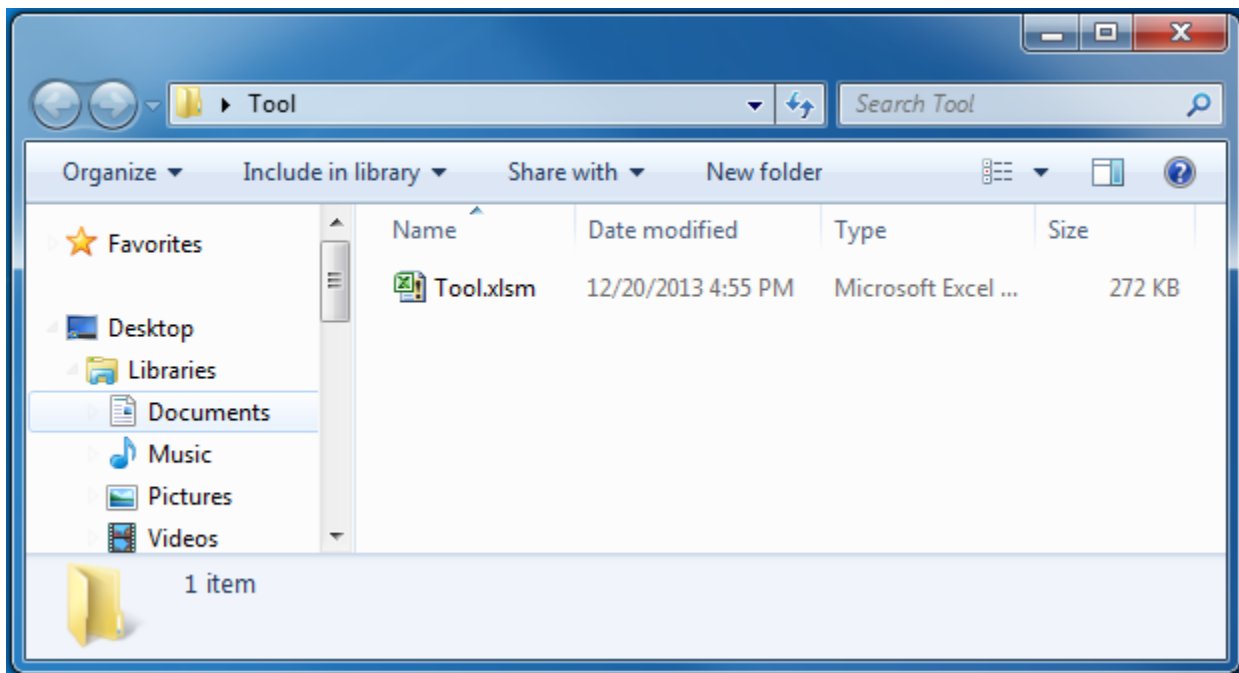
## CHAPTER 6

### How To Use The Tool (Tutorial)

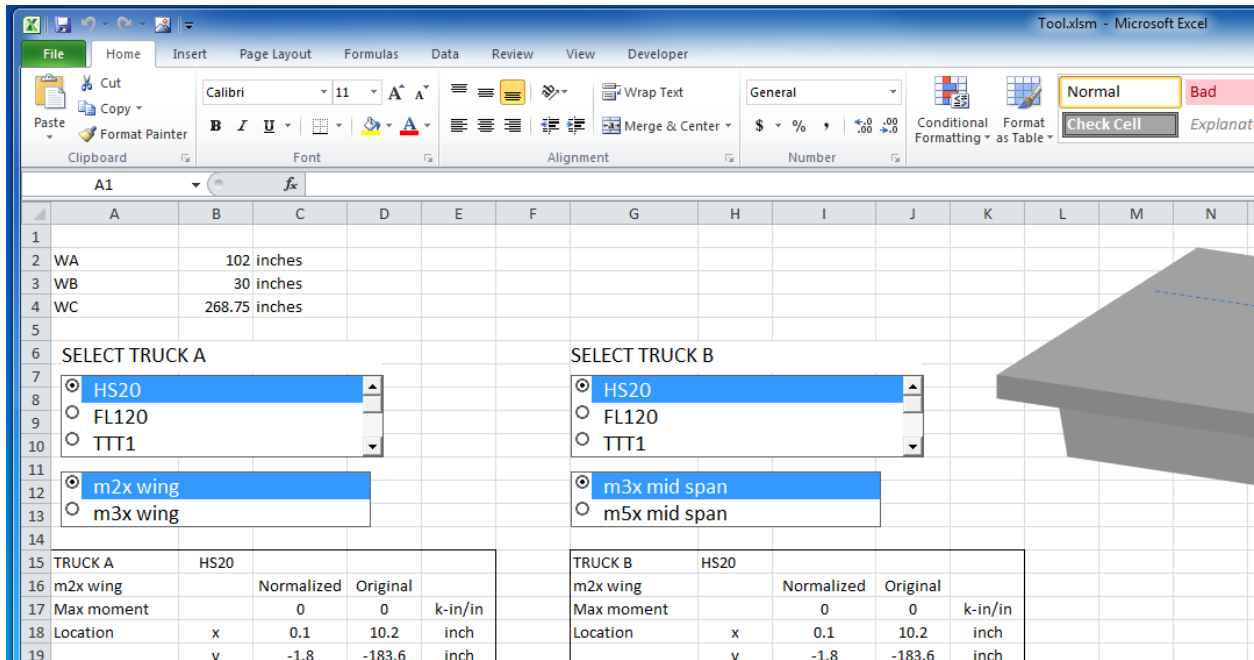
This section will explain how to use the tool that was developed in this research and discussed in Chapter 5. To use the tool, the user is required to follow the steps below. Keep a copy of tool.xlsm in backup in case it is accidentally deleted or gets corrupt.

**Step 1:** Make sure that the Excel file ‘tool.xlsm’ exists on the computer directory.

**Step 2:** Browse to the location of the file.



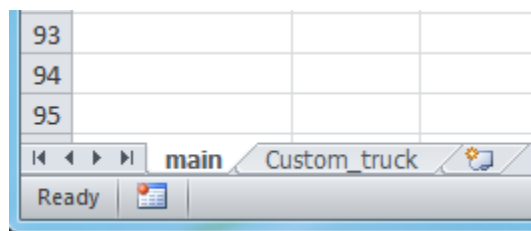
**Step 3:** Click to open the file ‘tool.xlsm’. The Excel file will appear on the screen. Part of the screen capture is shown in figure below.



**Step 4:** Enter WA value in cell B2, WB value in cell B3, and WC value in B4. For definitions of WA, WB, and WC, refer to the adjoining bridge deck figure in ‘tool.xlsm’ file.

	A	B	C
1			
2	WA	102 inches	
3	WB	30 inches	
4	WC	268.75 inches	

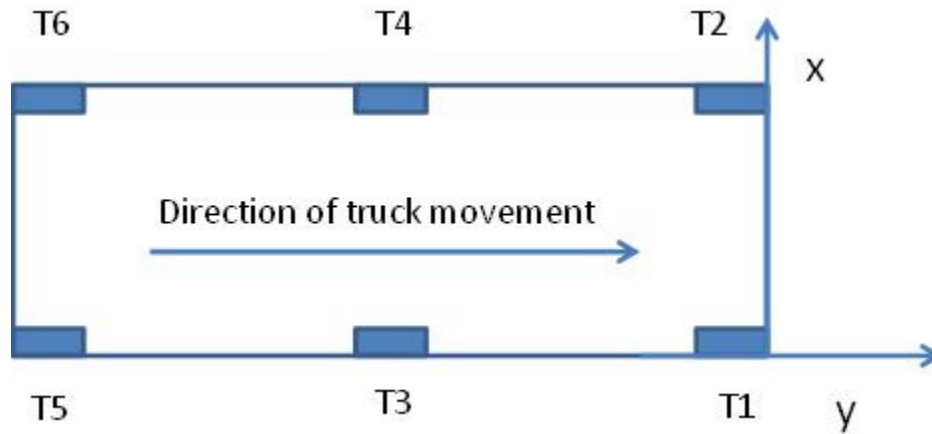
**Step 5:** Scroll down ‘SELECT TRUCK A’ and ‘SELECT TRUCK B’ lists to check if the trucks that need to be analyzed are available. If the trucks are not available, then go to ‘Custom\_truck’ tab in the ‘tool.xlsm’.



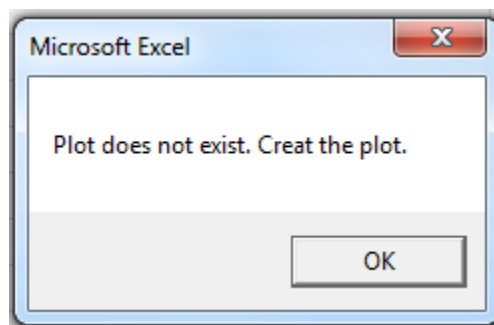
**Step 6:** In the ‘Custom\_truck’ tab, enter the number of wheels in cell B1. Depending on the number of wheels, an equal number of rows will be highlighted. This is to suggest the user to enter the corresponding data in all highlighted cells. The order of entering data with the direction

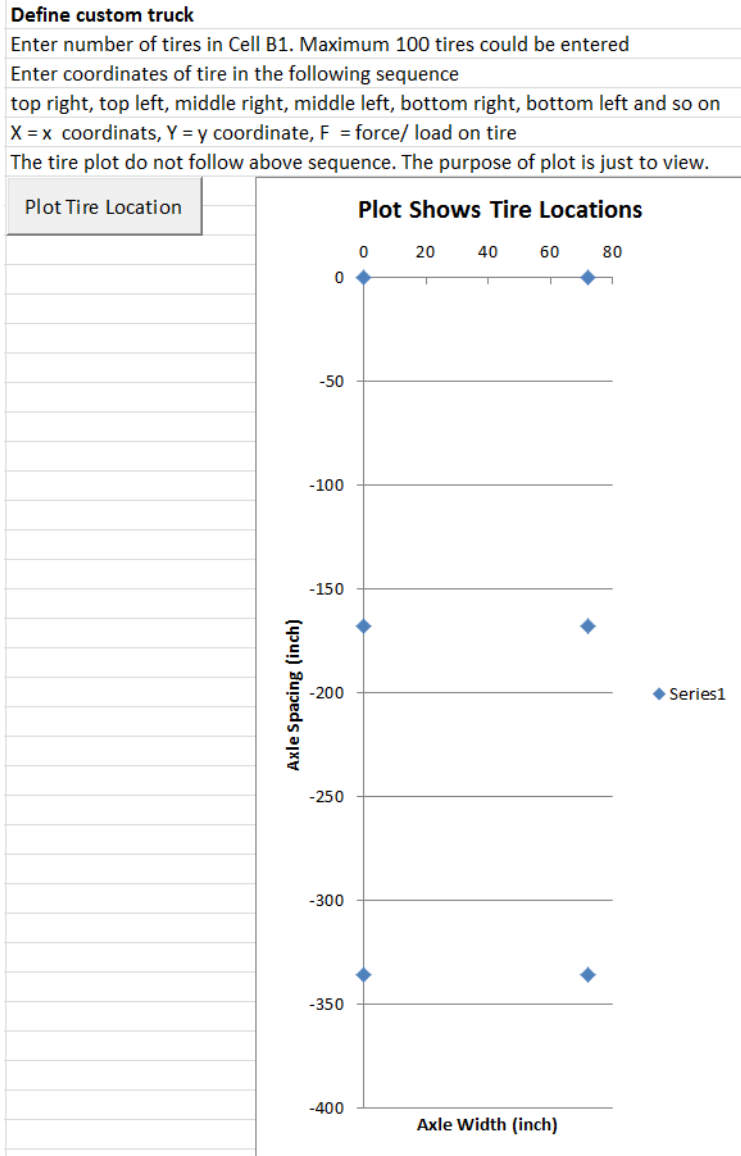
of truck movement and x, y coordinates are shown below. The side note is written for user. It is suggested to read the note and then start entering the wheel coordinates and corresponding load on the wheels. In the figure below, T1 - T6 are wheel numbers.

	A	B	C
1	Enter no of tires	6	
2	X inch	Y inch	F kips
3	0	0	4
4	72	0	4
5	0	-168	16
6	72	-168	16
7	0	-336	16
8	72	-336	16



**Step 7:** If the plot showing the wheel location does not exist or is accidentally deleted, then click 'Plot Tire Location' button. The following button dialog box will appear on the screen asking user to plot the tire location graph just for viewing. The plot of wheel will not be in the sequence in which it was entered. The purpose is just to view the data. It will not affect the result.





**Step 8:** If the desired truck is present in the list, then select truck type A and B from the list.

SELECT TRUCK A

HS20  
 FL120  
 TTT1

SELECT TRUCK B

HS20  
 FL120  
 TTT1

**Step 9:** Select the Homberg chart m2x wing or m3x wing and m3x mid span or m5x mid span.

m2x wing  
 m3x wing

m3x mid span  
 m5x mid span

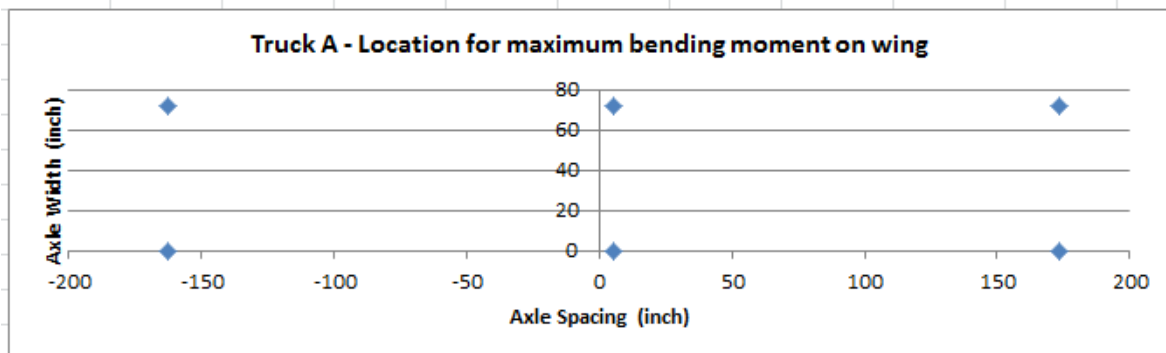
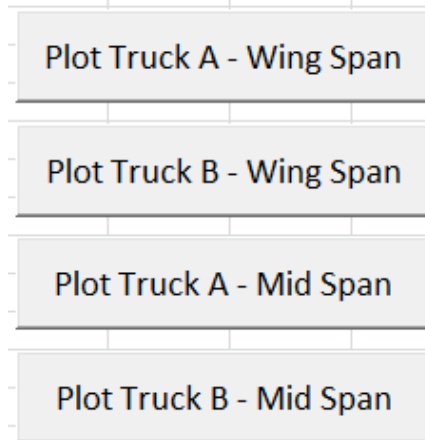
The results for HS20 truck A and HS20 truck B for m2x wing and m3x mid span will be printed in the Excel file from cells A15 to K34. In this tutorial, the HS20 truck was used in both the truck type A and B. The sample results are shown below.

TRUCK A	HS20			
m2x wing		Normalized	Original	
Max moment		0	0	k-in/in
Location	x	0.1	10.2	inch
	y	-1.8	-183.6	inch
Min moment		-2.47	-2.47	k-in/in
Location	x	0	0	inch
	y	1.7	173.4	inch
TRUCK A	HS20			
m3x mid span		Normalized	Original	
Max moment		0	0	k-in/in
Location	x	0	0	inch
	y	-1.8	-483.75	inch
Min moment		0.00	0.00	k-in/in
Location	x	0	0	inch
	y	-1.8	-483.75	inch

TRUCK B	HS20			
m2x wing		Normalized	Original	
Max moment		0	0	k-in/in
Location	x	0.1	10.2	inch
	y	-1.8	-183.6	inch
Min moment		-2.44	-2.44	k-in/in
Location	x	0	0	inch
	y	1.7	173.4	inch

TRUCK B	HS20			
m3x mid span		Normalized	Original	
Max moment		0	0	k-in/in
Location	x	0	0	inch
	y	-1.8	-483.75	inch
Min moment		0.00	0.00	k-in/in
Location	x	0	0	inch
	y	-1.8	-483.75	inch

**Step 10:** Four buttons are provided next to the result output to plot the truck position corresponding to the maximum moment caused by a particular truck. In the figure below, the HS20 truck position for maximum bending moment for m2x wing span Homberg chart is shown. The dots on the graph show the wheel locations. The user can move the mouse pointer over the dots and note the (x, y) location of a wheel for further analyses. Similarly, truck positions for maximum bending moment for truck and Homberg chart combinations could be printed.



## REFERENCES

ANSYS (2010), ANSYS User's Guide, Release 13.0, ANSYS, Inc., Canonsburg, PA.

Reddy, J. N. (1997). "On Locking-free Shear Deformation Beam Finite Elements," *Computer Methods in Applied Mechanics and Engineering*, 149, 113-132.

Roddenberry, M. D. and Kuhn, D. (2008). "Transverse Analysis and Field Measurements of Segmental Box Girder Wings," Research Report BD-543-21, Florida Department of Transportation, Tallahassee, Florida.